ESA/SRE(2011)13
July 2011

PLATO

Next-generation planet finder

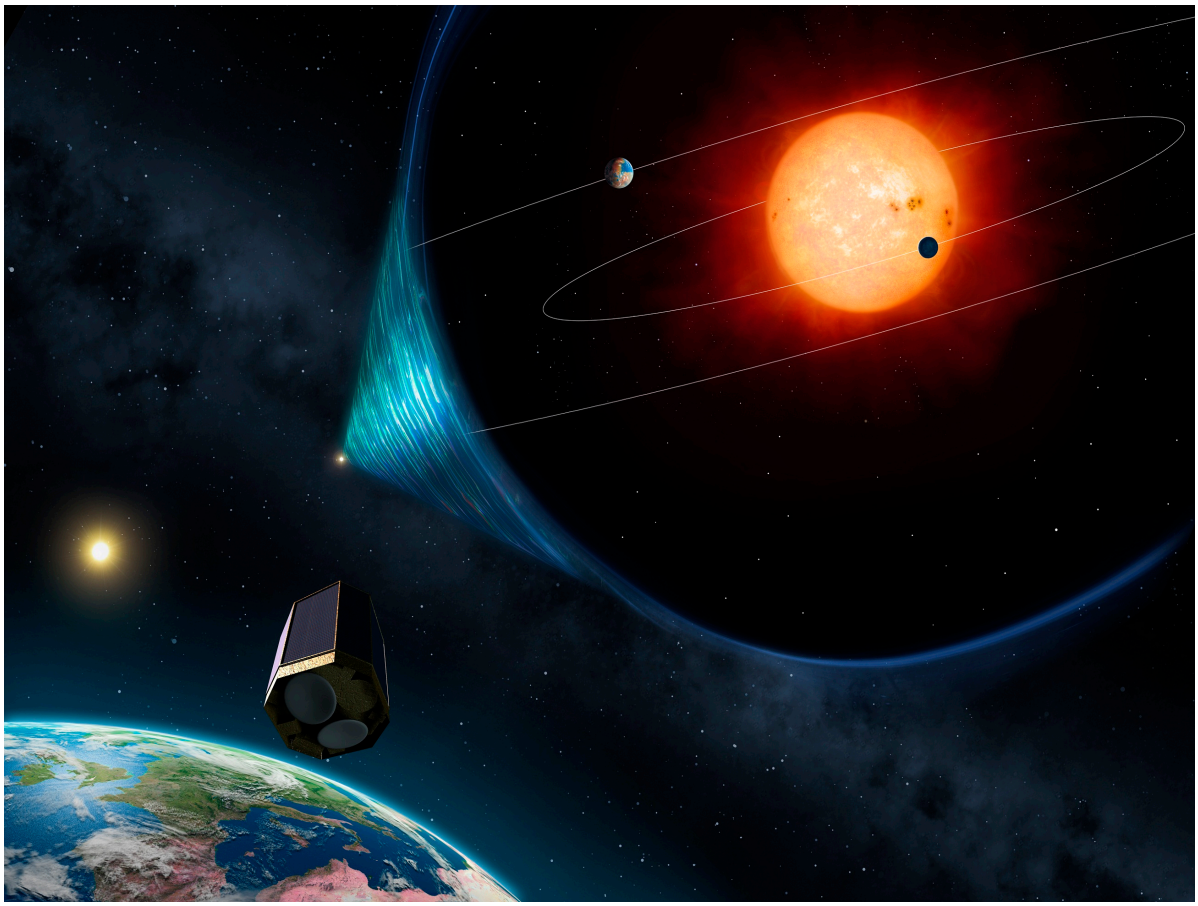

Definition Study Report

European Space Agency

Mission Summary
PLATO – the exoplanetary system explorer

Table 1-1: Summary of CV 2015-2025 candidate mission PLATO.

Science:	
Key scientific objectives	Detection of several thousand exoplanetary systems of masses between 1 and 20 Earth masses, including planets in the habitable zone, with accurate (~ 1%) determination of planetary bulk properties, (average density through mass and radius measurements), which will allow discriminating between different models of planets e.g. surface gravity and hence the ability to retain an extended atmosphere. Tens of thousands of larger planets are expected.
Observational concept	Ultra-high precision, long (up to several years), uninterrupted photometric monitoring in the visible band of very large samples of bright ($m_V < 11$) stars.
Mission concept:	
Primary data product	Very accurate optical light curves and centroid curves of large numbers of bright stars
Payload concept	• Set of 32 normal cameras organised in 4 groups resulting in many wide-field co-aligned telescopes, each telescope with its own CCD-based focal plane array; • Set of 2 fast cameras for bright stars, colour requirements and fine guidance and navigation
Observing plan	Two long monitoring phases (2 years each), each one with a single field monitored Two years additional "step & stare" phase with several successive fields monitored for a few months each.
Duty cycle	≥ 95%
Launch and orbit:	
	• Launch by Soyuz-Fregat2-1b from Kourou in 2018 • Transfer to L2, then large amplitude libration orbit around L2
Mission lifetime (Example):	
	• 0.25 years max for LEOP, transfer and commissioning • 2 years observation of sky region 1 • 2 years observation of sky region 2 • 2 years observation on step& stare mode • Possible extension for two additional years
Radiation environment:	
	• Sun-Earth L2 – relatively benign environment
Spacecraft specifications:	
Stabilisation	3-axis
Telemetry band	X-band (10 MHz maximum bandwidth)
Average downlink capacity	109Gb per day (Assumption: ground station contact for 4 hours per day, 3.5 hours for data downlink with a data downlink rate of 8.7 Mbps)
Pointing stability	0.2 arcsec rms over 14 hours
Pointing strategy	One 90 deg rotation around the line of sight every 3 months
Payload specifications:	
Optical system	6 lenses per telescope (1 aspheric)
Total number of telescopes	34 (32 normal cameras and 2 fast cameras)
Focal planes	136 CCDs (4 CCDs per camera) with 4510x4510 18µm pixels
Instantaneous field of view	2250 deg^2

Foreword

The PLATO mission was proposed in 2007 as a medium class candidate in response to the first call for missions of the Cosmic Vision 2015-2025 program. The proposal was submitted by Dr. Claude Catala (Observatoire de Paris) on behalf of a large consortium of scientists from laboratories all across Europe. The scientific objectives of the mission are to detect and characterize transiting exoplanetary systems of all kinds (providing unique data for both the exoplanets and their host stars). In particular, small, telluric planets in their habitable zones will be searched for, and studied. PLATO will detect multiple transits of exoplanets and, simultaneously, perform a detailed seismic analysis of the host stars, allowing a precise determination of their radii, masses and ages, from which the radii, masses and ages of the exoplanets will be derived.

Following favourable reviews by ESA's scientific advisory bodies, PLATO was selected in 2007 as one of the missions for which an assessment study were carried out in 2008 and 2009 by ESA, supported by the PLATO Study Science Team (PSST). In a first phase of the study (2007), the most efficient concept to achieve the science objectives was selected by the PSST, and the mission was further studied in the framework of an assessment study, involving two concurrent industrial contracts, as well as the PLATO Payload Consortium. The PLATO Mission Consortium (PMC), which involves more than 350 scientists and engineers in virtually all ESA member states, as well as a few members from the US and Brazil, will be in charge of the study and procurement of the instrument, of the PLATO data centre (PDC), and of the science preparation and exploitation activities (PLATO Science Preparation Management, PSPM). The members of the PLATO Consortium can be found at the web site http://www.oact.inaf.it/plato/PPLC/People.html All three studies were carried out in parallel and completed simultaneously at the end of summer, 2009.

The PLATO mission was subsequently selected for a definition study, starting in February 2010. The definition study again involves two concurrent industrial contracts for the definition of the mission profile, the satellite, and parts of the payload module (identified in this report as Concept A and Concept B respectively). The PLATO Mission Consortium carried out the study of the instrument, and a specific industrial contract for the study of CCD procurement was issued by ESA to support the PMC.

This report describes the results of the complete Definition Study, both of the scientific and technical results as well as managerial aspects. It results from a vast team effort, involving many different parties (ESA, PMC, PDC, PSPM, industrial companies), under general supervision by the PLATO science team (PST) and the ESA study team.

The members of the ESA PLATO Science Team (PST) were:

C. Catala	Observatoire de Paris, France
J.M. Mas-Hesse	CAB (CSIC-INTA) Madrid, Spain
G. Micela	INAF, Osservatorio di Palermo, Italy
D. Pollacco	Queens University, Belfast, United Kingdom
R. Ragazzoni	INAF, Osservatorio di Padova, Italy
H. Rauer	DLR, Berlin, Germany
S. Udry	Geneva Observatory, Geneva University, Switzerland

Input was also received from L. Gizon, MPI for Solar System Research, Lindau, Germany.

The team members from the ESA Directorate of Science and Robotic Exploration were:

M. Fridlund	Study Scientist
O. Piersanti	Study Manager
A. Stankov	Payload Manager
M. Baldesarra	System Engineer
L. O'Rourke	Science Operations Engineer

Members of the ESA planning and coordination office during the definition study have been P. Escoubet and Ana Heras

The report consists of the following parts. Following the Executive Summary (chapter 1), the main science goals and the expected scientific impact are presented in chapter 2. In chapter 3 we detail the Scientific Requirements of PLATO and in Chapter 4 we describe the payload and its expected performances followed by chapter 5, Mission Design, and Chapter 6 Preparatory Work and Follow-Up Observations. The Ground Segment and Operations is described in Chapter 7. Finally the Management of the mission is described in Chapter 8.

TABLE OF CONTENTS

1 EXECUTIVE SUMMARY

PLATO (PLAnetary Transits and Oscillations of stars) is the next generation planetary transit experiment designed to discover and characterize exoplanetary systems, both planets and their host stars of all kinds, and located in the solar neighbourhood. It builds on the accumulated experience provided by the successful CoRoT and *Kepler* missions. By focusing on bright and nearby targets, PLATO gives at least an order of magnitude gain over current missions, as what concerns planetary and stellar parameters. It will provide a full census of exoplanets down to small, low mass, terrestrial planets in the habitable zones of solar and late type stars. The brightness of the host stars is key to this goal allowing exquisite data to be obtained enabling seismic analysis of the host and, hence, allowing full characterisation of the detected exoplanetary systems, through a precise determination of the stellar radii, masses and ages, from which the same parameters of the exoplanets themselves will be derived. When combined with Gaia results, data from PLATO will reach the level that will revolutionise our knowledge of stellar evolution and transform our knowledge of exoplanets and their planetary systems.

This will provide a complete characterization of those exoplanetary systems, including their evolutionary status, and enabling us to deduce the nature of the planetary bodies (e.g. ocean or rocky planets etc). Such objects will be prized targets for future more detailed characterization, including the search for biomarkers in their atmospheres. These goals will be achieved by highly accurate time-resolved photometry of a large number of bright and nearby stars, coupled to a vigorous ground-based follow-up programme.

PLATO will capitalize on the strong European expertise in the field of exoplanet science, accumulated through the CoRoT mission and many years of ground-based efforts. It will also benefit from the outstanding achievements of asteroseismology, where European scientists excel through their leading roles in CoRoT and the seismology program of *Kepler*.

While it builds on the scientific heritage from both the CoRoT and *Kepler* missions, the major breakthrough to be achieved by PLATO will come from its strong focus on bright targets, typically with $m_V \leq 11$ which will allow planetary masses to be directly measured including Earth-sized objects. The PLATO targets will also include a large number of *very bright and nearby stars*, with $m_V \leq 8$. In order to be able to observe enough targets (> 85000) brighter than $m_v \leq 11$, the mission is designed to have a field of view orders-of-magnitude wider than any previous mission. PLATO will, for the first time, also be able to use the new tool of asteroseismology in a systematic way in order to characterise the host stars to a precision orders-of-magnitude better than anything attempted before. This will lead to an understanding of the parameters of the exoplanets themselves to accuracy on the order of 1 to a few percent. PLATO was highlighted in ESA's EPRAT report as a vital link in European studies of exoplanets over the next few decades.

The prime science goals of PLATO are:

- The detection of exoplanetary systems of all kinds, reaching down to small, terrestrial planets in the habitable zone;
- To accurately determine the bulk properties, like the average density through mass and radius measurements of a large sample of the lowest mass planets allowing discrimination among different models of the planets and, in particular, the phenomena affecting habitability (like the surface gravity and hence the ability to retain an extended atmosphere)
- The identification of suitable targets for future, more detailed investigations, including a spectroscopic search for biomarkers in nearby habitable exoplanets.

These ambitious goals will be reached by optical ultra-high precision, long (up to a few years), photometric monitoring of very large samples of low activity, bright stars, which can *only* be done from space. The high quality light curves will be used to detect planetary transits, and provide a seismic analysis of the host stars of the detected planets, from which precise measurements of their radii, masses, and ages will be derived. The brightness of the PLATO targets will also facilitate the use of future detection methods. PLATO will also detect small planets around nearby stars. Thus PLATO will be a pioneering mission searching out statistically significant samples of planets in the habitable zones of late type stars that can be studied in detail from ground based facilities. The nearest and brightest stars with planets will be *important targets* for

atmospheric investigation with future telescopes such as the JWST, E-ELT and possible future spectroscopy missions.

The brightness of the targets will allow full characterisation of the planets and their hosts. Their orbits, radii, masses and ages will be determined with unprecedented accuracy. Current results hint that large diversity exists amongst terrestrial-mass planets. PLATO results will allow comparative planetology at these masses for the first time leading to new science and redefining our ideas of planet habitability. With accurate stellar ages we will take the first exciting steps in understanding planetary evolution.

PLATO will address the basic question of the existence, distribution, evolutionary state, and characteristics of exoplanets in the solar neighbourhood. Answers to these questions are essential to understand how planetary systems, including our own, are formed and evolve, and also as a first and necessary step to understand whether life can exist elsewhere in the Universe, and locate potential sites for life. Since the discovery of the first exoplanet orbiting a solar type star in 1995 (Mayor & Queloz, 1995), this field has seen a remarkable development, with about 565 exoplanets known as of the end of June 2011. Most of these objects are giant planets in close-in orbits, but continuous progress in the precision of radial velocity observations is now enabling the detection of "super-Earths", with masses just a few times that of the Earth (but unable to constrain their radii and hence bulk properties). In space, the launch of the CoRoT satellite (December 2006), and NASA's *Kepler* mission (March 2009) has pushed the detection limits to lower radii e.g. CoRoT-7b - the first rocky planet with measured radius, mass, and hence bulk density (Léger et al., 2009; Queloz et al., 2009). The first *Kepler* rocky planet (Kepler-10b) has also been published (Batalha et al., 2011). Other *Kepler* results hint at significant diversity at low planetary masses, but accurate mass determination for the smallest planet candidates will be difficult due to the faintness of many of their host stars. In the future, we expect only few more rocky planets from CoRoT and *Kepler* during their lifetimes.

With their smaller field-of-views, CoRoT and *Kepler* have to target rather faint stars, up to m_v=15 and fainter in order to observe enough targets to detect the chance alignment of transits. Their ground-based follow-up, in particular in radial velocity monitoring, is therefore extremely challenging - even with the largest telescopes. Hence, ground confirmation and mass measurements are restricted to the largest of the CoRoT and *Kepler* planets, which impacts the scientific return of these two missions. While both CoRoT, and the *Kepler* mission, can detect the passage of a planet the size of our own world on such faint stars, *it is impossible to confirm the presence of such an object found by either spacecraft*. Even for the few objects that can be studied, our knowledge will be limited by the inability to measure the host star properties with sufficient accuracy. This is reflected in our estimates of the planetary properties and our ability to constrain their structure and state of evolution. Most important of all, neither CoRoT nor *Kepler* can observe more than a limited number of stars with a precision high enough to determine the astroseismologic spectrum with the precision required to determine the stellar parameters.

The main goal of PLATO is to alleviate these severe difficulties by focusing on large numbers of bright stars, typically 3 to 4 magnitudes brighter than CoRoT and *Kepler*. By utilizing a large set of small telescopes with extreme wide-field capability, PLATO will provide an order-of-magnitude impact on the field of exoplanetology by its ability to observe *all* its prime candidates (85 000) asteroseismologically, leading to a precision on the determined planetary parameters of ~ 1% and ages of systems 10 times better than *anything* achieved before. These targets will also be ideal for ground based follow-up. Furthermore, they will be the most important targets for studies with other facilities such as the JWST and E-ELT, and particularly important for studies of the surfaces, atmospheres and the search for biomarkers.

PLATO data will also allow rapid advances in other areas of stellar physics, stellar formation and solar system science, which when combined with Gaia results will see a step change in our understanding of stellar evolution.

The prime PLATO data product will be a large sample of high precision stellar light curves, obtained on very long time intervals and, with high duty cycle (≥95%). PLATO will obtain a photometric precision $<3.4 \times 10^{-5}$ in one hour for more than 20,000 late type stars brighter than about m_v=11 (allowing seismic characterisation of the host star), and 8.0×10^{-5} in one hour for 250,000 stars down to m_v=13 (allowing the detection of the transit of an Earth sized planet). In order to reach these numbers of stars, PLATO will monitor two wide fields, for 2 years (possibly 3 years for one field) each.

These sequences will be followed by a step-and-stare phase, lasting 1 – 2 year(s), and during which a number

of fields will be monitored for between 2 and 5 months each, and then re-observed as appropriate (including possible re-observation of the two fields that were monitored for 2 or more years in order to confirm the detection of small planets for which only 1 or a few transits have been detected). This phase will bring flexibility to the mission, allowing for instance to survey a very large fraction of the whole sky (maybe >50%), as well as to re-visit previously identified worthy targets. These phases will allow transit searches for Earth sized planet for $>10^6$ stars (80 ppm in one hour) and seismic characterisation in >85,000 stars (34 ppm in one hour). PLATO will thus achieve at least an order-of-magnitude improvement on previous missions, both quantitatively and qualitatively. PLATO can be launched in late 2018 on a Soyuz-Fregat rocket for injection into a Lissajous Orbit around the L2 Lagrangian point. This will give a nominal lifetime of 6 years after commissioning (spacecraft and consumables sized for 8 years), which is compatible with the example observation strategy outlined above.

PLATO is envisaged to consist of a spacecraft module and a payload module. The definition phase has been supported by two industrial contractors working independently and in parallel to design the spacecraft, while the instrument is provided by the PLATO Payload Consortium. The instrument consists of an ensemble of 32 "normal" cameras each with a very wide field-of-view (FoV) and CCD based focal plane. With a cadence of 25 seconds these units will monitor stars with $m_V>8$. Two additional “fast” cameras with 2.5 second cadence are used for stars with m_V ~4-8. The paucity of bright stars necessitates the wide FoV of the units while the science drivers dictate the required sensitivity (numbers of cameras). The ensemble of instruments is mounted on an optical bench. The cameras are based on a fully dioptric design with 6 lenses. Each camera has an 1100 deg^2 FoV and a pupil diameter of 120 mm and is equipped with a focal plane array of 4 CCDs each with 4510^2 18 μm pixels, working in full frame and frame transfer mode for the “normal” and “fast” cameras respectively.

The “normal” cameras are arranged in four groups of 8 cameras. Each group has the same FoV but is offset by a 9.2° angle from the PLM+Z axis and allows surveying a total field of ~2250 square degrees per pointing, but with different sensitivities over the field. This strategy optimizes both the number of targets observed at a given noise level and their brightness. The satellite will be rotated around the mean line of sight by 90° every 3 months, enabling a continuous survey of the same region of the sky.

The PLATO Ground Segment consists of four main elements:

- An ESA provided Mission Operations Centre in charge of satellite operations.
- An ESA provided Science Operations Centre (SOC) in charge of the scientific mission planning, the generation, validation, and distribution of the light and centroid curves. The SOC will also develop and operate the archives used to store and distribute all PLATO mission products to the science community.
- A PLATO Data Centre (PDC) provided by the Member States and which will generate the scientifically added-value mission products for archival and distribution by the SOC.
- A PLATO Science Preparatory Management Group (PSPM) who will carry out scientific preparatory and scientific operative activities, as well as supporting ESA in public relations and outreach activities. The PDC will generate the final science data products in full cooperation with the PSPM. It is foreseen that most validated PLATO data will be made public immediately. However, a small number of light curves (<1%) from targets selected prior to launch, will remain the property of the PLATO involved scientists for one year.

PLATO will lay the foundations for exoplanetary research for the next few decades. It will allow comparative planetology and ultimately redefine our thinking on habitability. PLATO targets will dictate instrumentation programmes on new large facilities and inspire future space missions that will aim to study in detail Earth-like planets around other stars and search for signatures of life in the Universe.

2 MAIN SCIENCE GOALS

2.1 Introduction

Since centuries mankind has been fascinated by the question of whether we are alone in the Universe. While this has always been a philosophical question, we are today, at the turn of the 3rd millennium, for the first time able to address the question whether planets with life could have developed elsewhere with quantitative measures. We are thus able to verify if our imaginations about other worlds are real.

In order to understand ourselves better we need to know what our true place is in the Universe. We have now reached the point in evolution where we have begun to enquire of our origins. Are we just one of many instances of life, evolving on a common type of planet? Or are we unique? Born in a very special place and under very extraordinary circumstances? We still do not know, but for the first time in our history we are able to address these questions as we now have the technology to do so.

In order to understand the origin of life and to determine where it is most likely to exist in the Universe, a full understanding of planet formation and the evolution of planetary bodies is vital. Along with improvements in our knowledge of main sequence stellar evolution, we need to measure accurately the distribution of planet sizes, masses and orbits, at least down to Earth-sized planets, and to determine which of these planets are likely to be habitable. Just as important, we need to determine their age. In this regard, terrestrial planets in the habitable zone *i.e.* the region in the stellar environment where physical conditions are such that water can be present as a liquid are of particular interest, since they are the prime sites for the development of life. Only then will we be able to relate all characteristics of the planets to the evolutionary history and age of the exoplanetary systems, and determine under which initial conditions and at what stage of their evolution planets can provide the necessary environment for life.

In this context, significant effort is now being spent at ESA within the Robotic Exploration programme in the search for present or past life on other bodies in the Solar System (e.g. ExoMars). Although success in these endeavours would be a great achievement, and would provide us with much needed information, the Solar System is just a miniscule speck in the Cosmos and within the Milky Way galaxy. Furthermore, as the Solar System originated out of the same primordial nebula at the same time, any rare and special conditions relevant to the origin of the Earth and life on it, would likely apply elsewhere in the Solar System *e.g.* Mars.

If we want to understand our real place in the Universe, we must thus look outside the Solar System.

As far as we know, life only arises on or near the surface of planets. We thus assume that life in the Universe is intimately connected with planets. Also, although some scientists have suggested ecologies in the atmosphere of Jupiter-like planets (*e.g.* Sagan & Salpeter 1976), the currently held opinion is that in order for life to arise and establish itself, you need a small 'rocky' world with liquid water and thus a benign temperature, just like our own Earth. The search for and study of planetary systems like our own, around other stars, and in particular the search for the signatures of life in exoplanetary systems, is thus a prerequisite towards generalising our understanding about the distribution of life in the Universe and how it may have once arisen on the Earth.

The first question that must be asked in this context is if planets are common in our Galaxy? At some level, this question has recently (in the last 20 years) been answered. Literally one planet orbiting a star other than the Sun is, at the moment, *found every week!*

More than 565 planets orbiting around other stars have been discovered so far, and more than 1000 – 1500 further good candidates are already known. All those that can be studied in detail, however, have turned out to be quite different from what we expected based on the structure of our own solar system, and they show a much larger diversity than we ever imagined. At this moment in time, we can only guess at all the types of planets that may exist. In particular the diversity of small planets in the so-called “habitable zone” around stars is only poorly constrained and remains one of the big future scientific goals that will help to address the fundamental questions on:

- How do planetary systems form and evolve?
- What makes a planet habitable?
- Is the Earth unique or has life also developed elsewhere?

PLATO is the next generation planetary transit experiment. Its objective is to characterize the bulk properties of exoplanets and their host stars in the solar neighbourhood. PLATO follows the ongoing very successful space missions CoRoT and *Kepler*, which have demonstrated the wealth of information that can be gained from such missions in particular for terrestrial extra solar planets like CoRoT-7b and Kepler-10b. These missions also demonstrated that planetary confirmation and characterisation is far more difficult than previously thought and requires data of high quality that in almost every case has not been possible given the brightness of the CoRoT and *Kepler* surveyed stars. It is clear that the next generation transit surveys must concentrate on bright stars allowing radial-velocity confirmation for Earth-mass terrestrial planets. Additional follow-up observations will then allow further characterization, e.g. by spectroscopy of planet atmospheres. PLATO is designed to be that survey and will therefore play a major role in addressing the fundamental questions raised above by answering the following scientific key questions of the mission:

- Did the Earth form in a special place in the Universe and/or under extraordinary circumstances?
- How diverse are planets and planetary systems?
- What are the characteristics of terrestrial planets in the habitable zones of stars?
- How do planets and planetary systems differ with age?

PLATO has a relevant role in all three major themes identified in the roadmap for research of extra solar planetary science by ESA's EP-RAT team: 1) detections, 2) characterization of the internal structure and 3) characterization of the exoplanetary atmospheres. In fact PLATO will detect a statistically complete sample of planets down to earth-size bodies. The EP-RAT report concludes "*In this respect PLATO has a key role in this roadmap, as it will constrain the internal structure of exoplanets down to the terrestrial mass regime. Since this mission is targeting bright stars, it will provide good targets for additional atmospheric characterization"*.

Furthermore, due to its high-precision, long-term (months to several years per field) monitoring of up to a million of stars potentially over 50% of the sky, the mission will impact not only the field of extra solar planets, but also stellar science in general. Together with the physical parameter obtained from Gaia, the asteroseismology of PLATO will change the face of stellar physics.

While the first exoplanetary search programme was described some 60 years ago (Struve, 1952) it took, for technical and sociological reasons, about 40 years before the first systematic search programmes were in place. They achieved their first successes a few years later. Latham and co-workers (1989) reported 'A Brown Dwarf or even a Planet' of 11 Jupiter masses orbiting the star HD 114762 (this object remains ambiguous to this day). Despite the efforts of the search programs, the first confirmed planets were found in the least expected area – orbiting pulsars! Timing studies of the radio signals emanating from these objects allow highly accurate determination of any orbiting body. The nature of these objects is also probably quite bizarre as they have presumably originated in the blast debris resulting from the supernova that the pulsar originates out of. At this time just a few such planets – ranging down to 0.02 Earth masses – have been found (Wolszczan & Frail, 1992).

Following closely behind these surprising discoveries, the first bona fide planet was reported in the autumn of 1995 (Mayor & Queloz, 1995), with others following soon after (Marcy & Butler, 1996; Butler & Marcy, 1996). Already these first objects produced surprises for those who had expected that all solar systems would look very much like our own. For example, these giant planets were orbiting very near to their primaries (*only a few stellar radii distant in some cases!*). Planets could clearly not have formed where they were found but must have migrated from greater distances. Other peculiar bodies such as planets with eccentricities more like comets in our own Solar System have been discovered but were completely unexpected. At some level, these first 'peculiar' planets were the results of the biases created by the technology and methods used for the first searches, which were significantly more sensitive to massive, short period bodies. While the discoveries have continued, at an accelerated rate to date, there has been no system like our own credibly reported.

Since 1995, we have found more than 550 planets orbiting around stars other than the Sun. While the building blocks of our own system appear to be there, like systems with multiple (5 or 6) planets, planets

similar to Jupiter, Neptune like planets and now even low-mass 'rocky' worlds like our own (*e.g.* CoRoT-7b: Léger et al., 2009, Queloz et al., 2009; Hatzes et al, 2011; Gliese 581e, Mayor et al., 2009a; Kepler-10b: Batalha et al., 2011a), they are always found in the wrong location (*e.g.* both CoRoT-7b and *Kepler*-10b are orbiting only 5 stellar radii away from their solar type host star and consequently experience surface temperatures of around 2000K), *i.e.* the structure of these exo-systems do ***not*** look like our Solar System.

There are several methods that have been used in order to detect exoplanets. The first method to be successfully applied involved measuring the radial velocities of many 'Solar type' stars. As a planet orbits its primary, the star will move back and forth along the line-of-sight due to the gravitational influence of the planet, and the Doppler effect will thus alternately blue- and red-shift the spectral signatures of the star. By measuring a large number of spectral absorption lines (typically several thousand per star) it is possible to measure the position of the line centre to an accuracy of a few parts in a thousand, consequently providing a velocity precision that today can be less than 0.5 m/s. Assuming enough observations have been made, this results in a usable radial velocity curve with the same precision and the presence of an influencing body can be inferred and its mass determined (actually the minimum mass of the planet unless the inclination of the orbital plane is known by another method – see below). Today, this method enables the detection of small planets (a few Earth masses) to be discovered close to low-mass stars, but the actual Earth orbiting a true sun-analogue would require another order-of-magnitude in precision and this is still some years in the future.

The next method that provided results was the transit method (Charbonneau et al., 2000). If the orbital plane happens to intersect the line-of-sight to the star, the planet will occasionally transit (part of) the stellar surface. The probability of a chance alignment varies between about 0.5% for a $1R_{\oplus}$ planet at 1 AU from a solar type star to several tens of percent for gaseous giant planets that are orbiting very close to red dwarf stars. By observing the light output of the star when the planet is transiting the stellar surface, the shape and depth of the light curve can tell us a lot about the size and other physical parameters of the planet (and of the star). Specifically, the transit constrains the inclination of the exoplanetary orbit so well that the true mass of the planet can be found from the radial velocity curve. By observing both the occultation of part of the light of the star by the planet, as well as the associated radial velocity curve, exact measurements of the planetary mass and diameter allow a determination of the body's average density and thus its mineralogy. Since this method – known most often as the transit method – requires a chance alignment to occur, any systematic investigation calls for the simultaneous observations of a large number of stars during an as long as possible time with an as high as possible duty cycle of the observations.

There are other methods that have had an impact on the field of exoplanet research. Microlensing studies for example (gravitational lensing where an intervening body enhances the light from a background object, in such a way that it reveals the presence of any planetary body orbiting the lensing object), can be used, to some extent, to estimate the frequency of long period planets surrounding M-type stars. This requires an even larger stellar sample to be observed simultaneously than the transit method, and is thus limited to the observation of very distant objects (with the accompanying problems when one tries to carry out detailed follow-up observations). As the lensing alignment will only occur once, these bodies can never be confirmed by any other technique or followed up for other science goals.

Astrometry is another promising method. It has so far played a relatively small role, since ground based and even ESA's very successful HIPPARCOS satellite only can measure with milliarcsecond precision that is not enough to detect the deflection in a star's movement in the plane of the sky. ESA's Gaia mission which will be able to measure changes in stellar positions with precisions of ~ 10 – 20 microarcseconds will, on the other hand, complete a census of large planets (Jupiter mass or larger) out to 200-500pc (depending on the size of the planet). It will also observe stars down to 15^{th} magnitude with millimagnitude precision and thus detect millions of exoplanetary transits for large planets. This will nicely complement the observations of PLATO. Gaia will also be of fundamental importance for PLATO as what concerns the determination of the stellar fundamental parameters.

The study of exoplanets is one of the fastest growing areas of modern contemporary astronomy. This is being driven by new discoveries that are revealing the large variety and extraordinary complexity of exoplanetary systems. Hardly a week goes by without a new "record" being set (*e.g.* the biggest or the smallest, water/CO in their atmospheres etc) and this in turn is fuelling an immense public interest in exoplanets in particular and astronomy in general. As the study of exoplanets is a new area of activity, it is to be expected that the research proceeds through a phase of discovery and this, in turn, is important as the exoplanet parameter

space is mapped out. For example, we have found gas giants of the same mass with more than a factor of two variation in radii, planets evaporating their atmospheres in gigantic clouds surrounding them, as well as a number of very large planets orbiting low-mass, cool stars. Each of these discoveries tells us about new and fundamental properties of planets that can help constrain models of their formation etc.

Essentially every new facility being contemplated for astronomy today has to address the issue of exoplanets. The very large ground-based telescopes in the 30 – 40m class, currently being planned all have aspects of exoplanet research as one of their main science drivers. This reflects the perceived importance given to the field by all parts of the astronomical community. Therefore, the next 15-20 years will see significant resources being made available on the ground. Nonetheless ground based resources will be challenged by limitations arising from the Earth's rotation and atmosphere, so that progress in key areas will be limited: in order to address the *direct* study of Earth-like exoplanets, instruments need to be deployed in space.

It is clear that the ground- and space-based assets will complement each other depending on the physical parameter one wishes to measure. Two pioneering missions have already been launched. CoRoT, developed by the French space agency CNES with the active partnership of ESA, Austria, Belgium, Brazil, Germany and Spain has already had its first successes (see above) with the detection of the first characterized 'super-Earth' rocky planet. This object is the first planet outside our Solar System that has been demonstrated to have an average density very similar to the one of the terrestrial planets in the Solar System. Having today discovered more than 26 confirmed planets, and having so far detected about 200 exoplanetary candidates, there is no doubt that CoRoT will make more discoveries over the next few years (Auvergne et al., 2009).

NASA's *Kepler* mission is following in the European footsteps. Already, more than a thousand transiting candidate planets have been reported by this mission, a handful of which have been confirmed as true exoplanets. *Kepler* has a much larger field of view than the CoRoT satellite (about 110 deg^2 as compared to 1 deg^2). Further, it is monitoring the same field (containing about 150 000 stars) for at least 3.5 years (and probably much longer), while CoRoT switches fields every 6 months (and actually have by now observed a similar number of stars). With its 3 times larger aperture, and using an integration time of 30 minutes the sensitivity of *Kepler* is also much larger, as well as being more sensitive for planets with longer periods than CoRoT (Borucki et al., 2010). Kepler has so far found an increasing frequency of small planets inline with some model predictions, and, somewhat surprisingly, a large population of transiting multiple planet systems (Latham et al., 2011).

It is possible that over the next few years either CoRoT or *Kepler* will find an earth-sized transit from a planet at a period corresponding to within the habitable zone of its host star. However, as the majority of survey stars are so faint that radial velocity confirmation and mass determination, especially for small planets is almost impossible. For example, for an average *Kepler* sample star a consideration of stellar noise suggests that an 80m telescope is needed for confirmation (and this would require multiple epochs each lasting several hours). Other kinds of characterisation such as atmospheric analysis would be equally challenging.

It is clear that if we are to make real progress in the study of exoplanets a next generation mission is needed. Such a mission should allow us to collect precise and reliable information on the distribution of exoplanets, including, most importantly, planetary radii (required for any type of comparative planetology and thus bringing other sciences into the field), orbits, masses and ages. The PLATO mission will provide such information. The targets will consist of a significant portion of the brightest - and nearest - stars in the sky (about 50% of the surface of the sky will be observed). It will also provide a target list for complementary observations of all aspects of exoplanetology and stellar physics.

By using a lot of relatively small, very wide-angle, telescopes and adding the signal from these, PLATO will be observing a sizable (in a nominal mission 40-50% of the sky) fraction of all bright stars in the sky simultaneous for year-long periods at a time. While solar type stars in the primary sample will generally be in the 4-11^{th} magnitude range (significantly brighter than the samples of CoRoT and *Kepler*), PLATO will also survey a sample of fainter M-dwarf stars. This will allow the collected ensemble of ground- and space-based auxiliary instrumentation to be brought to bear on any target discovered to have a transiting companion planet. The sensitivity of PLATO will be so high for solar-like stars that – from the same light curve as the transit will be studied – the astroseismologic power spectrum will be obtained with unprecedented precision. From this we will learn the structure of the interior of the star, its age, and thereby the history of the complete system. This will allow researchers from diverse areas of stellar research to unite to be able to accurately describe other solar systems and compare them with our own. For the first time, we

will have access to both the sizes as well as the orbital periods of planets representative for what we find in the inner Solar System. PLATO will transform our knowledge of this subject through its survey of habitable zone planets from late type stars.

This is the key synergy in the PLATO observations. Simultaneous observations of the transiting light curve which provides the planetary parameters in terms of the stellar parameters, and the astroseismologic observations of the host star which determines these same stellar parameters will become available for a large number of systems. Adding together the available Gaia data as well as the ground based supporting observations a much more complete picture of stellar and planetary physics and evolution will become possible.

Simulations, as well as experience with the ground based, Kepler and CoRoT data, demonstrate (see section 6.5 and especially Fig. 6.5 for details) that PLATO, during the nominal mission, will observe and fully characterise many thousands of planets with masses between 1 and 20 earth masses, and with a precision approaching 1% in mass and radius, while determining their ages to within 250 million years. Of these between 50 and 100 are expected to be Earth-sized planets in their host stars habitable zone. More candidates will have to await confirmation and follow-up later. Tens of thousands of (larger) planets will be discovered and characterised to a lower precision (5% - 10% on radius and mass) around fainter stars than the primary sample.

This will not be the end of this exciting field but only a very strong beginning. Based on the PLATO results, the design of future missions aimed at the detailed, direct study of individual, Earth-sized planets will be possible. Such missions could range from using again the transit method but this time in order to register spectral information (suggested as a scientific objective for the James Webb Space Telescope in the case of large samples of nearby red-dwarf stars with transiting planets). The direct study of exoplanetary surfaces will require much larger instruments of the next generation like interferometers or large coronagraphs but these instruments will also build on the work of PLATO which will have to find suitable objects before the larger instruments will be actively contemplated.

The simultaneous observation of exoplanetary and stellar parameters will provide an understanding of the formation and evolution of systems and give us a better understanding of how our own solar system formed and has evolved. PLATO will therefore bring in a new era in exoplanetology. Using stellar seismology as an active tool and thereby forging the star-planet connection will enhance our knowledge, not only about exoplanets, but also about ourselves.

At the same time, PLATO will bring in a new era in stellar physics. Together with the data coming from ESA's Gaia mission, the observations of the micro-variability of all classes of stars, carried out by PLATO will change the face of stellar physics and finally let us understand in Arthur Eddington's words "something as simple as a star". The first data acquired by the CoRoT and *Kepler* missions have clearly demonstrated that it is possible to measure accurately diameters, masses and luminosities of any kind of star. While this is now carried out for tens and hundreds of stars, PLATO will do it for hundreds of thousands of stars. The understanding of stellar objects at this level of precision will also impact many other important branches of astrophysics. Given the results from these space mission and the ground based searches, the one thing we should expect from such a transformational mission such as PLATO is to expect the unexpected!

2.2 Detailed science objectives

While building on the heritage from CoRoT and *Kepler*, the major breakthrough to be achieved by PLATO will therefore come from its strong focus on bright targets, typically with $m_V \leq 11$. The PLATO targets will also include a large number of *very bright and nearby stars*, with $m_V \leq 8$, as well as a large sample of cool M dwarfs down to $m_V \sim 15$-16.

The objective of PLATO is to detect and characterise a sample of extra solar planets sufficiently large and with a photometric accuracy precise enough that the data can be used to:

- Build a statistically significant sample of planets down to Earth-size orbiting main sequence F-, G-, K-type (Solar Type) and M-stars in their habitable zone

- Determine, through asteroseismology, the radius and mass of both the parent star and the planet(s) orbiting it with an accuracy of a couple of percent, and derive the age of the systems to an accuracy better than 10% in order to discriminate between different models of planetary structure.
- Derive a planetary mass function extending from Brown Dwarfs down to planets smaller than the Earth.
- Allow the selection of a sample of bright and nearby systems for further studies with ambitious facilities such as JWST, the E-ELT or future spectroscopy missions and provide reliable statistics for the occurrences of earth-like planets in the solar neighbourhood.
- Determine if bulk properties of planets (and their formation) depend on the stellar environment.

The above objectives are achieved by collecting long, uninterrupted, ultra-high precision photometric light-curves of a sample of >20,000 relatively bright stars ($m_V \leq 11$) observed for 2-3 years, and up to 90,000 such bright stars in total (including the step-and-stare phase). The same light-curves will be used for detecting exoplanets via transits and characterising their host star by asteroseismology. Furthermore, exoplanet detection down to Earth-sized planets is possible for stars with $m_V \leq 13$, and up to 1,000,000 of such stars will be monitored with PLATO thanks to its wide field-of-view over the mission lifetime (see chapter 6).

In addition to the seismic analysis of planet hosting stars, which is a key tool to reach the mission objectives, asteroseismology of the many other stars present in the field of view will be used to study stellar evolution. Light curves of stars of all masses and ages across the HR diagram, including members of several open clusters and old Population II stars, will be collected for this purpose.

Besides the core programme, PLATO will allow a broad range of studies involving photometric variability. Its high signal to noise, long time coverage and very large field-of-view will enable the study of variability on several time scales – between 1 minute and several years – on statistically significant stellar samples. These properties will be used to address many different questions, mainly (but not exclusively) in the area of stellar physics.

2.3 Planet Statistics: From hot-Jupiters to cool Earths

The discovery of extra-solar planets orbiting solar-type stars has been one of the major astronomical breakthroughs of the past 15 years (Mayor & Queloz, 1995; Marcy & Butler, 1996; Butler & Marcy, 1996). The regularly increasing number of known extra-solar planets is lending some confidence to observed features in statistical distributions of the planet and primary star properties. These features are thought to keep fossil traces of the processes active during the formation of the system and help constrain the planet formation models. We have learned that planets are common, especially those of lower-mass, and that Nature is able to produce a surprising variety of configurations. Understanding the physical reasons for such wide variations in outcomes remains a central issue in planet-formation and evolution theory, especially in the context of the determination of the conditions for the development of life. Our understanding of the Solar System formation and evolution will also be hugely improved by a better knowledge of exoplanet systems. Building on the expertise accumulated over the past decade from ground-based and space observations, and from progress of theory, PLATO will provide fundamental knowledge toward the detection and characterization of planets similar to our own.

2.3.1 Ground based detection

Spectroscopic surveys:

The spectroscopic results have continued to push towards longer periods and/or lower mass planets. The past few years have, however, seen a breakthrough in the field of extra-solar planets with the detections of light (2-20 M_{Earth}), solid (rocky/icy) planets around solar-type stars (*e.g.* Lovis et al. 2006, Bouchy et al. 2009, Mayor et al. 2009b) and M dwarfs (Bonfils et al. 2007, Udry et al. 2007, Mayor et al. 2009a).

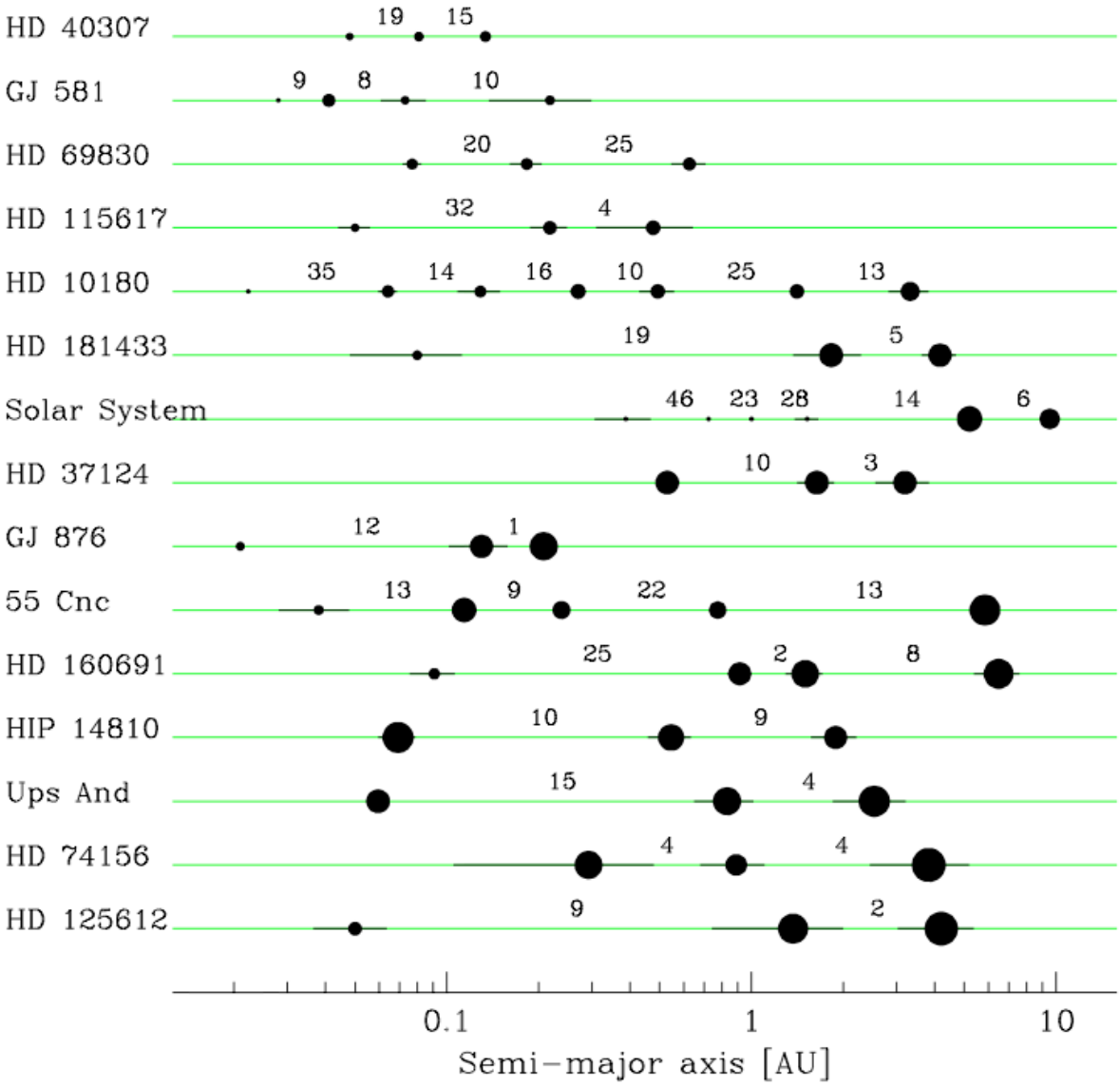

Figure 2.1: Close "packing" of super-Earth planets from radial velocity surveys (Lovis and Fischer, 2010)

Results from radial velocity programs suggest that the already published discoveries only represent the tip of the iceberg and that a new population of Neptune-mass and super-Earth planets is present. In particular, a recent census of planetary candidates among stars of the HARPS-GTO "high-precision" subprogram revealed that more than 40% of solar-type stars host low-mass planets (Udry et al. 2009), among which are about 30 ± 10% of close-in ice giants and super-Earths (Lovis et al. 2008, Mayor et al. 2009a). The existence of a large population of super-Earths is supported by discoveries of similar objects at larger separations using the microlensing technique (*e.g.* Beaulieu et al. 2006, Bennett et al. 2008). Planet-search surveys are now building up a detailed and unbiased view of objects with masses in the range of super-Earths and Neptune.

Of equal interest has been the realisation that multi-planet systems are common. Indeed the closer a system is examined we find, it seems, planets at all distances from their host stars. The Lovis and Fisher (2010) results demonstrate this in a graphical way (Figure 2.1). There is much to be learned from these systems and they will heavily constrain formation models.

One of the milestones for all planet detection surveys is to find a terrestrial planet in its host's habitable zone. Climate modelling of Gliese 581d, a super-Earth near the outer edge of the habitable zone, showed that this planet can provide habitable conditions if a few bar of CO_2 atmosphere is assumed (Selsis et al. 2007, v. Paris et al. 2010, Wordsworth et al. 2010, Hu and Ding 2011, Kaltenegger et al. 2011), making it a first candidate for habitability in certain conditions. It seems likely that the first Super-Earth planet firmly in the

habitable zone around M dwarfs will be discovered by radial velocity in the next few years. The detection of an Earth sized planet with an M-dwarf host will remain extremely challenging from the ground while their detection around solar-like stars will remain possible only from space and thus the province of PLATO.

Transit surveys:

Since the first exoplanet transit was detected in 1999, the numbers of objects known has been steadily increasing. Often using novel equipment, ground based discovery surveys were initially slow to find new objects as their data were often dominated by systematic noise. More recently these limitations have been better understood and transit surveys have started to realise their promise. The importance of the transit cannot be under estimated – the planetary orbit is tightly constrained by the transit geometry which allows the motion of the planet to be well understood and planetary mass precisely determined without the *sin* i uncertainty in the radial-velocity follow-up observations. Of equal importance its fractional size relative to the star can be accurately derived from the transit signal. In principle, the parameters (*e.g.* bulk density) that describe an individual planet can be determined with some accuracy and compared to theoretical models.

Over the last few years ground based transit surveys have produced around a hundred new detections almost entirely of large planets. The two dominant surveys are the SuperWASP project (57 planets) and HAT-NET (30 planets). These surveys have explored the parameter space of large planets finding the largest, most massive, retrograde orbits, shortest period etc.

Some of the most significant results have been the realisation that

1) planetary diversity is extremely important – planets of the same radius can have vastly different masses and hence densities,
2) while migration mechanisms are commonly assumed to have caused the population of hot Jupiters, at least a significant proportion of these objects (maybe the majority?) arrived in their present locations through scattering mechanisms.

Clearly, there is much still to learn about even the simplest and largest planets.

More recently ground-based techniques have pushed the extremes of planet detections. For example, WASP-33b was the first transiting planet detected orbiting a young A-type star and was confirmed through sophisticated tomographic techniques (detecting the planetary silhouette moving over the stellar surface during a transit with Doppler imaging).

Ground based transit surveys have struggled to find planets of Neptune size or smaller most probably because of limitations caused by the Earth's atmosphere and other systematic noise sources. However, with the realization that rocky planets may well be plentiful around M-dwarf stars, a number of ground-based surveys have started regular monitoring of a significant number of these objects such as *e.g.* the M-Earth Project (Irwin et al. 2008) with the expectation that around these small stars, super-Earth (or smaller) planets should be detectable. Given the low luminosity of the star, the habitable zones in these objects are close in, and it is likely that ground-based surveys could well be able to detect planets in these regions within a few years. GJ1214b was M-Earth's first success (Charbonneau et al. 2009) and there are likely to be a small number of additional successes. GJ1214b seems to have an extraordinary low bulk density and this has been interpreted as indications of a thick extended atmosphere. The faintness of typical M-dwarf host stars will make detailed characterization follow-up extremely challenging, even with the future giant telescopes or with JWST.

Other surveys (*e.g.* UKIRT/VISTA ROPACS) are also targeting field M dwarfs (i.e. not a specific object targeted survey), but have, so far, failed to find any planets. These deep surveys suffer from narrow fields of view and small numbers of targets (and thus need significant quantities of large telescope time).

There are several second-generation ground-based surveys currently being deployed or in planning. HAT-S is a multisite survey based on the HAT-N and has recently entered into operation. NGTS (http://www.ngtransits.org/index.shtml) is a development of the successful SuperWASP project and will be constructed at ESO's VLT site at Paranal over the next few years. Both surveys are targeting cool dwarfs.

Direct Imaging:

The first confirmed images of an exoplanet were obtained in 2004/5 with the VLT of the brown dwarf 2M1207 (Chauvin et al. 2004). Observations of more typical systems followed with planetary detections around the main sequence stars Beta Pictoris, Fomalhaut and HR8799 (Lagrange et al. 2010, Kalas et al. 2005, Marois et al. 2008), and several others have since followed. Given the difficulties in obtaining these data it is likely that even as new instrumentation becomes available, only massive cold or young very planets will be feasible targets. However, few other detection methods are sensitive to these objects and so direct imaging will complement spectroscopic and transit detections.

2.3.2 Space based detection

In order to detect small or long period transiting planets there is *no-option* but to collect data from space. Removing the restrictions imposed by the turbulence of the Earth's atmosphere enables photometry of sufficient quality to detect transit signatures from low signal-to-noise events. However, other noise sources such as some types of stellar activity begin to manifest themselves at these levels that can complicate detection (or indeed confirmation). While satellites such as HST have been used to conduct transiting surveys their limited fields of view (amongst other reasons) mean that they have in general been used to study previously known planets. In some cases they have been used to detect transits from planets found by spectroscopy such as the important recent announcement of the transiting super-Earth 55 Cnc e with the MOST satellite (Winn et al. 2011b) and (warm) Spitzer (Demory et al. 2011). CoRoT and *Kepler* are two missions that were designed from the outset for transit surveys.

CoRoT:

CoRoT was the first satellite mission dedicated to transit detection. With an aperture of 27cm and accessible field of view of ~37 square degrees the satellite sees few bright stars but instead has a brightness distribution of around 11-15th magnitude. CoRoT has detected some 200 exoplanet candidates and has announced 26 new planets. While some of these are relatively long period probably the most interesting object is CoRoT-7b (Fig. 2.2) with $R\sim1.6R_E$, $M\sim4\text{-}6M_E$ *and* orbital period 0.87 days. In this case the faintness of the host star, *V~11.7*, and its mild activity have made its mass determination difficult. CoRoT-7b was the first super-Earth planet discovered with a measured radius and density (Léger et al. 2009, Queloz et al. 2009).

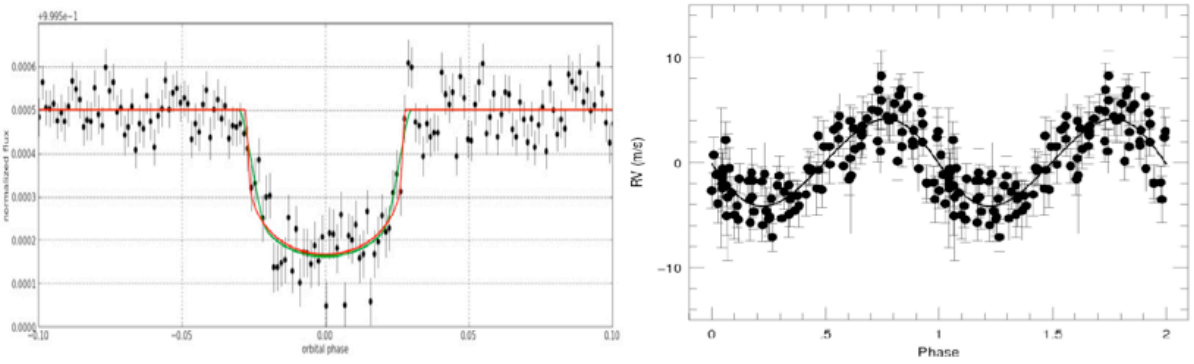

Figure 2.2: CoRoT-7b light curve (Léger et al. 2009) and radial velocity curve (Queloz et al. 2009). The faintness of the star and its activity level made the velocity determination problematic and extremely time consuming.

Kepler:

Kepler is a modified 0.95m telescope with a field of view of 116 square degrees. In general stars in the range ~10.5-15 magnitudes are targets for transit search (there are of course very few at the bright magnitude end and hence the bulk of its 150,000 main sequence stars >13th magnitude). As noted in chapter 5, confirmation of terrestrial planets at these brightness levels and *for any period* is challenging at best, and consequently nearly all earth-sized *Kepler* candidates are not confirmable via radial velocity measurements as bona fide planets. However, *Kepler* will lead to a far better understanding of the statistical size distribution of exoplanets (and not mass distribution), when assuming that most candidates are indeed planets. Nevertheless *Kepler* has made some extremely important discoveries:

1) As predicted from the population synthesis simulation the population is dominated by small (and presumably) low mass planets. Borucki et al. (2011) presented an analysis of the first 4 months of data and found about 1000 stars exhibit transit like events. Of these ~5% are of earth size, ~7% super-Earth and ~19% Neptune sized planets. Borucki et al. (2011) find 54 planets that appear to be orbiting in the habitable zones of their host stars. Borucki et al. (2011) show (see Figure 2.3) that the observed peak in the size distribution is at a maximum at 2-3 Earth radii and then declines at a rate inversely proportional to the area of the candidate. They warn that biases and errors at the smallest radii are not well understood and that these results should be seen as preliminary. This is similar to the results hinted at from the ground-based radial velocity surveys.

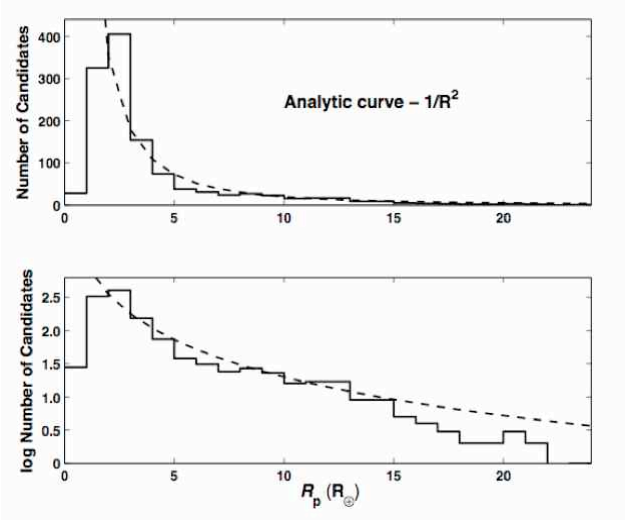

Figure 2.3: Distribution of candidate planetary radii from Kepler data (Borucki et al. 2011)

2) Multiple systems. This is a most remarkable result with ~33% of detected candidates found in multiple systems (17% of detected systems). While most have two planets a small number have >4 planets and indicate that these systems are flatter to <1 degree (a result quite at odds with our solar system). In some of these cases transit timing variations can be used to weakly constrain masses. The best example of this is Kepler-9b/c which is a double Saturn mass system (periods 18 and 37 days) and with probably a close in lower mass planet. The two gas-giants exhibits transit timing variations of several minutes. The most extreme multi-planet transiting system is Kepler-11 with 6 distinct planetary bodies.

3) While there are many small eclipses from *Kepler* candidates only Kepler-10b has been verified as a planet with an orbital period of 0.84 days (Batalha et al. 2011a). With $R \sim 1.4 R_E$ and $M \sim 4.6 M_E$ it is comparable to CoRoT-7b and must be a dense, rocky planet ($\rho \sim 8.8$ g cm^{-3}). At $V \sim 10.9$ the host star is one of the brightest in the *Kepler* survey and has been observed with the 10m Keck Telescope.

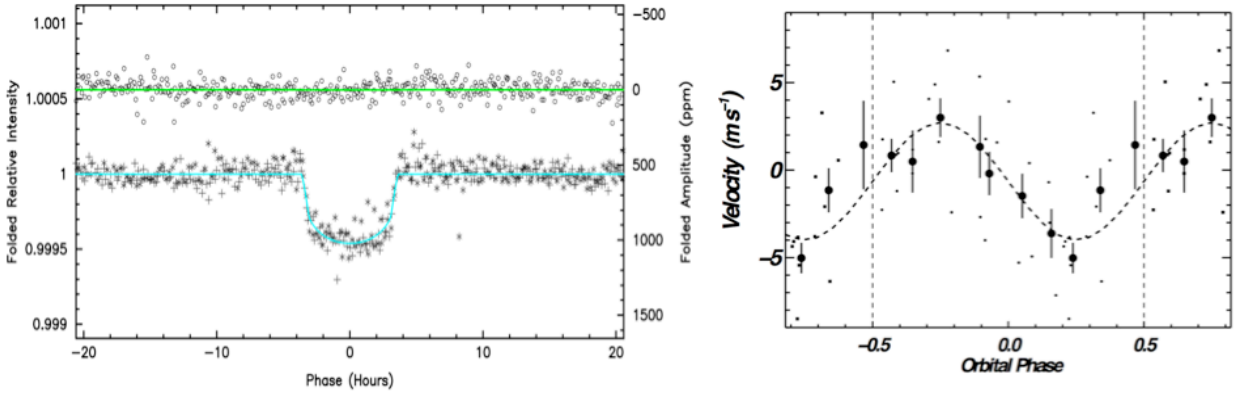

Figure 2.4: Kepler photometry and Keck spectroscopy of Kepler-10b (Batalha et al. 2011). The small points in the right hand panel are the individual observations and the larger points with error bars (derived from the spread in individual points) are binned. At V~10.9 this is at the limit of ground based capabilities. It is also worth noting that Kepler-10 is not an active star.

Figure 2.4 shows the Kepler-10 light and radial velocity curves and demonstrate that while the host star, Kepler-10, is not an active star, even at this brightness the mass determination is problematic. Statistically, *Kepler* will be fortunate to detect a single confirmable Earth-analogue system.

2.3.3 Conclusions from space based activities

The *Kepler* and ground based radial velocity surveys demonstrate that small, low mass planets are numerous. Currently, we know of only 4 terrestrial sized planets, CoRoT-7b, *Kepler*-10b, 55Cnce and GJ1214b – all are extremely short period solid bodies. Already we are seeing great diversity in their properties and hence a planetary mass cannot be inferred from their measured fractional radii. This is similar to the situation found for the giant planets, so maybe it should not be seen as too surprising. However it does imply that spectroscopy will be extremely important to understand the nature of planets.

The present observational findings on super-Earths both from the radial velocity and *Kepler* surveys are also in good agreement with the results of population synthesis models based on the core accretion paradigm for planet formation (Ida and Lin 2004, 2005, Alibert et al. 2004, 2005, Mordasini et al. 2009). These models predict the existence of a large number of low-mass objects with a distribution steeply increasing towards the lower masses, up to an overwhelming proportion of Earth-mass planets. The sharp rise of the number of planets predicted by the simulations below a few Earth masses is still out of the present instrumental sensitivity of radial velocity surveys, but, if real, will provide a fantastic reservoir of candidates to be detected by space transit missions like PLATO.

In addition to predicting a large number of Earth-size planets, interesting ideas, linked to population synthesis models, postulate differences in the internal composition of super-Earths, depending on their formation and evolution history: refractory elements in *born-again embryos* giving birth to a super-Earth through the perturbation of a forming giant planet, or volatile element content for failed cores (Ida and Lin, 2010). Precise measurements of the planet radii are needed to discriminate between these different cases.

While multiple planets are reasonably common within the radial velocity surveys, the large proportion found within the *Kepler* survey is somewhat surprising (it is worth remembering here that the radial velocity surveys are selecting a different host population to *Kepler* – the radial velocity survey have more massive planets and potentially longer periods). Latham et al. (2011) show that systems with short period gas giants are much less likely to have multiple transiting planets and suggest that a migrating massive planet would stir up or disrupt any internal super-Earth planets. Latham et al (2011) suggest that this may explain the population of large planets not orbiting in the host star's equatorial plane. An interesting question to pose is how have the multiple *Kepler* systems remained so flat?

2.3.4 Planet detection with PLATO

Transit search: Wide-field, long, continuous and high-precision photometric monitoring

Photometric transit. As already mentioned, because of the nature of the method, only the orbital parameters and a lower limit on the planet mass is known from radial velocity measurements alone. Much tighter constraints for planet models are obtained by the observations of a photometric transit of the planet in front of its parent star. Combined with radial velocity measurements such observations yield the exact mass, radius and mean density of the transiting planet, providing priceless constraints for the planet internal structure, as well as for the planet-evolution history.

Planetary transits can be detected through high precision photometric monitoring. A planetary transit in front of a star causes a decrease of the photometric signal

$$\Delta F = \left(\frac{R_p}{R_*} \right)^2$$

where R_p and R_* are the radius of the planet and of the star, respectively. The duration of a transit is given by:

$$d \approx \frac{P R_*}{\pi a} \sqrt{\left(1 + \frac{R_p}{R_*}\right)^2 - \left(\frac{a \cos i}{R_*}\right)^2} \qquad (2.3.1)$$

For a star like the Sun, the typical relative variations are $\Delta F = 10^{-4}$ with 13 hours duration for 1AU orbits for Earth-size planets, and $\Delta F = 10^{-2}$ for Jupiter-size bodies. Observations of recurring planetary transits can be used to measure the orbital period *P* and therefore the semi-major axis of the orbit, by applying Kepler's third law. In combination with the radial velocity method, the true mass and therefore the planet mean density can be derived.

Giant gaseous planets. Presently, more than 110 such systems are known, with only a handful of them transiting bright stars. They are the most interesting targets for complementary follow-up ground-based or space observations. Remarkably, more than 90 or so currently known transiting planets have been found in the past couple of years. Thus, in 2008, for the first time, the transit method was equally successful as the radial velocity technique. Most of the detected transiting planets have been found by novel, wide-angle ground-based facilities targeting bright stars such as WASP, HAT, TrES and XO projects (Pollacco et al. 2006, Bakos et al. 2004, Alonso et al. 2007, McCullough et al. 2005). Atmospheric limitations make the detection of small planets around solar type stars particularly challenging. Consequently, most known transiting planets have masses and radii comparable to Jupiter but with vastly shorter orbital periods.

Low mass planets. On the low-mass end of the distribution, the detection of transiting Neptunes and super-Earths will provide fundamental information to constrain the inner composition of these planets such as *e.g.* the relative fraction in mass between the iron core, the mantle or the atmosphere of the planet, or the fraction of water/icy among solids. Even if degeneracy problems exist and no unique solution is expected, basic estimates on the chemical species present in the planet could allow at least partially solving the problem. For example, an extended atmosphere will have a major effect on the radius and it should be possible, directly from the observations, to separate planets with thin and thick atmospheres. This is an important point related to the planet's habitability. While *Kepler* has already demonstrated it is sensitive to these objects, their host star brightness will, in the vast majority of cases, preclude confirmation and detailed investigation even once HARPS-North becomes available. Currently (even including *Kepler's* results) only a handful of confirmed transiting hot-Neptunes are known, however, the *Kepler* results demonstrate that ~19% of all transiting planets are of this class.

The prime goal for PLATO, of course, will be the lowest mass planets. In this area none of the other missions are competitive as confirmation will only be possible with bright host stars. The Queloz et al. (2009) and Batalha et al. (2011a) results for the super-Earths CoRoT-7b and Kepler-10b respectively, demonstrate the difficulties involved. These stars are amongst the brightest in the CoRoT and *Kepler* surveys and have proved extremely challenging (despite their periods being <1 day) even for confirmation let alone more detailed observations (e.g. atmospheric studies). Nonetheless the detection of these objects shows that this is possible and that the brightest targets are needed.

Necessity of long monitoring. Observations of transiting planets at large orbital periods are rare due to the decreasing geometrical transit probability ($P_t \propto P^{-2/3}$). A recent highlight is the observation of the primary transit of the 111-day-period Jupiter-like planet HD80606 b (Moutou et al. 2009, Fossey et al. 2009), previously detected by radial velocity observations (Naef et al. 2001). Although many more planets are known from radial velocity detections, the parameters range is not well sampled for planets with known primary parameters, especially towards long periods or/and small masses, and that long-lived continuous monitoring of bright stars are required to completely characterize planets on wider orbits. The significant bias in the observations toward larger planets, and more importantly the difficulty to confirm the transit candidates with ground-based follow-up for the faint CoRoT and *Kepler* targets, is likely to preclude any rapid firm conclusion on this issue. In the future, we expect more such detections of giant planets on long-period orbits as radial velocity surveys are extended and *Kepler* results are followed up. However, small planets in long period orbits will remain extremely difficult for either CoRoT or *Kepler* with the smallest objects being only accessible to PLATO.

We clearly need a new set of observations offering a relatively unbiased insight into the distribution of exoplanets in the (radius, semi-major axis) parameter space, down to Earth size planets, and up to at least 1 AU. The main thrust in future exoplanet research will be the detection and characterization of Earth-like planets within the habitable zone of Solar-like stars *i.e.* surveying true Earth analogue systems. These observations will be extremely challenging and can only be done from a space-based platform.

The impact on transit detection with PLATO

The impact of PLATO on exoplanet science will be directly related to the number of exoplanets that can be detected and fully characterized, and to the coverage of the planet parameter space (orbit, radius, mass) achievable by the mission. The key asset of PLATO in this respect will be the brightness of its target stars, which will be bright enough to enable an asteroseismic analysis to determine the star's mass and age, as well as for a fast and efficient radial velocity follow-up from the ground.

In this respect, we note that PLATO will provide a far better coverage of planet parameter space than *Kepler*, thanks to its extended surveyed area and to the brightness of its targets. *Kepler* will monitor up to 150,000 stars down to m_V = 14.5, for at least 3.5 years, in a field of about 116 deg^2. Many transit candidates have been discovered, including many Earth-sized planets. However, most of these transit candidates will be orbiting faint stars with m_V = 13.5-14.5, which represent the majority of the surveyed sample. The radial velocity follow-up of these transit candidates will be very difficult to perform, even impossible in most cases. Similarly, seismic analysis will be possible on only a handful of the host stars of the detected planets, although a substantial asteroseismic programme exists on *Kepler*.

While radial velocity follow-up of giant planets detected by *Kepler* can be performed with available facilities, such as the HIRES spectrograph on the Keck telescope, for small planet candidates, *Kepler* will have to rely on HARPS-North, which will not be on the sky before 2012, and even then, will provide radial velocity follow-up capabilities for small planets only for the few brightest stars in the *Kepler* sample.

On the contrary, PLATO thanks to its extended surveyed area (Fig. 2.5), will concentrate on bright stars (m_V < 11), and therefore will not suffer from the same limitations. It will also benefit from improved radial velocity performances of instruments in the Southern hemisphere, such as ESPRESSO on the VLT, and later CODEX on the E-ELT. A detailed estimate on the expected number of planets that can be characterized for their radius and mass by PLATO is given in chapter 6. In Fig. 6.2 a comparison of the expected performance for Kepler and PLATO is shown, including spectroscopic ground-based follow-up capabilities to determine planet masses down to Earth mass. Due to its target brightness PLATO will in particular be able to fill the parameter space of low mass and distant planets which is difficult to access with the Kepler mission.

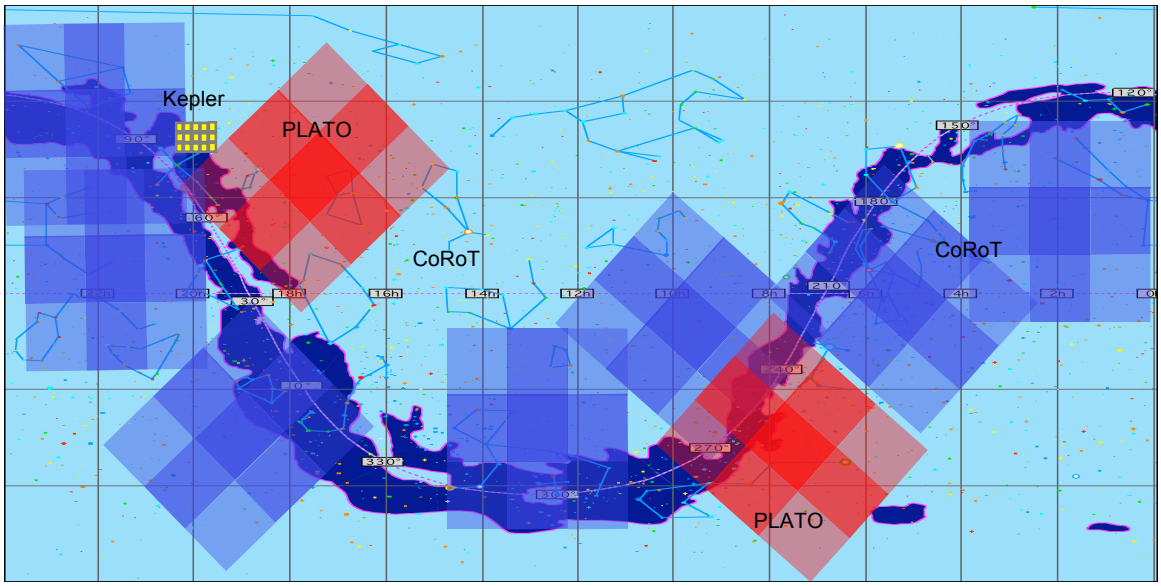

Figure 2.5: Schematic of the coverage of the sky by PLATO. Red indicate long pointings, blue the step-and-stare phase covering a large part of the sky. For comparison, the positions of the CoRoT and Kepler fields are shown.

Only PLATO with its extended surveyed area and its main focus on bright cool dwarfs will allow us to reach real Earth analogue systems and extend the search for exoplanets to small terrestrial planets in the habitable zone of their stars.

The impact of PLATO via other detection methods

Transit timing variations: Planetary transits can be studied further to search for variations in the mid-transit times caused by gravitational distortions due to additional planets in the system or moons around the planet

("transit timing variation" analysis). The usefulness of this as a means to constrain masses of planets that are otherwise too faint for radial velocity determination has been well demonstrated by *Kepler,* indeed for this mission timing variations may be the most useful way of estimating masses as in the faint *Kepler*-11 six planet system. However, for low mass planets masses derived by this method are not sufficiently accurate to be useful, in general, for obtaining bulk properties (except where the models are least degenerate).

Transit timing variations are particularly sensitive to planets in resonance orbits and can even be used to detect Trojan asteroids (1:1 resonance), which can be stable up to the mass range of the Super-Earths within the orbit of a Jupiter planet. The photometric precision of PLATO will allow the detection of perturbations with amplitude of a few seconds, which is a performance at least two times better than *Kepler* and four times better than CoRoT. Taken together with the larger number of objects, this should lead to new information.

Other types of timing techniques can also be used. For example, for sdO stars their pulsations can be used to infer the presence of planetary companions, eclipse timing in eclipsing binaries etc.

Astrometric detection of planets: The stellar reflex motion induced by a planet's revolution creates an astrometric wobble, which can be expressed as:

$$w = 3\frac{a}{d}\frac{m_{pl}}{M_{star}}$$

where w is the amplitude of the astrometric wobble in μas, a is the semi-major axis of the exoplanet orbit in AU, m_{Pl} and M_* the mass of the planet and its star (expressed in $m_{\rm Earth}$ and $M_{\rm Sun}$ respectively), and d the distance to the exoplanetary system in pc. Thus a 1 $M_{\rm J}$ exoplanet, orbiting a 1 $M_{\rm Sun}$ star at 1 AU, placed at 15 pc, so that the star has m_V = ~6, would induce a 60 μas wobble. PLATO will measure the astrometric position of each star in the surveyed field relative to all other stars in the field, which will provide a very precise reference frame. Preliminary simulations have shown that indeed relative centroid measurements are photon noise limited with negligible residual jitter noise. In this case, precisions of about 10 μas will be achieved down to m_V = 6 after one month of integration. This will be sufficient to detect all giant exoplanets with orbits near 1 AU, orbiting nearby bright stars, irrespective of the inclination angle of the orbital plane with respect to the line of sight. These astrometric measurements, coupled with measurements of reflected stellar light described below, will constitute a powerful tool for identifying exoplanetary systems around nearby stars, out to distances of 15-20 pc, and therefore can help select targets for further follow-up observations, for instance in interferometry and coronagraphy.

Reflected stellar light: The high-precision photometry of PLATO will allow detecting non-transiting planets by the modulation of the flux in the light-curve. The fraction of reflected stellar light by a close-in giant exoplanet along its orbit, which depends linearly on its albedo A, is typically $F_p/F_* \sim 9.1\text{x}10^{-5}\ A$ for a Jupiter size planet orbiting at 0.05 AU from its host star. Because the monitoring of such targets will cover several hundred planetary orbital periods, such a modulation will be detectable by PLATO down to m_V = 9-10 for albedos as small as A = 0.3. High precision photometric monitoring will therefore allow us to detect giant exoplanets in close-in orbits around stars down to m_V = 9-10, even for large inclination angles, where transits are not visible. For *nearby stars* this could be an important discovery technique as it is mostly free from the geometric constraints required for transit occurrence and will produce important targets for direct observation with the ELT etc. For example, reflected light from the 1.49 $R_{\rm J}$ exoplanet CoRoT-1b, which is orbiting an m_V = 13.6 star, was detected (Snellen et al. 2009) at a level of about $1.26\text{x}10^{-4}$, using CoRoT data having a noise level of 200 ppm/hr (Barge et al. 2008). This pioneering result demonstrates that PLATO, reaching a noise level below 30 ppm/hr on stars down to m_V = 11, will be able to detect on its main targets reflected light signals at least 7 times weaker, which could correspond to planets 2.5 times smaller in radius or 2.5 times further out, assuming a similar albedo.

Very bright stars, typically with m_V = 6, will be observed with a noise level of approximately 10 ppm/hr. Such a low noise level will enable the detection of stellar reflected light on planets with 0.15 R_J radii. We will therefore be able to detect super-Earths in close-in orbits, without suffering from geometrical probability, and identify a large fraction of nearby stars hosting close-in planets, that will become privileged targets for further observations, including searching for smaller and further out planets.

In addition, the exquisite noise level in the light curves of these very bright targets will give the possibility to study details of the atmospheres of giant planets in close-in orbits, such as global weather patterns. This kind

of ultra-precise studies on very bright stars constitutes a unique possibility of PLATO targets that is out of reach for earlier missions like CoRoT and *Kepler*.

***Rings, moons and binary planets*:** Planetary rings and large moons can also be detected by their modification on the shape and duration of the transit light-curve. For example, for a Saturn-analogue at 1 AU from the parent star, the ingress and egress take one hour for the planet and two hours for the ring. In addition, the planet ingress (egress) starts (ends) steeper for the planet than for the ring. Finally, the projected inclination of the ring with respect to the planet's orbital plane and the ring optical depth can be derived from the transit shape, which provides valuable information for the formation and evolution studies of the system. Furthermore, we may expect discoveries of planet configurations not found in our own Solar System, like e.g. binary planets.

2.3.5 Future experiments in Exoplanetology and Astereoseismology

Spectroscopic developments e.g. laser-combs on instruments such as ESPRESSO/VLT, will mean that radial velocity measurements will continue to improve and hence these surveys will be able to detect lower mass and longer period planets. IR spectrographs such CARMENES/Calar Alto (Quirrenbach et al. 2010) and SPIRou/CFHT are also likely to become available in the 4-8 year time scale and these will attempt surveys of the brightest M dwarfs and could potentially be sensitive to small planets in the habitable zones of their hosts.

Several new ground based transit surveys are also being planned or are currently in commissioning. HAT-S has multi-longitude coverage (Chile, Namibia, and Australia) and has recently become operational. NGTS is in the construction phase and will be based at the VLT Paranal site in Chile. Both these surveys are designed to detect hot-Neptunes and possibly smaller planets. They are unlikely to be sensitive to orbits longer than about 10 days or so.

Other facilities that will come on-line in the near future are the SPHERE/VLT and GPI/Gemini. These are direct AO imaging instruments designed to explore the cold-Jupiter planet distribution.

Gas Giant planets may also be detected through their auroral emission at low frequencies. When the full LOFAR array is in operation surveys of nearby stars will be undertaken.

In space, Gaia is due for launch in 2012. The astrometric precision is likely to mean it is sensitive to large planets and possible super-Earths around the very nearest stars. A recent study on the planet detection potential of Gaia (Casertano et al. 2008) predicts several thousands of gas giant planets out to 3-4 AU for stars within 200 pc. Beyond this we are only aware of proposals such as TESS – a whole sky transiting planet experiment and Elektra, a similar proposal operating in the near infrared (neither of these are sensitive to long periods and thus not to objects in the habitable zone around solar type stars). Other satellites will of course be extremely useful (e.g. JWST) but will not be survey instruments.

2.4 Planetary system characterisation

With increasing statistics of extra-solar planets we have been surprised to find large diversity of planets and planetary systems, spanning a much wider range in parameter space than found in our own Solar System. We are close to being able to compare properties of large numbers of planetary systems (Comparative Planetology) in different environments and at different evolutionary stages, putting our solar system into a wider context for the first time.

The fundamental parameters radius, mass, density and orbit form the basis for the characterisation of planets, followed by further detailed information on, e.g. their atmospheric composition and the potential for development of a biosphere. Numerical models of planetary interiors are being developed to address key questions with regard to their internal structure, bulk composition, and thermo-chemical evolution. For exoplanets, such models are primarily constrained by their observed masses and radii. Inherent composition degeneracies can be reduced or even eliminated if cosmo-chemical arguments and specific environmental conditions are taken into account. Furthermore, knowledge of the axial moment-of-inertia and surface composition would help reduce principal model degeneracy. From a full statistical sample of planets with well determined fundamental parameters, it will be possible to obtain scaling laws for key physical and chemical properties that are essential to better understand the origin and evolution of planetary bodies

(EPRAT-Report, ESA). The detection of a significant number of small rocky transiting planets, which form the focus of PLATO, would be a major step forward to this emerging new field of comparative planetology.

However, despite more than 500 confirmed planets and more than one thousand published candidates, we are still far from a full statistical overview of planetary system diversity, in particular with respect to small and distant planets. *A major goal of the PLATO mission is to provide planetary systems that are well characterized for their prime parameters: planet mass, radius, mean density, orbit, and age of the system and parameters of the host stars.*

Planet and star masses. Radial velocity techniques provide only the mass function, and a good measurement of stellar mass is needed to derive the planetary mass. However, planetary model interior degeneracy problems require very precise determinations of the bulk parameters enabling the calculation of the ratio of heavy (iron, silicates...) and light (water, hydrogen...) elements in the planet's interior. In fact, one must determine the planetary radius to within 2% to clearly distinguish between different scenarios (Valencia et al. 2007, Seager et al. 2007, Grasset et al. 2009). Presently, stellar masses can be determined from their spectra and stellar evolution models with a precision of the order of 20%. *The asteroseismic analysis of the PLATO light curves will be able to provide 1-4% error in the stellar masses which will lead to an improvement of the precision of planetary masses of about one order of magnitude.*

Planet and star radii. Planets that are seen to transit their host star have tightly constrained orbital inclinations and the added benefit that the depth of the eclipse is directly related to the planet and star size, R_p / R_*. If the stellar mass and radius are accurately known the planetary bulk density can be estimated, allowing for a first classification of planets (e.g. gas giants, Neptune-like, terrestrial). By combining Gaia data and ground-based spectroscopy, *stellar radii can be derived to excellent accuracies, giving an overall improvement of more than a factor 3 in the accuracy of planet radii.*

Given this, it is not surprising that the detection of large numbers of transiting planets has become a major goal in recent years. As techniques improve and instrumentation increases in sensitivity, it is likely that there will be a gradual shift in focus towards detailed characterization of the brightest and most interesting planets. The mean planet density naturally depends on the planet mass and radius. *The above mentioned accuracy improvements will therefore lead to an improvement by a factor of 10 to 50 for planet densities.* This is extremely important to better constrain the planet internal structure.

Planet and star ages. Finally, the understanding of exoplanetary system evolution requires an estimate of their ages, which can only be determined by a measurement of the age of their central stars. For the next generation transit surveys, like PLATO, it is therefore crucial to take into account also an accurate determination of stellar parameters to better constrain the input for planetary system evolution modelling. *For the bright star sample, asteroseismology from PLATO light curves is able to indicate the age and mass of the star in an independent way and with higher precision than available with other methods* (see below for a more detailed description of the method).

One recent example is the determination of the density of the planet *Kepler*-10b (Batalha et al. 2011a), where asteroseismology played a crucial role in the analysis of the interior structure of the planet. Similar analyses on planet hosting stars have been successfully carried out by the CoRoT and *Kepler* missions (Gaulme et al. 2010, Christensen-Dalsgaard et al. 2010). The properties of a limited sample of bright stars have been determined with accuracies near the 2% limit for the radius and as good as 15% for the age (Metcalfe et al. 2010).

2.4.1 Radii and masses: Constraints on the interior composition of planets

The impact of PLATO concerning terrestrial and ice planets

Transit observations have led to some remarkable results. As explained earlier we have found almost a factor of two variations in the size of giant planets of similar masses (the cause of it is unexplained) and begun to study their internal structure through comparison of their bulk density with theoretical models. Although still based on small statistics, the situation seems to be similar for super-Earths, for which the *Kepler*, CoRoT and M-Earth candidates present fairly different radii (1.4, 1.7 and 2.7 R_E) despite estimates of their masses that

are not very different (4.6, 4.8 and 5.7M_E, respectively). This demonstrates once more the variety of possible outcomes from planet formation processes.

Fig. 2.6, left, shows the mean density versus the planet mass, indicating the large number of known gas giant planets, many of them with densities well below Saturn. Although the branch of ice and terrestrial planets is still little populated, we already see indications for a similarly wide range of planet parameters as observed for gas giants. The large diversity of densities observed for giant planets seems to be also the rule for super-Earths and ice planets. A main goal for PLATO is to populate the diagram at the lowest planet masses by taking advantage of its bright target stars that allow the derivation of masses from radial-velocity follow-up even for small terrestrial planets.

The situation is also evident in Fig. 2.6 right (Winn et al. 2011b) that shows the distribution of known super-Earths (planets between 1 and 10 Earth masses) in the mass/radius diagram. Over plotted lines correspond to different interior models and mean densities. There is a significant diversity of mean densities in a relatively reduced interval of masses, between the rocky planets CoRoT-7b, *Kepler*-10b, and 55 CnC e and the most likely icy-gaseous planets *Kepler*-11d, e, f.
Structural models of solid exoplanet interiors are constructed by using equations of state (EoS) for the radial density distribution, which are compliant with the thermodynamics of the high-pressure limit. Model calculations for different EoS and fixed bulk compositions indicate that difference in calculated planetary radii will be much smaller than typical measurement uncertainties from transit photometry (Wagner et al. 2011). Nevertheless, planetary mass and radius impose equally important constraints on model planets as massive as the Earth, whereas in the upper mass range structural models are chiefly constrained by precise determinations of planetary radius.

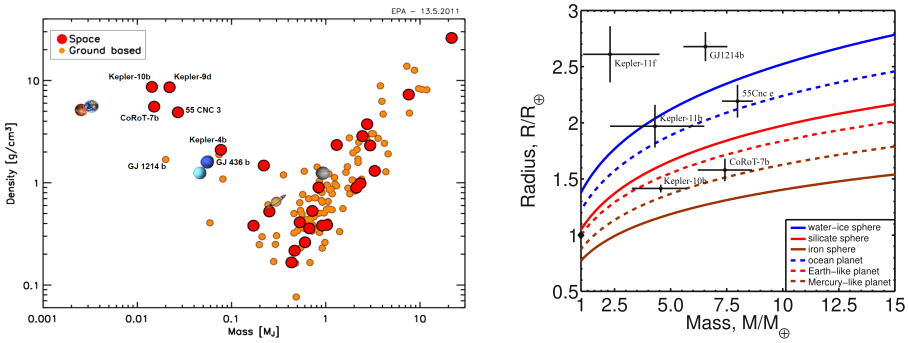

Figure 2.6: Left: Density of known transiting planets less than 30 Earth masses. Right: Calculated mass-radius relationships for terrestrial planets with different internal composition (Winn et al. 2011b). The right hand panel shows the mass-radius plot for earth and super-earth like planets. Included here is the six planet system where the model dependant masses have been derived through induced timing variations.

Indeed, Valencia et al. (2007) have shown that precisions better than ~5% in planetary radius and ~10% in planetary mass are needed to distinguish between bulk terrestrial planet properties, like ocean planets and dry rocky planets. *The data expected from PLATO, therefore, will allow us to derive high-precision mean planet densities and to constrain models of planet interiors, even for very small, terrestrial planets*. See section 5 for the estimated planet characterization performance.

The impact of PLATO concerning gas giants

Gas giants are crucial in understanding the history of planetary systems. Although the statistics of transiting gas giants is constantly increasing from existing surveys, there is still much to be learned from PLATO due to the brightness of its target stars. In our Solar System, Jupiter and Saturn's migration after their formation shaped the architecture of the whole system (Tsiganis et al. 2005, Walsh and Morbidelli 2011). Present uncertainties on the interior composition of these planets however provide a major hurdle for understanding the origin of the solar system (e.g. Guillot 2005). By greatly improving the accuracy of stellar and planetary parameters on a statistically significant ensemble of planets, and by discovering rare 'Rosetta stone' planets, Plato will provide constraints on the compositions of giant planets in general and will consequently shed a new light on the formation of planetary systems, including our own.

Determining compositions from a statistically significant sample of transiting gas giants: The composition of giant exoplanets is becoming accessible thanks to the discovery of tens of transiting exoplanets (Guillot et al. 2006, Burrows et al. 2007, Miller et al. 2011). However uncertainties are numerous: The fact that most transiting exoplanets are inflated compared to predictions (e.g. Guillot 2008, Laughlin et al. 2011) implies the existence of a missing physical mechanism affecting their evolution and preventing a reliable determination of their global composition. Similarly, planets around young, spotted stars pose particular problems that prevent a clear interpretation of their characteristics in terms of origins (Guillot and Havel 2011). The structure of brown dwarfs and M-dwarfs is also difficult to interpret, probably linked to our poor knowledge of their atmospheres (Burrows et al. 2011) or to magnetic interactions (Chabrier et al. 2007).

The most important asset of PLATO in this respect lies in the extremely significant increase in precision of the determination of the parameters of these systems. These are currently limited by our poor knowledge of stellar evolution models. Thanks to the possibility to perform asteroseismology on the target stars, the planets discovered by Plato around bright stars will have 3 times better radius determinations and 5 times better mass determinations. For this subset of planets, more accurate tests of the correlations between the various stellar and planetary parameters will be possible.

With this new extended and more accurate ensemble of transiting giant planets, PLATO will provide the basis to understand the contraction of giant planets and in particular determine what is the source of additional heating of close-in planets. It will provide clear constraints on the dependence between stellar and planetary metallicity. At this point, our lack of knowledge of the complexity of the problem prevents us from predicting in which area PLATO will bring the most significant advances. Some likely areas include the determination of the maximum mass of heavy elements accreted by massive planets and brown dwarfs, the determination of whether all giant planets have a small core, an accurate comparison of the compositions of giant planets around stars of various masses…etc.

Consequence of the accurate determination of the age of planetary systems: Because giant planets progressively cool and contract, an accurate determination of their age is crucial for a precise determination of their interior structure. Unfortunately, the age of stars is traditionally very poorly constrained (to with a few Gy for stars on the main sequence). Furthermore, young planets that are the most important in order to decipher the conditions in which planetary systems are formed, orbit around active stars and the determination of their parameters has remained at best elusive (see e.g. Gillon et al. 2010, Czelsa et al. 2009, Guillot and Havel 2011). With the possibility to distinguish pre-main sequence from main-sequence stars, and with relative age determined within 10%, PLATO will essentially remove the age ambiguity that severely hinders the interpretation of their sizes and determination of their composition. It will discover young transiting giant planets and provide a crucial determination of their age. This will help to understand whether processes such as tides (e.g. Ibgui et al. 2011) and giant impacts (e.g. Ikoma et al. 2006, Guillot and Havel 2011) affect the sizes and structures of these young planets.

Obtain constraints on the core sizes from measurements of apsidal precession: The k2 Love number may be thought of as a measure of the level of central condensation in a planets interior. Its measurement can inform us on the presence of a central core. Its measurement from the shape of the planet as obtained during ingress and egress (Seager and Hui 2002) is probably too difficult to determine (Barnes and Fortney 2003), even with PLATO. However, it can be measured from the planet's apsidal precession (Ragozzine and Wolf 2009). This requires the discovery of short period, (slightly) eccentric planets, the possibility to determine accurately primary and secondary transits and a long time-base. All these are possible only with *Kepler* (with luck) and PLATO (much more extensively).

Discovery of 'Rosetta stone' planets: It is important to realize that an important contribution from survey missions like PLATO will also come from detections that we can not predict and which has to do with the discovery of 'Rosetta stone' planets: planets that, by their location and characteristics defy available theories and enable us to really make decisive progresses in the field. By exploring > 50% of the sky, PLATO will discover these rare planets.

2.4.2 Planet albedo and reflected light

High-accuracy photometry allows not only the measurement of the primary transit, but also the occultation of the planet by the star (secondary transit). This technique is more successful in the near infrared because

the emission of hot Jupiters with high equilibrium temperatures is stronger in these wavelengths. However, the method's feasibility has also been demonstrated in the visible band from space-based photometry, such as in the cases of CoRoT-1b (Alonso et al. 2009a, Snellen et al. 2009; see Fig. 2.7) and CoRoT-2b (Alonso et al. 2009b, Snellen et al. 2010a), where even the reflected light from the planet was characterized, determining its albedo (see also Rowe et al. 2008). Recently, *Kepler* observations of the planet HAT-P-7b (Pál et al. 2008) have detected for the first time the tidal distortion created by a transiting planet on its star (Welsh et al. 2010). A similar result has been obtained by the satellite CoRoT for the transiting brown-dwarf CoRoT-3b (Deleuil et al. 2008). This provided even a measurement of the relativistic beaming effect (Mazeh and Faigler 2010). The measurement of the albedo and the reflected light is not limited to hot Jupiters; it has been also applied to the study of terrestrial-sized planets, such as the case of *Kepler*-10b (Batalha et al. 2011a).

The noise level in the light curve of CoRoT-2b was in the order of 130 ppm/hr whereas in the case of HAT-P-7b the rms level was 60 ppm on an m_V~10 mag star. The performance of PLATO (30 ppm down to m_V~11) is expected to be at least 4 times better than CoRoT and at least 2 times better than *Kepler*, allowing the detection of weaker signals around the majority of targets. PLATO will provide a wealth of information for the characterization of the atmospheres in the complete range of sizes from terrestrial to Jupiter-like planets.

PLATO observations will provide fundamental information on the structure of planetary atmospheres allowing a better understanding of their dynamics (Snellen et al. 2010a), the re-distribution of heat to the night-side (Harrington et al. 2006, Knutson et al. 2007, 2009, Crossfield et al. 2010), and the thermal inversion of the atmosphere (Spiegel and Burrows 2010 and references therein).

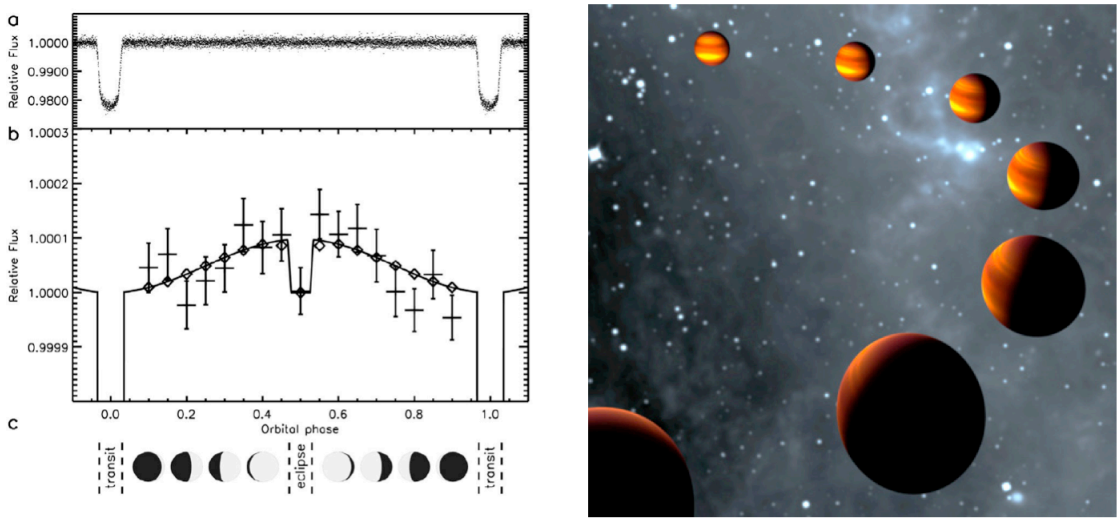

Figure 2.7: Phase effects in the light curve of CoRoT-1b (Snellen et al. 2009). Non-transiting planets are also detectable with this method.

2.4.3 Input to follow-up characterisation: atmospheric composition and loss

Scientific Impact

Dedicated follow-up observations from ground and space allow characterizing detected transiting planets further. Spectroscopic and spectrophotometric measurements during primary and secondary transits provide the atmospheric composition from molecular absorption lines in the visual and infrared range. While transit spectra of planets around bright host stars are sensitive to chemical abundances in the atmospheres, spectra in the infrared range obtained near secondary eclipse of planets around nearby stars are sensitive also to the temperature structure of the atmosphere.

The Hubble Space Telescope (HST) and the Spitzer Space Telescope (Spitzer) have been highly successful in the characterization of extra-solar planetary atmospheres through high contrast measurements during primary and secondary transits (see Seager and Deming 2010 and references therein). These facilities have provided observations which have characterized the chemical composition of atmospheres by detecting

atoms and molecules such as sodium (Charbonneau et al. 2002, Redfield et al. 2008, Vidal-Madjar et al. 2011), water (Grillmair et al. 2008, Swain et al. 2008, 2010), methane (Swain et al. 2008), carbon monoxide and carbon dioxide (Swain et al. 2009, 2010, Madhusudhan and Seager 2009). Escaping atomic hydrogen from the exosphere of HD 209458b was confirmed with HST (Vidal-Madjar et al. 2003), but also other ions such as CII or SiIII have been detected (Linsky et al. 2010). Evidence for the vertical atmospheric thermal inversion or its absence has been proved by Spitzer (Machalek et al. 2008, Charbonneau et al. 2008). Some planets have shown minimal contrast between their day-side (permanently illuminated due to their tidally locked orbits) and their night-side (HD 189733b, Knutson et al. 2007) whereas others show important contrasts (ups And b, Harrington et al. 2006). These investigations are fundamental for our understanding of the composition and dynamics of planetary atmospheres as well as their interaction with their environment and escape to space (see Lammer et al. 2009 and references therein).

In addition, the detection and study of extended upper atmospheres around exoplanets of all types provides promising insights into the interaction of the host star's plasma environment with the planet itself, as well as shedding light into the evolutionary stage of these bodies and their atmospheres and possible magnetic obstacles. Depending on size, mass and composition, upper atmospheres under non-hydrostatic conditions can interact with the stellar plasma flow so that huge hydrogen coronae and energetic neutral atoms (ENA) can be produced via charge exchange. By observing the size of the extended upper atmospheres and related ENA-clouds of detected transiting planets with future space observatories such as the WSO-UV (Shustov et al. 2009), conclusions can be drawn on the stellar wind properties, the planetary obstacle shape (e.g., magnetosphere) and the structure of the upper atmosphere (Lammer et al. 2011a, 2011b).

The host stars of PLATO planets will be amongst the brightest (and hence closest) known. Consequently they will be the natural targets for atmospheric studies (either through transmission or emission spectroscopic studies), including the search for biomarkers in terrestrial planets in the habitable zone. While the latter spectroscopic observations may prove difficult, the value of these targets would remain as suitable instrumentation is developed (indeed their existence would help drive such developments forward).

2.4.4 Prospects for future observing facilities

Follow-up with complementary space facilities

The James Webb Space Telescope (JWST, Gardner et al. 2007) with its large mirror size and high thermal stability will continue Spitzer's legacy, enabling, for a wide range of stellar brightness, the study of smaller exoplanets, including potentially habitable ones, as well as moons transiting giant planets. JWST will be able to detect the thermal emission of hot Jupiters at a SNR=25 for stars at ~150pc. Low-resolution spectra of NIRSpec will enable the detections of various molecules such as, H_2O, CO, CH_4, and CO_2 of transiting Jupiter-like planets orbiting out to 1 AU for host stars with mV=13.4 mag. It could even potentially discover the signatures of biomarkers in the atmospheres of super-Earths orbiting in the habitable zone of nearby M-dwarfs (Belu et al. 2011). The magnitude range of PLATO is m_V=5-13; therefore JWST will be able to fully characterize the hot Jupiters found by the PLATO mission.

PLATO will contribute potential targets for the proposed EChO (Exoplanet Characterisation Observatory) Mission. EChO is a dedicated exoplanet space-mission which will characterize the thermal structure, atmospheric composition and albedo of exoplanets using simultaneous, wide-range visible and IR spectroscopic observations. EChO will build on current work of Hubble and Spitzer using e.g. transit observations to improve understanding of the atmospheres of exoplanets. EChO has the goal of studying atmospheres of hot and warm planets down to Super-Earth around G-M stars and Super-Earths in Habitable Zone around dM stars. EChO also aims to help constrain current models of temporal and spatial variability in exoplanetary atmospheres e.g. for the atmospheric circulation of large exoplanets. Currently, EChO is under study as a potential M3 mission of ESA.

Imaging and spectroscopy with the E-ELT

The European Extremely Large Telescope (E-ELT) is the scientific project for a 30-40 m diameter telescope. It will be able to correct for atmospheric distortions and provide images 15 times sharper than those of HST. Recently, in September 2010 the E-ELT successfully passed the Phase B Final Design Review at ESO.

The Exo-Planet Imaging Camera and Spectrograph (EPICS) is an instrument project for the direct imaging and characterization of extra-solar planets with the E-ELT (Kasper et al. 2010). EPICS can resolve contrast between the host star and the exoplanet of 10^{-8} at 30 mas and 10^{-9} beyond 100 mas angular separation. It will provide spectral characterization of exoplanet chemistry with medium resolution spectroscopy (R~3000) as well as polarimetric imaging in the near infrared (between 600 and 1650 nm). Among its goals, EPICS aims to characterize Neptune mass planets and massive rocky planets around nearby stars, including those located in the habitable zone. EPICS will provide ground-based characterization of the atmospheres of the transiting extra-solar planets found with PLATO.

CODEX, the high resolution visual spectrograph for the E-ELT (Pasquini et al. 2008) would be able to detect the signal of 1 Earth mass planets in the habitable zone of low activity slowly rotating solar like stars (Dumusque et al. 2011b). CODEX will be able to measure the mass of Earth-like transiting planets detected by PLATO.

2.4.5 Planetary system evolution

Planet ages

Well characterized planetary systems, for which the age of the system is well-determined, will be crucial to advance our understanding of planetary evolution processes. The large number of known hot-Jupiters that transit their star (hence for which the planetary radius is known) has already motivated numerous theoretical studies of planetary evolution (simulating accretion, migration and loss) with age (e.g. Liu et al. 2008, Fortney et al. 2007, Lecavelier des Etangs et al. 2004, Kirsh et al. 2009). Such studies are critically constrained by uncertainties in planetary age, which PLATO will address.

Furthermore, one can only understand the evolution of planetary atmospheres and their water inventories if the evolution of the radiation and particle environment of the host stars, and thus its age, is well-known. Observations of young solar proxies indicate that the early Sun was a much more active source of energetic particles and electromagnetic radiation in the X-ray and EUV spectral range ($\lambda < 100$ nm) (*e.g.* Zahnle and Walker 1982, Micela 2002, Ribas et al. 2005). The short wavelength radiation is of particular interest because it can ionize and dissociate atmospheric species, thereby initiating photochemistry that can change atmospheric composition. The soft X-rays and EUV radiation is absorbed in a planetary thermosphere, whereby it can heat and expand it significantly (*e.g.* Kulikov et al. 2006, 2007, Lammer et al. 2008, 2009, Tian et al. 2008). This results in high atmospheric escape rates from primitive atmospheres. For numerical studies of atmospheric loss processes, it is therefore crucial to know the parameters of the whole system as well as a good estimate of the system age.

Finally, lessons from our Solar System imply that the factors determining habitability are many and varied - a complex interplay between *e.g.* geochemical, biological and physical factors. The terrestrial planets, Venus-Mars-Earth, are/were habitable but at different geological ages. Even though PLATO itself can not directly address the question of planet habitability, it will put detected terrestrial planets into a context of well-known ages, which will be valuable information when studying such planets further with suitable future spectroscopic instruments.

As the database of transiting hot-Jupiters as well as for small-sized planets expands, it will be informative to apply planet evolution models addressing the topics discussed to a wide range of scenarios. To succeed in this, the age of the system needs to be well constrained, *as will be done for planet host stars with PLATO.*

Planetary orbits

Spectroscopic observations during the transit itself also give information about the alignment of the planetary orbit to the spin axis of the host star via the Rossiter-McLaughlin effect. This alignment angle provides fundamental information on the possible evolution of planetary systems and on the influence of mechanisms such as migration, the Kozai effect, or tidal dissipation (Fabrycky and Tremaine 2007, Triaud et al. 2010, Winn et al. 2011a and references therein). In turn this provides hints about the orbital dynamical histories of these planets.

Most hot-Jupiters have misaligned orbits (Triaud et al. 2010), a result that is best explained by the Kozai effect or other scattering mechanism, a strong indication of stochastic processes during the planet formation or evolution. It also indicates the presence of further large planets in the system.

PLATO will provide a large sample of bright transiting planetary systems where this projected obliquity can be measured. A comparison of statistically significant samples of aligned and misaligned systems will put important constraints in the mechanisms leading to the formation of planets, allowing us to measure the competition between several concurrent models of planetary formation and evolution.

One of the main goals of PLATO is to provide precise and reliable measurements of the planet host stars' characteristics, in particular their radii, masses and ages. Stellar radii and masses to within a few percent will be necessary to measure the planetary radii and masses to comparable accuracy. Ages with a precision of a few tens of percent will be necessary to study the time evolution of the star-exoplanet systems.

2.5 Stellar Exoplanet host stars

One of the main goals of PLATO is to provide precise and reliable measurements of the planet host stars' characteristics, in particular their radii, masses and ages. Stellar radii and masses to within a few percent will be necessary to measure the planetary radii and masses to comparable accuracy. Ages with a precision of a few tens of percent will be necessary to study the time evolution of the star-exoplanet systems.

Every physical body, e.g. a building, has its own eigen-frequency, which is determined by its own internal structure and density profile. Similarly, eigen-frequencies of stars are determined by their internal structure, which is why they can be used to measure internal density profiles. The efficiency of the approaches comes from specific properties of stellar oscillations which are outlined below.

2.5.1 Corot, Kepler and the impact of PLATO data on characterisation of planet host stars

With the MOST, CoRoT and Kepler space missions, high-precision, long-duration, high duty-cycle photometric stellar light-curves became available to the community for the first time. These data sets lay the ground for a new era on the study of stellar interiors and stellar evolution. However, with the increasing number of detections of small, terrestrial extra-solar planets, a desperate need for even more precise parameters of exoplanet host stars developed. This need is one of the main drivers for the PLATO mission approach, optimizing for exoplanet search around bright stars with the possibility to obtain asteroseismology of their hosts. Here, we give examples on what has been achieved in this respect already from CoRoT and Kepler, demonstrating the feasibility of this approach and its future potential for PLATO.

The CoRoT satellite has observed several solar-type stars in its asteroseismic programme. We take here the example of HD 49385, the coolest star observed so far in the asteroseismic programme of CoRoT and whose frequency spectrum is shown in section 2.4.3. HD 49385 is a G0V type star with an apparent magnitude $m_V = 7.4$ (taking into account the difference in collecting area between CoRoT and PLATO it would correspond to a star with $m_V \approx 10$). The effective temperature and luminosity are estimated to be $T_{eff} = 6095 \pm 50\ K$ and $log\ L/L_{\odot} = 0.67 \pm 0.5$. Placing the star in the HR diagram results in a mass estimate of $1.36 \pm 0.15\ M_{Sun}$ and age of $3.8 \pm 1.2\ Gy$, owing to the uncertainty on the details of the physics in the star's interior, and in particular on its initial core chemical composition. This star has been observed with CoRoT during 136.9 days, with a duty cycle of 88.2%. Deheuvels et al. (2010) were able to exploit about 30 oscillation modes present in this spectrum. A grid of stellar models was computed, with different masses, ages, helium abundances, metallicities and overshooting distances. Deheuvels et al. (2010) then searched for the model offering the best fit with the fundamental parameters and the seismic parameters. This modelling showed that we could expect a much better accuracy than with classical methods in the determination of the stellar mass, radius and age. Using only a mean value of the large spacing and of the small spacing d_{01} (see below for details on asteroseismic analysis parameters and techniques), but working with fixed metallicity, one finds $M/M_{Sun} = 1.36 \pm 0.04$ and age$= 3.9 \pm 0.4\ Gy$, to be compared to the much larger uncertainties of determinations without asteroseismic observables. Because the star is an evolved main-sequence star, its power spectrum shows the existence of at least one mixed mode. The modelling of individual modes and particularly the mixed mode enables Deheuvels et al. (2011) to put tight constraints on the age of this star. More recently, HD52265 has been monitored by CoRoT for 117 days. It is a metal poor star hosting a giant planet in a close-in orbit (Ballot et al. 2011). Figure 2.8 shows the power spectral density in the 1500-2550

μHz domain. The comb-like structure is typical of p mode oscillations.

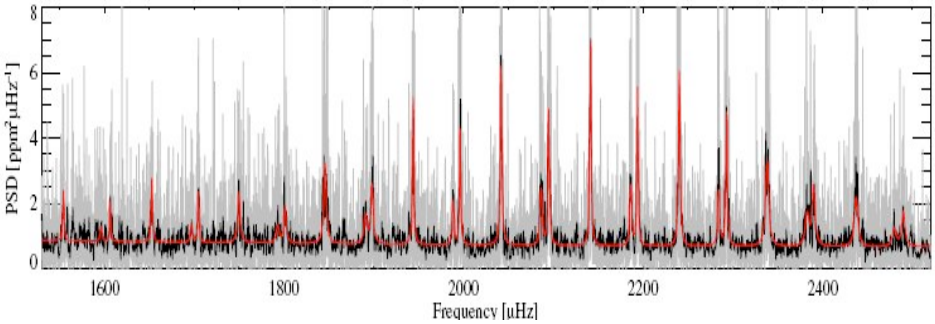

Figure 2.8: Power spectral density of HD 52265, a planet host star, in the frequency range of the oscillations at full resolution (grey curve). The black curve represents the result of a smoothing by an 11-bin wide boxcar and the red curve corresponds to the fitted spectrum. From Ballot et al. (2011).

The mean large separation $<\Delta\nu>$ and the ν_{max} frequency that can be derived from the observed frequencies respectively are (98.5 ± 0.1) μHz and (2090 ± 20) μHz and spectroscopic T_{eff} = 6100± 81 K (Ballot et al 2011). From these values they derive the mass and the radius of the star as (1.232 ± 0.065)M_{sun} and (1.371 ± 0.025) R_{sun} respectively. A more precise determination based on using of individual modes is ongoing.

Two years of *Kepler* observations (Borucki et al. 2010) have provided seismic data on a wealth of solar like stars with predominance for rather evolved main sequence stars. For instance, Metcalfe et al. (2010) using various independent evolutionary codes and analysis, determined the seismic radius mass, age for an evolved main sequence bright (V=9) bright G star KIC 11026764. They used individual frequencies obtained from a seismic analysis of 33.5 days of its *Kepler* photometric light curves. A fitting approach including individual frequencies and spectroscopic constraints (T_{eff}, log g , Fe/H) yield the radius, and age with respective *internal (statistic)* 1.5%, 1%. The radius is well constrained with the large separation. Mixed modes are observed in KIC 11026764 and are responsible for providing a very precise determination of its age. *Systematic* errors were taken into account as represented by the distribution of parameter values resulting from the use of different evolutionary and oscillation codes. Such errors were estimated to the level of 1-2% for the radius, 1-40% for the age. The mass is constrained only within 10%. As a whole, the precision achieved for KIC 11026764 is about 3% in the radius, and about 10% in the mass and 18% in the age for the set of best models. With longer observations, as expected with Plato, inversion for mass and fitting methods using mixed modes for age determination will be possible.

As another example, *Kepler* has detected a star hosting a rocky planet Kepler 10b and which is bright enough for asteroseismic analysis. This detection shows the potential of this observation and analysis concept, which will be also applied to PLATO data, and demonstrates its effectiveness and strength. Batalha et al. (2011a) used 19 individual frequencies derived from 5 months observations and a fitting method based on a search in a stellar model grid. Starting with high resolution spectroscopy that yielded an effective temperature, T_{eff} = 5705 ± 150 K, surface gravity, log g = 4.54 ± 0.10 (cgs), metallicity, [Fe/H] = –0.15 ± 0.03 and v sin *i* = 0.5 ± 0.5 km/s, an iterative procedure involving the seismic modelling finally led to mass, radius and age determinations to the respective precision level of 6.7% , 2% , 38%.

Meanwhile, a number of stars have been analyzed by asteroseismology by CoRoT and Kepler. Figure 2.9 shows the mean large separations as a function of the effective temperature for *Kepler* data for 78 stars together with evolutionary tracks for models with masses in the range 0.8 to 1.5 M_{sun}. The same stars are represented on the right of Fig. 2.9 in a diagram $<d_{02}>/<\Delta\nu>$ versus $<\Delta\nu>$. Isochrones in step of 1 Gy are represented from the ZAMS to red giant stages. The figure clearly shows that the mean large and small separations provide accurate ages and masses for un-evolved stars (White et al., 2011).

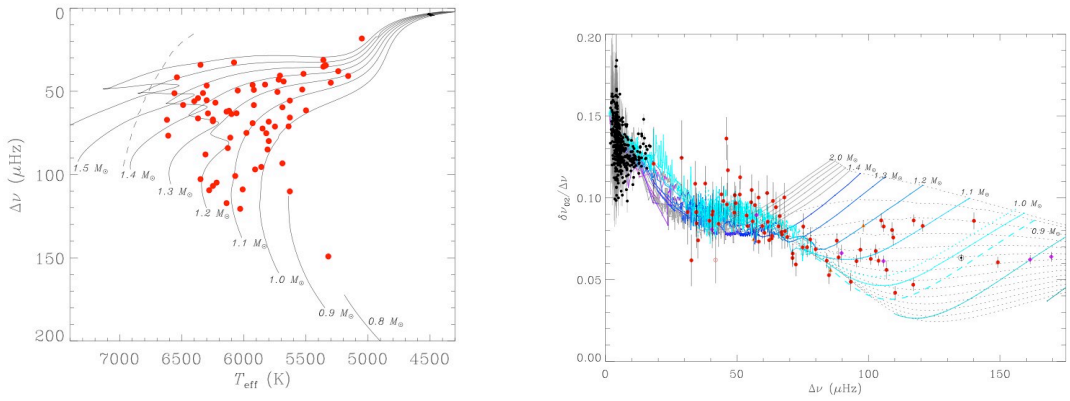

Figure 2.9: Left: Mean large separation as a function of the effective temperature for 78 solar like oscillating stars observed by Kepler over 10 months (red dots). The theoretical tracks for models with different stellar mass (solid lines) are from Christensen-Dalsgaard (2008). Right: Mean small separation <d_{02}> normalized to the mean large separation as a function of the mean large separation for the same stars than on left (red dotes) and evolutionary tracks (blue solid lines). Horizontal dotted lines are isochrones with 1 Gy step (top right: ZAMS, bottom left: beginning of the red giant ascending branch). From White et al. (2011).

Furthermore, one of the most striking results from CoRoT and *Kepler* seismic observations is the solar oscillation of red giants. The quality of the seismic data for these stars allows the determination of not only mass, radius but also precise stages of evolution and related ages (Bedding et al. 2011). One also obtains important information on the structure of the star and potentially on its helium content (Miglio et al. 2010). All this will concur to test one important but still poorly modelled ingredient of stellar models, i.e. transport processes (heat, chemical element, angular momentum). Indeed some transport processes that occur during the main sequence phase have consequences for the further evolution of the star that are more easily detected -and therefore more easily tested- when the star is on its red giant phase.

Most of the above examples represent the precision of fitting methods that are used to determine the stellar parameters taking into account the actual uncertainties on the input observational data. This does not take into account any bias coming from uncertainties, unknown, missing or inappropriately modelled input physics in both model atmosphere and stellar interior models. This nevertheless shows that techniques based on seismology that can yield the required accuracy already exist, provided that the observational (seismic and non seismic) data and that the models have a sufficient quality level. Improvements in the physical description of stellar models will be validated by seismic studies and will lead to successive generations of increasingly more realistic stellar models.

The expectations on the nature and the quality of the seismic input data from PLATO are based on results of extensive hare-and-hounds exercises using artificial seismic data, which have been performed by the asteroFLAG consortium (Chaplin et al. 2008), and on direct experience of analysing seismic data from the photometric CoRoT observations (*e.g.* Appourchaux et al. 2008). The results show that for PLATO we should be able to extract high-precision estimates of individual mode frequencies of main-sequence targets brighter than $m_V \approx 12$. For F, G and K main-sequence targets at $m_V = 11$ typical frequency uncertainties of individual modes in G and K stars will be about 1 part in 30,000, while in the hottest F stars the uncertainties may rise to about 1 part in 10,000. Together with the above examples from CoRoT and *Kepler* this indicates that with the much longer monitoring performed by PLATO one can expect to achieve accuracies of a few % for radius and mass and a few tens percent for the age using asteroseismology.

2.5.2 Stellar radii: Input from Gaia

Gaia data will have a major role to play in the characterization of PLATO exoplanet host stars. In the absence of interstellar absorption, Gaia will deliver relative precisions on the luminosities of FGK main-sequence stars at distances up to 200 pc in the range 0.7 – 5.5% (Lebreton 2008).

On the other hand, measurements of effective temperature to within 1% will be achievable through dedicated high resolution, high signal-to-noise spectroscopic observations obtained as part of the ground-based follow-

up programme. The above performances on luminosity and effective temperature, coupled together, will lead to stellar radii with a relative precision within 2% for un-reddened stars such as most of the PLATO targets.

In addition, as explained below, the Gaia stellar radii coupled with the seismic observations of PLATO will lead to model-independent masses with a relative precision of a few percent. They will also play an important role in placing tight constraints on stellar interior structure models of the exoplanet host stars that will provide stellar ages.

2.5.3 Stellar masses and ages: Seismic determination with PLATO

Classical methods used for the determination of masses and ages of stars rely on a comparison of the star's location in the HR diagram with theoretical evolutionary tracks. Unfortunately this method has severe limitations. Even if stellar evolution theory were fully understood, the location in the HR diagram does not uniquely determine the properties of a star. Moreover, there are many uncertainties in evolution theory, most importantly linked to uncertainties in the calculation of theoretical tracks, in particular due to poor knowledge of the internal metal mixture of stars. Uncertainties on physical processes in stellar interiors (microscopic diffusion, rotational mixing, etc.) imply that the metallicity can be wrong by up to a factor 2 when using initial surface values for the abundances derived from high-resolution spectroscopy. This propagates into relative uncertainties of 20% for the stellar mass. Moreover, stellar ages on the main sequence remain essentially unconstrained. The characterization of planet host stars, and in particular the measurement of their masses and ages, must therefore be obtained with another, more accurate and more reliable method. Seismic analysis is this much-needed method. Indeed measurements of the oscillation frequencies of the PLATO targets will allow much tighter constraints to be placed on the fundamental stellar parameters of exoplanet host stars. This improvement arises because the individual oscillation frequencies can be estimated to high levels of precision not usually encountered in stellar observations.

The oscillation modes of solar-like stars are acoustic waves trapped inside the star, and are governed by the sound speed c(r) and density ρ(r) throughout the star. The corresponding oscillation frequencies of a star are then determined by its structure; hence, from an observed set of frequencies, we can infer properties of the structure of the star. There are basically two approaches to such an analysis usually referred to as *forward* and *inversion* techniques.

General: Information from frequency diagrams

The *eigen-frequencies* $\nu_{n,\ell,m}$ are described by 3 "quantum numbers" (n,ℓ,m), where n is the radial order and ℓ, m the latitudinal degree and azimuthal order of the spherical harmonic $Y_{\ell,m}(\theta, \varphi)$ representation of the geometry of the mode.

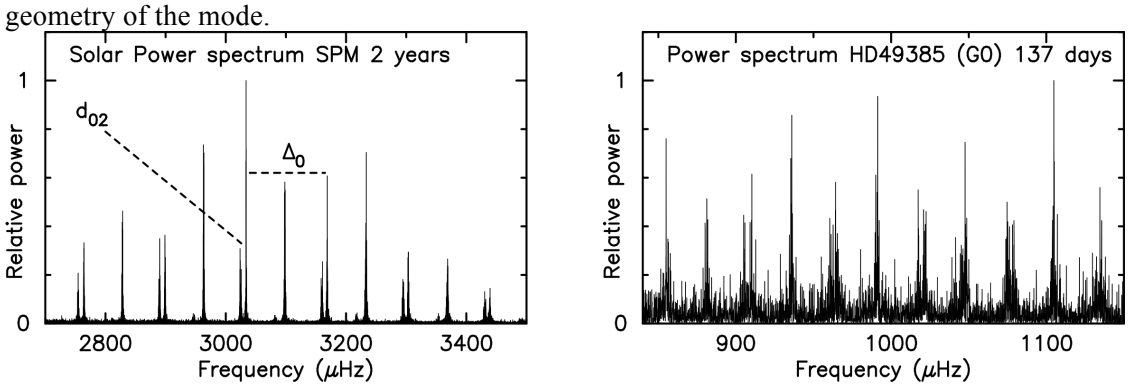

Figure 2.10: Left: Solar power spectrum from 2 years of SPM photometric data. The almost equally separated large peaks are modes of degree ℓ = 0, 1 with successive n values, the prominent smaller peaks close to modes of degree ℓ = 0 are ℓ = 2 modes. Low amplitude modes of degree ℓ = 3 close to modes of ℓ = 1 can just be seen in this figure. Right: Power spectrum of HD 49385 from 137 days of observation with CoRoT. The large separation Δ_0, and small separation d_{02}, provide information on the structure, mass and age of a star.

For a spherical star there is no dependence on the azimuthal order m; this degeneracy is lifted by rotation (and/or magnetic field). For slow rotation the frequencies $\nu_{n,\ell,m} = \nu_{n,\ell} + m < \Omega >$, $m = -\ell, \ell$; where $< \Omega >$ is a weighted average of the interior rotation which depends on the internal structure of the star and the particular Eigen mode. This can be used to probe the internal angular velocity of a star. Measurements of modes with ℓ

values up to 3 are expected for PLATO targets, for which the stellar disk cannot be resolved. The oscillation frequencies, including the rotational splitting, are determined by fitting the peaks in a power spectrum of the light curve with a Lorentzian line profile. Two examples are given in Fig. 2.10 – one from 2 years of photometric observation of the Sun with SPM on SoHO, the second from 137 days of observations with CoRoT of the G0 star HD 49385. Determining frequencies of modes with $\ell = 0, 1, 2, 3$ with the solar data is quite straightforward giving estimated errors < 0.1μHz, while for the 137 day run on HD 49385, we can extract frequencies with errors ~ 0.3μHz. The goal with the much longer monitoring to be performed with PLATO is to achieve accuracies ~ 0.1μHz.

Frequency separations: The power spectra exhibit an almost equal spacing between the large peaks; these are usually described in terms of separations such as the large separations $\Delta_\ell = \nu_{n,\ell} - \nu_{n-1,\ell}$ between modes of the same degree ℓ and adjacent n values and the small separations, *e.g.* $d_{02} = \nu_{n,0} - \nu_{n-1,2}$ between the narrowly separated peaks corresponding to modes $\ell = 0, 2$ (see Fig. 2.10). Additionally we have the small separations $d_{01} = \nu_{n,0} - (\nu_{n-1,1} + \nu_{n,1})/2)$ which are particularly valuable when only modes of degree $\ell = 0, 1$ can be reliably determined. These separations provide diagnostic information on the star's structure. The large separations give an estimate of the star's acoustic radius which is related to the stellar mean density, while the small separations such as d_{01}, d_{02} give diagnostics of the interior structure. Periodic modulations in these separations give diagnostics of the location of the boundaries of convective cores and envelopes. The diagnostic power of the frequencies and separations can be further enhanced by techniques which model, or subtract off, the contribution of the outer layers of a star which are poorly understood (Kjeldsen et. al. 2008, Roxburgh and Vorontsov 2003a).

Model independent inversions for the stellar mass

Among the possible *inversion techniques*, the most suitable one is *model independent* and seeks to infer the internal density profile which is the best fit to the observational data set. Integration over the stellar radius of the density profile then yields the seismic mass of the star.

The result that frequencies are almost independent of ℓ provides the basis of a *model independent* inversion procedure to determine the internal density profile inside a star from an observational set of frequencies (see e.g. Roxburgh and Vorontsov 2003a for more details on the technique).

Once we know the density profile, the total mass of the star can be simply computed as integral of the density over the (assumed known) radius of the star. Note that the regions where the density is not best constrained make only a small contribution to the total mass: in the centre the radius r is small and in the outer layers the density is small. The resulting density profiles can then be compared with those predicted by stellar evolution models to estimate the evolutionary age of the star (see Section 2.4.5 below). Although the results are not dependent on the initial stellar model, it is advisable to start with model close to the real star. Mass and radius for the initial model can be derived for instance from observed average seismic properties (see Sect.4.2.4). It should also be stressed that the derivation of a model-independent mass requires that the radius R of the star is determined by other means; this is a necessary condition since the frequencies are invariant under a scaling of M and R that leaves M/R^3 invariant. As mentioned earlier, radii of the PLATO exoplanet host stars will be known to an accuracy better than 2% thanks to Gaia, which translates into *a well constrained model-independent exoplanet host star mass with a relative precision better than 2%.*

Model fitting to obtain masses and ages

Among the *forward techniques*, *model fitting* is extensively used to compare an observed data set with a set of frequencies predicted from a grid of stellar models and select the model which best fits the data. This approach provides the seismic mass, radius and age of a star.

In this approach, we compare the properties of the set of observed frequencies with the predictions from a grid of evolutionary stellar models in order to find the model that best fits the observables (*e.g.* Brown et al. 1994, Miglio et al. 2005, Metcalfe et al. 2009). The grid is composed of stellar models that are computed under a range of assumptions about the physical processes that govern stellar evolution. The search in the grid is restricted to satisfy the fundamental properties of the star (magnitude, effective temperature, gravity, metallicity, projected rotational velocity, etc) and the oscillation frequencies. In practice one seeks for a minimisation of the differences between observed and computed, seismic and non-seismic, parameters.

Several methods can be used to carry out such minimisation (see for instance Stello et al. 2009, Quirion et al. 2010).

The unknown effect of the surface layers on the absolute values of the frequencies can be overcome by different techniques (e.g. Kjeldsen et al. 2008, Roxburgh and Vorontsov 2003a). The best fit model then gives values for the mass, radius, age and internal structure of the stars.

The minimum seismic information necessary in the fitting process can be estimated following Metcalfe et al. (2009). The authors found that with half a dozen surface-corrected frequencies available at each of $\ell = 0$ and $\ell = 1$, it becomes possible to constrain the model-dependent masses to within 3%, and the corresponding ages that the star has spent on the main sequence to within 5%, if we assume the heavy-element abundances to be known to within a factor of two. Note that this result assumes that the model physics is correct. With the addition of more frequency estimates (i.e. of $\ell = 2$ modes, and of more overtones) further improvement of the parameter uncertainties will be possible. For a main-sequence target observed at $m_V = 11$, we would expect to be able to measure more than ten overtones of its $\ell = 0, 1$ and 2 frequencies (see Sect.4.3 for a concrete example).

Mixed modes as precise age indicators: Main sequence stars that are evolved enough or sub-giant stars present some particular non radial modes ("mixed modes") that deviate significantly from uniform frequency spacing. These modes yield a strong (though model-dependent) constraint on the age of the star. The reason is that the star becomes more centrally condensed when it evolves and frequencies of oscillation modes behave like g-modes in the core and p-modes in the envelope ("mixed modes") increase to fall in the range of detected modes. Their frequency deviate from the regular spacing of asymptotic pure p modes and can therefore be identified. This behaviour changes very quickly with stellar age. Both CoRoT and *Kepler* have observed stars presenting such particular modes.

For the non-seismic parameters, the largest source of observational uncertainty comes from the estimated heavy-element abundances. From the precision on the luminosity expected from Gaia, it would in principle be possible to constrain the abundances seismically to a precision of about 10% (Metcalfe et al. 2009), thus further improving the accuracy of the star's mass and age.

One must stress that the efficiency of model fitting to the observed frequencies depends on our ability to model stellar evolution, and the reliability of these models. Indeed, we stress that any technique that aims at determining the stellar age from observed properties of the star, be they classical observables, oscillation frequencies or quantities such as the small separation derived from such frequencies, depends on reliable modelling of the star. Thus the asteroseismic investigation of stellar structure and evolution is an essential part of the characterization of planet hosts. Some advances in our understanding of stellar modelling are starting to come from investigations with data from CoRoT and *Kepler* but the superb PLATO data will provide a further dramatic improvement in the understanding of stellar evolution and hence in our ability to characterize the properties of the planetary hosts.

Average seismic parameters and scaling relations

The above techniques assume we have individual frequencies. However when the S/N ratios in the seismic data are insufficient to allow robust extraction of individual p-mode frequencies, it will still be possible to extract average estimates of the large and small separations $\langle\Delta_0\rangle$ $\langle\Delta_1\rangle$, $\langle d_{01}\rangle$, $\langle d_{02}\rangle$ and their ratios over one or more frequency ranges, owing to their regularity. These average values provide a set of seismic data well-suited to constraining the exoplanet host star parameters (cf. Christensen-Dalsgaard, 1988). Coupled with classical observations of L, T_{eff} , $[Fe/H]$, $\log g$ delivered by Gaia (or even more precise by other means) this has considerably better diagnostic power than the classical observables alone. For very low signal-to-noise data the mean large separation $\langle\Delta\rangle$, some indication of its variation with frequency, and possibly an average value of the small separation d_{02}, can be determined from frequency windowed autocorrelation of the time series (Roxburgh and Vorontsov 2006, Roxburgh 2009b, Mosser and Appourchaux 2010).

In any case, for most stars, measurement of the average large separation should allow the stellar density to be constrained to a precision of several percent from model fitting. With an accurate knowledge of the effective temperature and/or luminosity, a seismic radius can be determined with a similar precision. The use of the average large separation together with the radius from Gaia measurements can also provide a seismic mass with a precision higher that provided by the classical observables alone.

Finally, it must be stressed that scaling relations have been shown to relate the averaged large separation, <Δν>, and the frequency at maximum in a power spectrum, $\nu_{max,}$ to the mass, radius and effective temperature of the star (Kjeldsen and Bedding, 1995):

$$\frac{R}{R_\odot} = \left(\frac{135}{\langle\Delta\nu\rangle}\right)^2 \left(\frac{\nu_{\max}}{3050}\right)\left(\frac{T_{eff}}{5777}\right)^{1/2}; \qquad \frac{M}{M_\odot} = \left(\frac{135}{\langle\Delta\nu\rangle}\right)^4 \left(\frac{\nu_{\max}}{3050}\right)^3 \left(\frac{T_{eff}}{5777}\right)^{3/2}$$

where the radius and mass are normalized to the solar values, and the mean large separation <Δν> and $\nu_{max,}$ is in Hz.

As an example, let us consider the case of two stars KIC 11395018, a G star with a magnitude V=10.8, and KIC 11234888, a late F star with a magnitude V=11.9. Both stars have been observed during 8 months with *Kepler*. Mathur et al. (2011) obtain a precision on the averaged large and small separation of 2% and 1 % respectively. The precision on the mean density derived from the mean large separation is about 5%. The precision on the stellar radius and mass derived according to Eq. (2.4.6) above are of 10% and 20 % respectively. Note that with a precision of 2% on the radius from Gaia for these two stars, the precision on the mass derived from the mean large separation would be 10 %, i.e. would be improved by a factor 2.

Mass and radius determinations that are based on average seismic quantities will also be used to yield a first, very rapid determination of mass and radius for a large sample of stars. These seismic radius and mass will also serve as initial input for the more precise forward and inversion techniques described below for the planet host stars.

2.6 Complementary Science

Besides the core program, PLATO will enable a broad range of studies involving photometric variability. It will provide us with a unique database of stellar variability, with precisions of the order of a few 10^{-5} per hr, and on all time scales between 1 minute and a couple of years. These exquisite results will be used to address many different scientific questions, mainly (but not exclusively) in the area of stellar physics. Some of these additional science programs are briefly mentioned below.

PLATO's high signal to noise, long time coverage and very large field-of-view, will make possible the study of variability on several time scales for statistically significant stellar samples. It will be possible also to study very small and short term variations easily distinguishable from instrumental noise thanks to the large number of independent telescopes. We discuss here the major advance in our understanding of stellar evolution that will come from using the PLATO data and some of the additional science cases in which PLATO will have significant impact on stellar astrophysics in general. The following list is non-exhaustive and is mainly for illustrative purposes of what kind of science will be covered by PLATO as important by-products.

2.6.1 Asteroseismology and stellar evolution

The asteroseismology discussion in the previous section is focused on the exoplanet host stars, which are low- mass main-sequence stars. However the mission will provide data that far exceed, in terms of extent and quality, any previous dataset for the study of stellar interiors. PLATO will greatly strengthen our understanding of stellar structure and evolution which remains a basic, yet at the moment somewhat shaky, foundation for a large part of astrophysics. An improved understanding of stellar modelling is essential also for estimating the ages of the host stars of planetary systems and putting the discovered planetary systems, (and therefore also our solar system) in an evolutionary context.

Convection, convective overshooting and various other mixing and transport processes are poorly understood and yet play a major role in stellar evolution, determining evolutionary time scales, and must be taken into account for measuring stellar ages. As a consequence, for example, the ages of the oldest globular clusters are still very uncertain and, for some values of the parameters in the models, can be higher than the estimated age of the Universe (van den Bergh 1995, Clementini and Gratton 2002, and Krauss and Chaboyer 2003).

The large range of values for parameters modelling core overshooting needed to fit data on young open

clusters (Mermilliod and Maeder 1986), on eclipsing binaries (Claret 2007), and on the oscillation frequencies of a few massive stars (Aerts 2008), prevents the reliable determination of stellar ages for stars with convective cores. This implies that our knowledge of convective and rotational mixing processes inside massive stars is very incomplete, resulting in huge uncertainties in masses, ages, internal composition and structure of supernova progenitors, and hence in the modelling of the explosion and the resulting nucleo-synthesis yields. Uncertainties in convective overshooting can lead to uncertainties in the ages of open clusters by up to a factor of two (Perryman et al. 1998). In view of these difficulties, it is clear that the age ladder of the Universe, which rests on stellar age estimates, is still highly unreliable. Moreover, the ages of field stars are even more uncertain than those of cluster stars. This has serious consequences for the use of results from Gaia to investigate the evolution of the Galaxy.

The asteroseismic investigations of a large number of stars of various masses and ages constitute the necessary tool to constrain efficiently our modelling of stellar interiors, and improve our understanding of stellar evolution. Some progress should be achieved using data on the bright stars observed by CoRoT in its seismology program and any bright stars included in the limited asteroseismic programme of *Kepler*, but a thorough investigation into stellar evolution requires a large number of bright stars sampling all stellar parameters (mass, age, rotation, chemical composition, environment…), including main-sequence members of open clusters, and old Population II stars. The PLATO mission, both with the long runs and with the step & stare phase, will provide the necessary data to reach this goal since the data will allow us to study the oscillations of a large fraction of the target stars (with or without planets), and to investigate the seismic properties of various classes of stars.

Asteroseismic investigations of stellar interiors will compare the density structure obtained as described in Section 4 with the results of stellar modelling. Furthermore, the model fitting will undoubtedly result in highly significant residuals as evidence that the parameterized representation of the model physics is inadequate at the accuracy of the PLATO data; the challenge will then be to determine how the physical description must be improved. This will, for example, allow detailed investigations of the uncertain mixing processes associated with convective cores in main-sequence stars, which is believed to be of great importance to their subsequent evolution.

Moreover steep gradients in the stellar interior produce a quasi-periodic modulation of the oscillation frequencies (cf. Vorontsov 1988, Gough 1990). For stars with sufficient precision in the measurement of the frequencies this will allow us to probe the properties of the boundaries of convective cores using both solar-like pressure (p) modes (cf. Roxburgh and Vorontsov 1994a, 2001) and the gravity (g) modes that are excited in more massive stars (Miglio et al. 2008), and hence place tight constraints on the overshooting of convective motions into the layers above. This can provide a more accurate calibration of the ages of such stars. Sharp features in the outer layers give information on the depth or radius of convective envelopes, overshooting below the envelope and on the He abundance (Monteiro et al., 1994, 2000, Roxburgh and Vorontsov, 1994b, Roxburgh 2009a).

Members of *open clusters* will be targets of special interest. Their uniform initial chemical composition and age, and nearly common distance, provide very stringent constraints on the modelling, increasing the information obtained from the oscillation frequencies. In young clusters, we may in particular observe the β Cephei stars as well as slowly pulsating B stars, and bring important constraints on the evolution of massive stars. In the older clusters, oscillations in sub-giants (similar to those observed in η Bootis, Carrier et al. 2005) can be studied. Therefore, the asteroseismic analysis of members of open clusters chosen to sample an age sequence, will allow us to constrain severely stellar evolution modelling. It is foreseen that the step & stare phase at the end of the mission can be used to optimize this open cluster coverage, by monitoring several fields for a few months each.

The simultaneous measurement of stellar rotation, derived from PLATO light curves, will allow us also to determine the effects of rotation on stellar structure. This analysis will be performed on the bright stars for which asteroseismic studies (and therefore individual age determination) will be possible. With these bright stars it will be possible to calibrate the gyro-chronology relation. This relation presently relies for old stars mainly on the solar age and rotation (i.e. Barnes 2007). In particular PLATO will give access to the very long periods associated with very small photometric variations.

3 SCIENTIFIC REQUIREMENTS

The main scientific objective of PLATO is to detect and thoroughly characterize a very large number of exoplanetary systems, including both the exoplanets and their host stars. To achieve this goal PLATO will require monitoring the visible flux from a large number of bright stars, with very high accuracy, during a long time and with a high cadence. These light curves will show the signatures of planets transiting in front of their parent stars. The same light curves will allow us to measure the micro-variations in flux of these stars, which will be used to perform a seismic analysis of them. The exoplanet transits and the stellar seismic analysis will yield the fundamental physical parameters of the exoplanets *and* their stars with ultra high precision. Combining the long uninterrupted high precision photometric monitoring from space with ground-based follow-up observations, such as high-resolution radial velocity spectroscopy and interferometry, a full characterization of the planetary systems will be obtained. The primary targets of PLATO are therefore stars that are sufficiently bright to allow both high photometric accuracy from space and precise follow-up measurements from ground.

All exoplanetary transits detected by PLATO will be investigated in detail, leading to an extensive knowledge of exoplanet populations (including the mass function for exoplanets) and enabling us to relate the physical properties of both the planets and their central star for an unbiased statistical sample. In particular, telluric exoplanets in the habitable zone will receive special attention. The mission is designed to guarantee the identification and study of a statistically significant number of such planets.

Each bright star with a detected transit will be followed up from the ground, performing high precision radial velocity measurements, in order to confirm that the detected event is indeed due to a planet, and also in order to measure the planet mass. These follow-up observations will be facilitated by the brightness of the PLATO targets, and will be most efficient for spectral types later than F5. Additional ground-based high resolution spectroscopy will be used to confirm or measure the stellar fundamental parameters (T_{eff}, *log(g)*, chemical composition, rotation velocity, etc).

The knowledge of the planet orbital period, the planet/star radius ratio and the planet/star mass function, coupled to the measurement of the star's radius, mass and evolutionary state, will allow to derive all the planets fundamental physical parameters (mass, radius, orbit, age), assuming the stellar and planet ages to be similar. Additional ground- and space-based follow-up observations will also be obtained for the brightest targets, in particular in- and off-transit photometry (visible and IR) and high signal/noise spectroscopy providing information on the planet atmospheric composition and dynamics by differential observations.

In addition to the main goals focusing on the observation of the brightest stars of the sample, PLATO will also perform a more extensive survey of exoplanetary transits in front of a very large number of fainter stars. Also, in complement to the seismic analysis of planet host stars, asteroseismology of the many other types of stars present in the field of view will be used for a more complete study of stellar physics and evolution. Observations of stars of masses and ages all across the HR diagram, including members of several open clusters and old population II stars, will be obtained for this purpose. In order to maximize the surveyed sky area and the number of monitored stars at all magnitudes, the mission will comprise two long monitoring phases of two successive fields. A third step-and-stare phase at the end of the mission will be used to extend the sample of stars surveyed for short period planets and for stellar structure studies, as well as for revisiting targets of the first two pointings in an optimized way, to confirm longer period exoplanets.

All the star count tests performed during the assessment phase show that the numbers we are using for the selected fields are reasonably reliable, with some uncertainties on the actual number of cool dwarfs and sub giants. During the implementation phase of the mission the precise final pointing(s) will be defined on the basis of a specifically designed observational campaign, likely based on medium-band photometry, including filters sensitive to temperature and gravity. Spectroscopy of a subsample will help in calibrating and testing the photometric classification. Based on the outcome, the best observational strategy will be defined. Finally early Gaia results (2015) will be used for the selection of the individual targets within the selected fields of view.

This chapter describes in detail the scientific high level requirements needed to achieve the objectives of the PLATO Mission, including the stellar sample definition, the observation strategy and the required

photometric accuracy. These are the basic requirements from which the lower level engineering requirements that define the design of the mission have been derived, leading to the payload concept described later in this report.

The depth of a planetary transit is given by the ratio of the areas of the planet and its transited star, which is of the order of $\Delta F_{star} / F_{star} \approx 10^{-4}$ in the case of Sun-Earth analogues, while transit durations are typically of the order of 12 hours. In order to detect such transits at more than 4σ, a dimensioning requirement, we need to obtain a photometric noise level lower than about 2.5×10^{-5} in 12 hours, i.e. about 8×10^{-5} in one hour. This is the minimum requirement for the detection of an Earth-like planet in front of a solar-like star.

However, the measurement of several points across the transits will be necessary, implying lower levels of noise. In practice, a minimum of 5 to 6 points across the transit are necessary to characterize its shape, in particular the ingress and the egress parts. We therefore require a photometric noise level below 3.4×10^{-5} in one hour, for the highest priority star sample of the mission.

Recent results from CoRoT have shown that detecting, measuring and identifying oscillation modes in solar-type stars requires a noise level in amplitude Fourier space below about 2.0 ppm per $(\mu Hz)^{1/2}$ (Michel et al. 2008, Deheuvels et al. 2010, Garcia et al. 2009, Ballot et al., 2011), which is equivalent to 3.2 ppm in 5 days, or 1.3 ppm in 1 month, and which translates approximately into a noise level of 3.4×10^{-5} in 1 hr, *i.e.* similar to that for the detection and characterization of Earth-like transits.

The duration of the observations needs to be longer than 2 (goal 3) years, so that at least 2 (goal 3) consecutive transits for Sun-Earth analogues can be detected.

For the seismic analysis of the target stars, the total monitoring time must be sufficient to yield a relative precision of 10^{-4} for the measurement of individual mode frequencies, which is needed to perform the inversion of the oscillation spectra. For solar-type stars, this comes down to an absolute precision of 0.2 to 0.1 μHz, which translates into a minimum monitoring time of 5 months for a reasonable S/N of 10 in the power spectrum.

In the following sections we describe the specific requirements that define the PLATO mission.

3.1.1 PLATO light curves and additional products

R0a PLATO must provide long, high duty cycle, high precision photometric time series in visible light of a large number of bright stars. The basic PLATO data products consist of the white-light curves with derived characteristics of the stellar samples specified by the requirements below (see **R2** and **R5**).

R0b In addition, it is required that part of the payload (*e.g.* a small subset of the telescopes or individual detectors if a multi-telescope concept is chosen) provides photometric time series in at least two separate broad bands (see **R8**). These will be used in particular to constrain the identification of the detected oscillation modes in bright classical pulsators.

R0c PLATO must also provide relative astrometric measurements of the targets of the bright samples (defined in **R2** below). These astrometric measurements will allow to search for giant planets through the detection of the associated star wobble, and will also be used to identify false positives, due for instance to background eclipsing binaries. Astrometric measurements may also be used to evaluate a posteriori instrument jitter properties.

3.1.2 Surveyed fields

R1 Two successive fields must be monitored, followed by a step & stare phase, during which additional fields will be surveyed. During the step & stare phase, the instrument may also have to come back to the two fields observed during the two long monitoring phases. During the step & stare phase, the instrument must be capable of accessing other fields at any position in the sky, at a proper time for these observations to be feasible.

3.1.3 Stellar samples and corresponding photometric noise levels

Because the transit depth is inversely proportional to the square of the star's radius, transiting planets will be preferentially searched around the small radii cool dwarf stars, which indeed will be similar to our Sun. However, the stellar sample will be extended also to sub-giants, which have radii only slightly larger than dwarfs. The restriction to cool stars is also motivated by the need for subsequent radial velocity follow-up observations. Their spectra supply the large number of lines necessary to get very accurate radial velocity measurements and are thus eminently suited for the programme. Consequently, the core star sample for the PLATO mission will consist of cool dwarf and sub giant stars that are bright enough for the photometric precision required for the detection of small planets and for seismic analysis to be reached.

R2 Five complementary stellar samples have been defined as targets of the PLATO mission, and are described below by order of priority :

P1: Given the probability to detect transits of planet in the habitable zone of solar-type stars, estimated to be about 0.1% (geometric probability × fraction of stars with such planets), we estimate that at least 20,000 cool dwarfs and sub-giants need to be surveyed for a sufficient amount of time to detect long period orbits (~1 year), i.e. typically for 2 to 3 years. This number of surveyed stars implies an expected number of telluric planets in the habitable zone of the order of 20, which we consider as the main objective for PLATO. This would represent a very significant improvement compared to *Kepler*, considering in addition that such exoplanetary systems detected by PLATO would also be fully characterized. Additionally we would expect to detect many transits of larger planets and/or closer around these stars. Therefore, more than 20,000 dwarfs and sub-giants later than spectral type F5, with a noise level below 3.4 x 10^{-5} in 1 hr, must be observed with the required duty cycle for more than 2 (goal 3) years. **This sample, with m_V typically between 8 and 11, is the backbone of the PLATO mission, and is considered as the highest priority objective.**

P2: The search for planetary transits around very bright and nearby stars presents a specific interest, as these sources will become privileged targets for further ground- and space-based observations. We therefore request the monitoring of a relatively large number of very bright stars with the goal of detecting a few telluric planets in their habitable zone. Hence, more than 1,000 dwarfs and sub-giants later than spectral type F5 and brighter than $m_V=8$ must be monitored with a noise level below 3.4×10^{-5} in 1 hr, with the required duty cycle for more than 2 (goal 3) years.

P3: The detection of an even larger number of short period planets around such very bright stars will also be used as input for further instruments aimed at characterizing their planetary atmospheres. Hence, more than 3,000 dwarfs and sub-giants later than spectral type F5 and brighter than $m_V=8$ must be monitored with a noise level below 3.4×10^{-5} in 1 hr, with the required duty cycle for more than 2 months. The P3 sample is an extension of the P2 sample, i.e. P2 sample is included in P3 sample.

P4: Due to the specific interest of investigating planets around cool dwarfs an additional sample of more than 5,000 cool dwarfs brighter than $m_V=16$ must be monitored with a noise level better than 8.0×10^{-4} in 1 hr, with the required duty cycle for more than 2 (goal 3) years. In addition, an equivalent number of such cool dwarfs must be monitored during the step & stare phase of the mission, with the same noise and duty cycle characteristics.

P5: Finally, to increase the statistics we need to observe a very large number of stars with the required precision to detect telluric planets around solar-type stars, *i.e.* 8×10^{-5} in 1 hr, even if accurate seismic analysis will not be available. For these detections, we will rely on other, less precise and less reliable techniques to assess the mass and age of the host stars. These other methods, *e.g.* based on a correlation of stellar rotation with age, will likely be improved by a proper calibration using the seismological measurements of the P1 sample. The minimum number of such stars required to get a statistically significant result is around 245,000, out of which we expect several hundred transits from telluric planets. As for the first sample we would also expect many more transiting larger planets. Hence, more than 245,000 dwarfs and sub-giants later than spectral type F5, with a noise level below 8×10^{-5} in 1 hr, with m_V typically between 8 and 13, must be observed with the required duty cycle for more than 2 (goal 3) years.

The above noise levels are specified as corresponding to photon noise only. With the addition of requirement **R6b** below, ensuring that the measurements remain photon-noise limited, similar noise levels are expected when taking into account all sources of noise.

3.1.4 Duration of monitoring

R3a & b: The total duration of the monitoring of the first and second fields must be longer than 2 (goal 3) years.

R3c: The step and stare phase at the end of the mission must have a duration of at least 1 (goal 2) year. During this phase, previously monitored fields, as well as additional fields, will be surveyed for at least 2 months and up to 5 months each. In addition, further visits to the previously surveyed fields will be organized in an optimized way to study long period exoplanets (several years), whose transits could occur at any time during the step and stare phase.

3.1.5 Time sampling

The duration Δt_{tr} of a transit of a planet with semi-major axis a and orbital period P in front of a star with radius R_{star} is given by $\Delta t_{tr} = P\ R_{star}\ /(a/\pi)$. For true Earth analogues $\Delta t_{tr} = 13$ hours. More generally, the duration of a transit around a single star may last from about 2 hours (a “hot giant" planet around a low-mass star) to over one day, for planets on Jupiter-like orbits (5 AU distance). Planets in the habitable zone, however, will cause transits lasting between 5 hours (around M stars) and 15 hours (for F stars), for equatorial transits.

Because individual transits have durations longer than 2 hours, a time sampling of about 10 to 15 minutes is in principle sufficient to detect all types of transits, as well as to measure transit durations and periods. However, a higher time resolution is needed in order to accurately time ingress and egress of the planet transits for which the S/N in the light curve will be sufficient. The accurate timing will allow the detection of third bodies, which cause offsets in transit times of a few seconds to about a minute, and will allow to solve ambiguities among possible transit configurations through the determination of ingress and egress time of the planet. In practice, a time sampling of about 50 sec will be necessary to analyze in such detail the detected transits.

The needed time sampling for the asteroseismology objectives can be derived directly from the frequency interval we need to explore, which is from 0.02 to 10 mHz. In order to reach 10 mHz, the time sampling must correspond to at least twice this frequency, i.e. of the order of 50 sec.

R4a: The sampling time for intensity measurements of stellar samples P1, P2 and P3 must be shorter than 50 sec.

R4b & c: The sampling time for intensity measurements of stellar sample P4 & P5 must be shorter than 10 min, and shorter than 50 sec after a first transit detection, for a precise timing of further transits.

R4d: The sampling time for relative astrometric measurements of stellar samples P1, P2, P3, must be shorter than 10 min, and shorter than 50 sec after a first transit detection. Astrometric measurements with a time sampling of 50 sec are also required for samples P4 and P5 after a first transit detection.

3.1.6 Photon noise versus non-photonic noise

R6a: the photon flux of the target stars must be sufficiently high to ensure that photon noise allows achieving the photometric noise requirements.

R6b: all other sources of noise must remain at least 3 times below that of the photon noise, at least for stars of sample P1, in the frequency range 0.02-10 mHz. Downward of 0.02 mHz, the non photonic noise level is allowed to rise gradually, to reach a maximum of 50 ppm per $(\mu Hz)^{1/2}$ in Fourier amplitude space at a frequency of 3 μHz, for stars with $m_V = 11$.

3.1.7 Overall duty cycle

The probability that N successive transits of the same planet are observed is given by $p_N = d_f^N$, where d_f is the fractional duty cycle of the instrument. In order to achieve an 80% probability that all transits of a three-transit sequence are observed, a duty cycle of 93% is needed, ignoring gaps that are much shorter than individual transits. The requirement for planet-finding is therefore that gaps which are longer than a few tens of minutes do not occur over more than 7% of the time, with a loss by gaps as small as 5% being desirable.

A similar requirement is also imposed for seismology. Gaps in the data produce side lobes in the power spectrum, which make mode identification ambiguous. Periodic gaps in the data must be minimized, as they will produce the most severe side lobes in the power spectra. It can be shown that periodic outages representing 5% of the total time produce aliases with a power of about 1.5% of that of the real signal. Such side lobes are just acceptable, as they will remain within the noise for most of the stars observed. It is therefore required that periodic data gaps are below 5%.

Non-periodic interruptions have a less catastrophic influence on the power spectrum, and can therefore be tolerated at a higher level, provided the time lost is compensated by a longer elapsed time for the observation. Random gaps in the data representing a total of 10% of the monitoring time yield side lobes with a power lower than 1% of that of the real signal, which will be adequate for this mission. The requirement on random data gaps is therefore that they do not exceed 10% of the elapsed time.

R7a: Gaps longer than 10 minutes must represent less than 7% (goal 5%) of the total observing time per target, for the longest possible observation period (3 years).

R7b: Periodic gaps of any duration must represent less than 5% (goal 3%) of the total observing time, and less than 2% at any given frequency in Fourier space, over periods of 5 months.

R7c: The total amount of gaps, periodic or non periodic, of any duration, must represent less than 10% (goal 5%) of the total observing time over periods of 5 months.

3.1.8 Colour information

In addition to the measurement of oscillation frequencies, asteroseismology requires the identification *(ℓ,m)* of the detected modes. Knowing the ℓ identification for the dominant modes of each of the bright target stars of PLATO implies a significant reduction of the free parameter space of stellar models and is a requirement to guarantee successful seismic inference of their interior structure parameters and ages. For oscillations in the asymptotic frequency regime, the derivation of frequency spacing's is enough to identify the modes. For most main-sequence stars excited by the κ mechanism, when the modes do not follow particular frequency patterns, the identification of ℓ can be achieved by exploiting the difference in amplitude and phase of the mode at different wavelengths. Therefore, some degree of colour information must be present in the PLATO data.

R8: Part of the payload must provide photometric time series in at least two separate broad bands (see **R0b**). At least two of the telescopes, or a dedicated subset of individual detectors, must provide photometric monitoring in at least two separate broad bands (one band per telescope). The photometric bands must be maximally separated, in such a way that the photon flux integrated in the common wavelength range represents less than 10% of the total photon flux. Less than 50% of the photons are allowed to be lost due to this broadband photometry.

3.1.9 The need to go to space

The science goals of PLATO require the detection and characterization of a very large number of planetary transits, as well as the seismic analysis of their host stars. As explained above, this requires very high precision, very long duration and high duty cycle photometric monitoring, which cannot be done from the ground. The Earth's atmosphere causes indeed strong disturbances that limit the achievable performance to milli-magnitude accuracies, mostly through scintillation noise. The small amplitude of the photometric dips caused by terrestrial planets is therefore beyond the range of ground-based observations.

Alternative techniques can be used from the ground to detect new exoplanets, and this field has seen tremendous progress in recent years. The most efficient of these relies on radial velocity measurements,

performed by high resolution spectroscopy. The most severe drawback of the radial velocity technique is that the resulting mass determination suffers from the sin *i* ambiguity, except in the rare cases where the inclination angle *i* can be estimated. Photometric transit techniques are the only ones that can overcome this difficulty. In addition, long, uninterrupted observations, that only space-based instruments can provide, are necessary to optimize the probability of transit detection, as well as to avoid side lobes in stellar oscillation power spectra. Achieving a high duty cycle ($\geq \sim 95\%$) is very difficult from ground, even if a network of multiple telescopes, or a powerful observatory in Antarctica, would be available. Space is therefore necessary to achieve the goals of PLATO, on one hand because of its stability and the absence of photometric disturbances, and on the other hand because it offers the possibility to perform the long, uninterrupted observations that are needed to detect exoplanets and to perform seismic analysis of their host stars.

4 PAYLOAD AND EXPECTED PERFORMANCE

The purpose of this chapter is to provide a summary of the PLATO instrument description and expected performances. It covers the cameras, their focal planes, all related electronics and the onboard data processing system (DPS). The PLATO instrument as defined here, plus the optical bench on which the 34 cameras are mounted, constitute the PLATO payload.

4.1 Basic Instrument Concept

The instrument concept is based on a multi-telescope approach, involving a set of 32 “normal” cameras working at a cadence of 25 s and monitoring stars fainter than m_V=8, plus two “fast” cameras working at a cadence of 2.5 s, and observing stars in the magnitude range 4 to 8.

The cameras are based on a fully dioptric telescope including 6 lenses. Each camera has a 1100 deg^2 field of view and a pupil diameter of 120 mm.

The 32 “normal” cameras are arranged in four groups of 8 cameras. All 8 cameras of each group have exactly the same field of view, and the lines of sight of the four groups are offset by a 9.2° angle from the PLM +Z axis. This particular configuration allows surveying a total field of about 2250 square degrees per pointing, with various parts of the field monitored by 32, 24, 16 or 8 cameras. This strategy optimizes both the number of targets observed at a given noise level and their brightness. The satellite will be rotated around the mean line of sight by 90° every 3 months, resulting in a continuous survey of exactly the same region of the sky.

Each camera is equipped with its own focal plane array, comprised of 4 CCDs with 4510×4510 pixels each, working in full frame mode for the “normal” cameras, and in frame transfer mode for the “fast” cameras. The CCD working temperature is -65°C. The focal plane is cooled down through a thermal link with the telescope, the energy being radiated away by the baffle. The power dissipated by the front-end electronics linked to each focal plane is evacuated by the optical bench (PLM).

There is one Data Processing Unit (DPU) per 2 cameras performing the basic photometric tasks and delivering a set of light curves, centroid curves and imagettes to a central Instrument Control Unit, which stacks and compresses the data, then transmits them to the SVM for downlink. Data from all individual cameras are transmitted to the ground, where final instrumental corrections, such as jitter correction, are performed. The DPUs of the fast cameras will also deliver a pointing error signal to the AOCS, at a cadence of 2.5 s.

Each assigned target star will be allocated a CCD window around it from which all the pixel values will be read out and transmitted to ground, forming a small image called an "imagette". The size of this window is typically 6x6 pixels (9x9 pixels for the fast cameras), large enough to contain the whole image of the target star. These imagettes will be used on ground to derive the PSF at different positions of the detector, a step which is needed to define the photometric extraction masks, and to verify the quality of the photometric and centroiding data being obtained by the onboard automatic processing (see section 6.7.1).

4.2 Instrument Breakdown

The instrument is composed of the following main sub-assemblies:

- 32 normal cameras, organized in four sub-groups. Each camera is composed by:
    - A Telescope Optical Unit (TOU): its mechanical structure supports the optical lenses and the baffle with thermal and stray-light functionalities,
    - A Focal Plane Assembly (FPA), which supports the four CCD detectors, which also includes the 4 flexi-cables of the 4 detectors, to be connected to the FEE,
    - The Focus Adjustment Shims (FAS) between TOU and FPA, used as the adjustment device to put the detectors at the best optical focus,

    - The thermal equipment including: MLI at least around the FPA and its I/F cables with FEE, the heaters and temperature sensors used for the camera temperature control and the temperature sensors used for monitoring the temperature at various points on the camera,
    - The Front End Electronics (FEE) box, located close to the FPA, including mainly the 4 video chains, the CCDs phase-drivers and the temperature sensor acquisition and conditioning.
- 2 fast cameras, with similar sub-systems called fast TOU, fast FPA, fast FEE..., differing from the normal cameras by a narrower optical bandwidth (to provide a chromatic photometry), and the use of the same detector but in frame transfer mode (to allow for faster readout and to provide the position error information to the SCAO, but with half the number of light sensitive pixels).
- Electronic units, composed of:
    - Ancillary Electronics Units (AEUs), mainly composed by the DC-DC converters used to power the associated FEE, and the synchronisation board used to have a fully synchronised acquisition by all the cameras. Physically, they are grouped together in 5 boxes, 4 for normal cameras, and 1 for fast cameras,
    - Normal Data Processing Unit (N-DPU). Each N-DPU is associated to 2 FEEs. They are grouped together by 4 in the same box called Main Electronics Unit (MEU). There are 4 MEUs (16 N-DPUs) for the 32 normal cameras, each one including its own power supply electronics.
    - Fast DPU, functionally associated to the fast FEE. There are 2 Fast DPUs, one per fast FEE, grouped in one box called Fast Electronics Unit (FEU), also including its power supply.
    - Two Instrument Control Units (ICU), used in cold redundancy, and functionally completely independent. Each, if active, can exchange data with all N-DPUs, all Fast DPUs, and with the SVM. The 2 ICUs are grouped in a single box with their own power supply.
    - On-board software, operating on the DPUs and ICUs, which can be modified during the flight.

The cameras are located inside the PLM, protected from the Sun by the sunshield. The electronics can be located either in the PLM or in the SVM.

4.3 Instrument Factsheet

By definition:

- A telescope is the unit including the optics, the barrels, the support structure, the dedicated baffle and the dedicated thermal hardware
- A detection subsystem is an FPA + FEE + related harness
- A camera is a subassembly which includes a telescope and a detection subsystem
- The DPS includes: MEUs, FEUs, ICUs, related power supplies and software
- An instrument is the full functional chain including a camera, and all the electronics and software associated to the camera and internal harness up to the interface with the SVM.
- The payload is the full set of instruments.

Characteristics	Value	Comments
Optics	Full refractive design with 6 lenses and 1 entrance window	Axi-symmetric design
Optics spectral range	500 – 1050 nm	
Pupil diameter	120.0 mm	For one telescope
Normal camera field of view	~ 1100 deg^2 ~circular, diameter 38.7 deg	For each telescope
Normal camera detector	Full frame CCD 4510×4510 18 μm square pixels	
Fast camera field of view	~ 550 deg^2	For each telescope. Only 50% of the focal plane light sensitive.
Fast camera detector	Frame transfer CCD 4510×2255 light sensitive, 18 μm square pixels	
Plate scale	15.0 arcsec / px	For both normal or fast telescope
PSF surface	Always included within 9 px	
Payload field of view	Overlapping FoV of 2232 deg^2	32 cameras looking on 301 deg^2 24 cameras looking on 247 deg^2 16 cameras looking on 735 deg^2 8 cameras looking on 949 deg^2
Equivalent pupil size	678.8 mm for 32 cam 587.9 mm for 24 cam 480.0 mm for 16 cam 339.4 mm for 8 cam	
Focal plane layout	4 CCDs in a square	
CCD temperature	< -65°C	By passive cooling
Read-out frequency	4 Mpx / sec	For both normal or fast telescope
Read-out noise	55 e- rms / px	Global for detector and electronics, at nominal read-out frequency
Read-out noise fast cameras	90 e- rms / px	Global for detector and electronics, at nominal read-out frequency
Normal camera CCD cycle period	25.0 sec fixed	
Fast camera CCD cycle period	2.5 sec fixed	To be confirmed with AOCS needs
Normal camera exposure time	~ 22.0 sec fixed	+ a shorter exposure time for on-ground, at room temperature, tests
Fast camera exposure time	~ 2.3 sec fixed	
Pointing error rate	2.5 sec fixed	
Number of telescopes	32 Normal + 2 Fast	
Power needed by payload	~ 820 W	Including 20% uncertainties
Mass of the payload	~ 600 kg	Including 20% uncertainties
Electronics	1 FEE / camera 1 DPU / 2 cameras 2 ICUs in cold redundancy	FEE and CCD activities are fully synchronised
Science Operation Centre	Under ESA responsibility	
Orbit type	Sun-Earth system L2	
Life time in orbit	> 8 years	
Eclipse	none	
Observation phases	1st and 2nd: 2 or 3 years	1 pointing / phase
Step & stare phase	> 1 year	With several pointings
Attitude	90° rotation around the LoS every 3 months	

4.4 System Design

4.4.1 Overlapping field-of-view concept

The main driver for choosing the instrument basic configuration is related to the need to optimize simultaneously the number and the brightness of observed cool dwarfs and sub-giants. The concept of overlapping field-of-view, offering a very wide field of view covered by a variable number of cameras, is derived from this main idea.

In addition to this basic motivation, the overlapping field-of-view allows us to re-observe, during the step & stare phase, some stars for which particularly interesting planets were detected in the long monitoring phases of the mission (in particular for instance telluric planets in the habitable zone), but only with a sub-set of telescopes, therefore without reaching the ultimate photometric precision. During the step & stare phase, these targets can be put in the part of field observed with all 32 telescopes, allowing the best photometric precision.

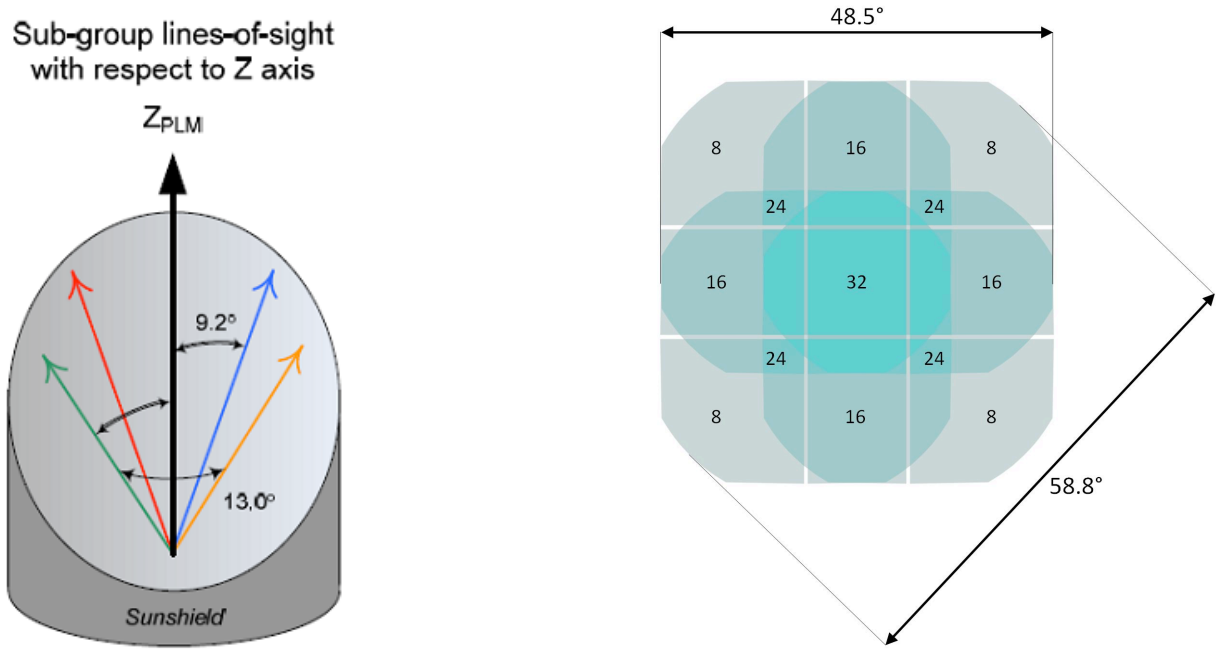

Fig 4.1: The overlapping line-of-sight concept (left) and the resulting field-of-view configuration (right)

The overlapping field of view configuration includes 4 sub-groups of cameras, each with 8 cameras, all the cameras of one sub-group having the same LoS, and the 4 sub-group LoS being tilted by a 9.2° from the Z axis of the PLM.

The result of this configuration is an overall very wide field of view (2250 deg^2, diameter ~53°), with a variable pupil size across the field:

- The centre, seen by the 32 cameras, offers the largest pupil size, but is limited in size to 301 deg²
- A second zone, seen by 24 cameras, offers an intermediate pupil size with a FoV of 247 deg²
- A third zone, seen by 16 cameras, offers an intermediate pupil size and a FoV of 735 deg²
- A fourth zone in each of the 4 corners of the FOV, seen by only 8 cameras each, with the smallest pupil size, and with a total FoV of 949 deg²

3Opto-mechanical architecture

The opto-mechanical architecture of the payload results from optical, thermal and mechanical constraints:

- All 34 cameras must be as identical as possible (except the focal plane detectors, which will be different in the fast cameras, operating in frame transfer mode)
- They must be mechanically and thermally independent (only linked by the PLM optical bench)
- The link of the telescope to the optical bench (or a camera support) must be isostatic, and shall ensure an orientation of the camera around its optical axis
- Any camera must not obstruct the FoV of any other camera
- The 32 normal cameras are grouped in 4 sub-groups of 8 cameras with a common LoS
- The 2 fast cameras are co-aligned with the Z_{PLM} axis
- The inner surface of each individual baffle shall not see the sunshield for both thermal and stray-light reasons
- Each camera (excluding its FEE) must be thermally decoupled from other cameras and from all satellite structural elements
- The FEE shall be located close to its associated FPA

The tilt of the normal cameras with reference to the PLM reference (9.2°) is given by a specific part: the skew spacer, supplied by the satellite contractor. This part interfaces the cameras and the optical bench. The orientation of the camera I/F plane can be obtained directly by manufacturing or by addition of shims which could be used for adjustments of the camera axis with reference to Z_{PLM} axis. One can also note that the skew spacers are all identical: only their orientation around Z_{PLM} axis changes as a function of the direction of the tilt. We have four angular positions of these spacers 0, $\pi/2$, π and 3 $\pi/2$ rad.

All cameras are externally identical and have identical interfaces. They are fixed on skew spacers via 3 bipods positioned at 120° around Z_{CAM} axis (see TOU mechanical design below). The 3 bipods are strictly identical.

	Cutting angle	Orientation around Z_{CAM}
Fast Camera	30.00°	0
Normal Type 1 & 4	37.03°	± 9.05°
Normal Type 2 & 3	24.30°	± 14.23°

Table 4.1: Baffle angular characteristics

Baffles are needed for both thermal control of the cameras and stray-light protection. Their external surface is insulated (MLI) from the radiation of other cameras and all other surfaces of the payload. Their internal conical surface is used as a radiator toward deep space. Their higher end is cut at an angle of 30° with respect to the XY_{PLM} plane so that their inner surface cannot "see" the sunshield. There are three different shapes for the baffles: one for fast cameras and only two for covering the four different tilts of normal cameras. The basic characteristics of the three groups of baffles are listed in Table 4.1.

Figure 4.2 shows the overall mechanical configuration.

The FEE boxes are located approximately 65 mm below the bottom of the focal plane assembly, in compliance with the required free length of CCD flexi-cables. They are mechanically linked to the PLM, rather than to the cameras.

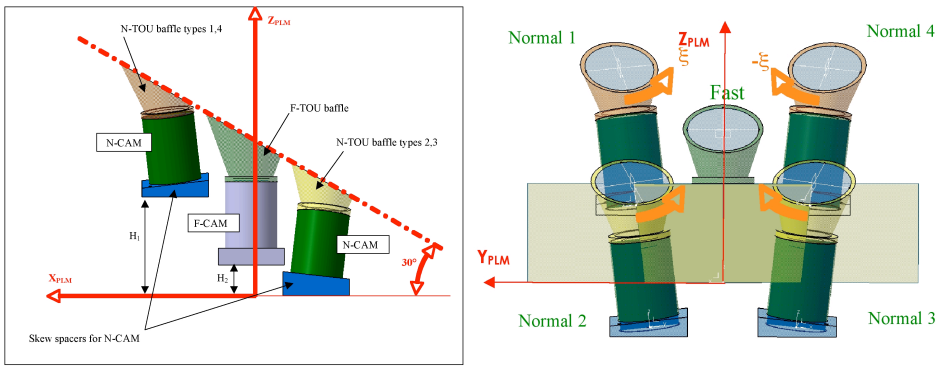

Figure 4.2: Mechanical configuration.

4.4.2 Thermal Architecture

The FPA power is evacuated along the +Zcam axis, by way of the baffle which radiates it away toward deep space. The structure of the telescope is highly conductive in order to minimize temperature gradients, while the baffle is dimensioned for the evacuation of the FPA power by radiation.

The detector temperature is specified as lower than -65°C, for dark current and radiation effect minimization. The optics will necessarily be cold because (i) the front window sees the sky under a large solid angle , (ii) the last lens, close to the cold detector, is also cold, (iii) thermal gradients inside the optics should be avoided for performance aspects. The optics temperature is specified at -80°C at the temperature reference point (TRP), compatible with the temperature specified for detectors. The FPA thermal control system will maintain the optics at the selected temperature, measured at camera TRP, while maintaining the FPA below its maximum specified temperature.

The performances of the camera are strongly related to its temperature stability. To ensure thermal stability, the camera (w/o FEE) is strongly isolated from temperature variable (or not controlled) sources (sunshield inner surfaces, optical bench...). The fixation bipods of the camera and the flex-cables between FPA and FEE have low thermal conductance, and MLI is installed on critical surfaces for radiative coupling limitation. The FEE is cooled through the optical bench, being developed by the spacecraft contractor.

Moreover, it is planned to have the possibility to slightly change the camera temperature, in order to optimise the PSF size and shape. This is obtained by controlling the camera temperature in a small range around its nominal working temperature: presently a range -75°C to -85°C is required, but could be easily extended later on to yield a better PSF optimization of each camera.

All electronics boxes will be kept within specified temperature ranges, and with specified stabilities, by the overall thermal control provided by the SVM. The temperature control is provided by the SVM, so that the temperature of the equipments can be controlled during all the phases of the mission, even when they are not powered.

Fully independent of the temperature control, a temperature monitoring system measures the temperature in several points on the camera, using 2-5mK resolution sensors, in limited temperature ranges, and at a sampling rate of 1 sample / 6.25 sec for normal cameras and 1 sample / 2.5 sec for fast cameras. Thus, temperature variations can be monitored at very high sensitivity. These sensors, located on the camera structure, are acquired and conditioned by their associated FEE, and their data are added to the headers of image data. This allows the possibility to monitor temperature variations as low as 0.1 mK by use of filtering or averaging on timescales in the order of minutes.

The main characteristics of the thermal architecture are:

- Thermally strongly coupled FPA and telescope structures
- Inner surfaces of the baffle with good emissivity (black anodise)
- Coupling between baffle and structure used as parameter for temperature range trimming.
- FPA + telescope structure + baffle units are as isolated as possible from the rest of the satellite and from the sky.

- The fixation bipods and the flex-cables between FPA and FEE have as low thermal conductivities as possible.

Baffle outer surfaces, telescope structure, FPA, bipods and FEE top surface are covered by MLI, for radiative flux limitation.

4.4.3 Electrical architecture

Digital electronics

Digital functions are implemented into several units: the CCD image processing is performed by either the normal DPUs (located in the MEUs) or by the fast DPUs (located in the FEUs). All data processed by the DPUs are transmitted to the ICU for additional treatments. Each MEU also hosts two SpaceWire routers to merge the data from the 4 N-DPUs. A SpaceWire router unit is also implemented in each ICU to merge data from the 4 MEUs and the 2 FEUs. For redundancy, the SpaceWire router unit of ICU-A and that of ICU-B can be switched on simultaneously by the active ICU Processor Unit, and work in hot redundancy.

For commandability and monitoring purposes, the 4 normal AEUs and the F-AEU are also connected to the SpaceWire network. The ICU-PSU (Power Supply Unit inside ICU) is also driven by the active ICU Processor Unit by a dedicated SpaceWire link.

Due to the large number of cameras the data flow architecture is hierarchical: each camera has its front end electronics (FEE) in charge of the readout of all four CCDs of an FPA. Therefore each FEE includes a phase sequencer, 8 analogue processing and 14-bit digitization electronics as well as adjustable biases.

In addition each N-FEE includes two high performance SpaceWire bidirectional serial interface, in order to (i) transfer the digitized CCD raw data, (ii) receive low level commands from digital electronics, (iii) transfer digital housekeeping to the ICU via the MEU. Digital data are then processed in the N-DPU sub-systems of the MEU. Each F-FEE includes 8 SpaceWire bidirectional serial interfaces, with the same functionalities as above.

When processed the digital data are gathered by the ICU which is ultimately in charge of the generation of telemetry packets towards the SVM mass memory. Similarly, all sub-system housekeeping parameters are gathered by the ICU, which is in charge of generating corresponding telemetry packets. Bidirectional data transfer between DPU and ICU is achieved by mean of 4 (MEU) + 2 (fast DPU) SpaceWire links. Configuration commands are received by the ICU from the SVM. According to their destination, the commands are processed and routed either to MEU, FEU, N-AEU, F-AEU or MEU-PSU. Finally the command is routed to FEE (through DPU) when applicable.

Clock and synchronization signal distribution

EMC coupling between harness cables or between electronic boxes is inevitable. In order to avoid that these interferences result into variable patterns in the images, and ultimately into unacceptable noise in the final photometric signal, the general concept is to synchronise all activities on a single clock signal, especially those of low level analogue electronics (detectors, attached video electronics, power supplies, active thermal control). With this precaution, a possible EMC coupling between two or several subsystems, will only results on a fixed pattern in the data, which can be managed like others stable perturbations.

All activities of the cameras are synchronised by a unique reference clock distributed to all sensitive boxes: FEEs (normal and fast), AEUs (normal and fast), detectors (by the way of FEEs) and active thermal control.

Two synchronisation signals are needed:

- A reference clock signal at a high frequency, which is used by the master FPGA located inside the FEE as its frequency reference. This FPGA manages the activity of the CCD (frame transfer, line transfer, pixel readout, reset, DC-restore signal…) and of the video electronics (clamp, start conversion…).
- A "PPS" signal at a lower frequency, which gives the start signal to all cameras, and marks out the first detector readout start.

The proposed solution consists of a low power, low mass box located close to the centre of the optical bench, including reference oscillators, frequency dividers, commutation logic for switching on main or redundant chain, and line drivers for sending the needed synchronisation signals.

Power distribution

Secondary power generation for analogue electronics is concentrated in the AEU units. Each unit hosts a bench of 5 independent DC/DC converters (one converter per telescope). Each AEU has a redundant interface with a platform regulated power line. Secondary power generation for ICU MEU and FEU is performed locally in each unit.

Redundancy concept

A high level of redundancy is reached in the PLATO payload, mitigating the impact of electronic unit or function failure. As a first step, single point failures were identified, and suppressed whenever possible via cold redundancy.

The ICU is at the heart of the payload, and losing this function would imply the loss of the whole payload. The ICU function is therefore fully redundant. The ICU function is divided in three sub-functions: power supply of the ICU function, processing function and router function. These 3 sub-functions are redundant and cross-strapped.

When redundancy is not applicable, the principle is to split the functions into sub-sets in order to limit the effect of a failure by limiting its propagation. Analogue electronics and associated power converters rely on this type of architecture: rather than having a single large DC/DC converter to feed all the FEEs, a bench of DC/DC is used. In case of a failure of one of the FEE (e.g. over-current) only the corresponding DC/DC converter is affected. This can be easily managed by having current limiters in the converter. Thermal control lines, comprising 3 temperature sensors, use the median value for feedback power to two redundant heaters.

The general philosophy we have adopted is the following: one failure in a normal chain equipment (as example an AEU) should affect only one normal camera with the risk of loss of this camera only, except for the N-DPU whose failure would affect two cameras simultaneously; two failures in the same normal chain equipment could affect more than 1 normal camera; the two fast chains are fully independent, and one failure in a fast equipment should affect only one chain with the risk of loss of only this fast camera.

4.4.4 Data treatment architecture

With 32 normal cameras working at the cadence of 25 seconds and 2 fast cameras working at the cadence of 2.5 seconds, the amount of raw data produced each day is close to 189 Terabits. This volume must be compared to the ~109 Gbits which can be downloaded each day to the ground. The role of the on-board treatments will be to reduce the flow rate by a factor > 1000 by down-linking only light curves, centroid curves and imagettes at the cadence required by the science. Data flow studies have shown that it is possible to individually download to the ground the processed data from each camera, rather than the average of all cameras only. Such a possibility will reduce the complexity of the on-board treatments (no on-board averaging of the data and fewer corrections to be implemented on board).

Main data processing algorithms

The final goal of the data processing is to provide light-curves that fulfil the requirements in terms of white noise and coloured noise. Due to the limited bandwidth of the telemetry, light-curves must be calculated on-board. Because the performances of the DPUs are too limited to perform a 2D PSF fitting for such a high number of targets, simpler algorithms such as mask photometry are baselined. We give below a summarized description of the algorithms to be run, either onboard or on the ground. A more complete description is available in the documentation provided for the Preliminary Requirement Review and in the “final implementation plan” documentation.

Weighted mask photometry: Instead of using a classical aperture (binary) mask, we will use a weighted mask derived from a simple analytical function, e.g. a Gaussian. Such a method, by putting more weight in the centre of the star image than in its wings, can reduce the pollution induced by the presence of a neighbouring fainter star.

Mask update: To prevent the star from going out of the mask due to the differential aberration we will update the mask positions frequently. Discontinuities induced by mask updates can be minimized using weighted mask photometry, provided masks are updated frequently.

Photometric correction of the satellite jitter: Jitter correction can be easily performed as soon as we know accurately the PSF associated with a given target and the displacements of that target at each instant, as well as the positions and intensities of the neighbouring contaminants. Since the PSF, the mask and the star displacements differ from one camera to another, the jitter correction is different from camera to camera. Since the light-curves from all individual telescopes will be down-linked, this correction can be done on-ground with methods that are being developed, based on similar techniques derived in the framework of CoRoT.

Outlier detection and rejection: The photometry of a star will be obtained by averaging (on-ground) intensity measurements originating from different cameras. Furthermore, for most targets, the star intensity is time-averaged on-board. Before performing such averaging (in time and space), we will discard those measurements that depart significantly from a reference level. This reference level will be obtained on-board on the basis of the median and the standard deviation computed by considering the measurements from the different cameras simultaneously monitoring the same star.

PSF modelling: In order to correct the light-curves from photometric variations induced by satellite jitter and differential aberration, it is crucial to derive the PSF associated with each target. The PSF is changing across the field of view. It will obviously not be possible to derive the PSF associated with each of the ~125,000 stars. Instead, we will acquire during calibration time series of imagettes for several thousands reference stars. From this set of imagettes, we will derive a model of the PSF using an inverse method. Then, in order to derive the PSF of all other stars, we will perform an interpolation of the PSF model on the location (X,Y) of the target and – if needed – on the colour (B-V) of the target.

Sky background modelling: Zodiacal light is expected to be the major contributor to the background, and is expected to vary on a monthly basis, as well as across the field. The background will therefore be frequently measured and modelled, e.g. by a bivariate polynomial. The parameters of this model will be fitted and used during observations to derive the background associated with each target.

Accurate positions of the targets: We need to define masks at any given time for around 125,000 stars, which requires an accurate determination of the star positions on the CCD. As soon as we know the pointing direction of a given camera, the optical distortion, the placement of the CCDs and the distortion of the CCD grid, it is possible to define a set of coordinate transforms relating the star coordinates on the sky (a,d) to its CCD coordinates (X,Y). This will be done using a set of ~1,000 reference stars from which transformation matrices for each camera will be derived.

Data processing system architecture

The PLATO data processing system is made up of an on-board segment and a ground segment.

The PLATO science ground segment (SGS) will be responsible for the main instrumental corrections and will produce calibrated light curves and calibrated centroid curves as level-1 products. The SGS will also perform some a posteriori verification of the onboard processing as well as some calibration (e.g. PSF modelling). Feedback from SGS to the on-board processing will include updates of the mask determination procedures, of other photometry algorithm parameters, of star sample selection, etc.

The payload onboard data treatment is divided into 7 modes, which are briefly described below:

- OFF mode: all the equipments of the payload are off.
- ICU Initialisation: the ICU initialises and establishes the communication with the SVM; ICU is not yet able to take control of the other payload equipments, so in this mode, the ICU is the only equipment of the payload that can be controlled and monitored.
- Stand-by and service mode: the ICU is able to manage the whole Payload. All payload management services can be performed except scientific processes. This mode is mainly used in the following cases:
  - Payload equipments switching on (except ICU switching on)
  - SW maintenance
  - Uploading of star catalogue in ICU memory
  - Waiting in case of LoS loss (during antenna steering, wheel unloading, or 90° rotation)
- Fine pointing initializing: the F-DPU acquires the guide stars and initializes the FGS filter. This mode is run until the F-DPU is able to deliver FGS data to the SVM.

- Configuration for observation: the ICU sends the star catalogues to the DPUs. The N-DPU and the F-DPU acquire the target stars and configure themselves for the observation. This mode is run at the beginning of a new pointing and after each 90° rotation.
- Periodic calibration: the N-DPU and F-DPU process the CCD images in order to update the focal plane geometry model, PSF models, background models and masks.
- Observation mode: the N-DPU, the F-DPU and the ICU perform the scientific processes and produces science TM as described in the chapter on the observation mode (see below).

There are 16 normal DPUs (N-DPU), each connected to two N-FEE. Each N-DPU is responsible for processing the data from two normal cameras. The processing cadence for normal DPUs is 25 sec.

There are 2 fast DPUs (F-DPU). Each F-DPU is responsible for processing the data from one fast camera. The processing cadence for fast DPUs is 2.5 sec.

In the observation mode, the main tasks of the DPUs are:

- To acquire and store full-frame images sent by the FEE (normal DPUs: one 4510×4510-px image / 6.25 sec per normal camera; fast DPUs: four 4510×2255-px images / 2.5 sec).
- To extract the star windows (normal DPUs: ~ 2×163380 6x6-px windows / 25 sec; fast DPUs: ~400 7×7-px windows / 2.5 sec).
- To transmit the imagettes to the ICU.
- To correct data (smearing, offset, background, gain).
- To compute target flux and centroids.
- To update photometric masks and star positions at a cadence of about 5000 seconds to correct for differential kinematic aberration.
- To transmit computed flux and centroids to ICU at the acquisition cadence (25 sec for N-DPUs and 2.5 sec for F-DPUs).

The F-DPUs have a supplementary function: they are responsible for providing pointing error measurements directly to the SVM AOCS.

In observation mode, the role of ICU is:

- To detect and remove outliers by comparing the N measurements from the N telescopes sharing the same LoS (N=8, 16, 24, 32).
- To stack for each telescope the flux and centroids (only the selected data are stacked).
- To compute for each telescope the mean (and the standard deviation) of the stacked measurements (stacked flux and stacked centroids) at a cadence depending of the sample category (50 or 600 sec).
- To compress the data before transmitting them to SVM.

In “configuration for observation” mode, the DPUs are responsible for:

- Identifying the list and the raw positions of the reference stars.
- Computing a background model.
- Computing the accurate positions of the reference stars and the distortion matrix.
- Identifying all the targets and deriving their accurate positions.
- Computing the masks and the window positions of all targets.

The role of the ICU in “configuration for observation” mode is mainly to provide to the DPUs some configuration parameters (catalogue, etc.), to schedule the DPU tasks, to manage the data flow and to perform cross checking operations between data from telescopes of the same LoS.

Figure 4.3 gives an overview of the PLATO data processing system architecture and of the data flow rates. This chart focuses on the sharing of the main functions and the data flows. It is a simplified view of the hardware architecture and does not replace the one given in section “Digital electronics”: the SpaceWire routers are not shown and the DPU assembly boxes (MEU) are not drawn.

4.5 Telescope Optical Unit

4.5.1 Optical design

There is no difference in the TOU design for normal and fast telescopes, but the latter will include low-pass or high-pass filters under form of special coatings on an optical surface of the optical train.

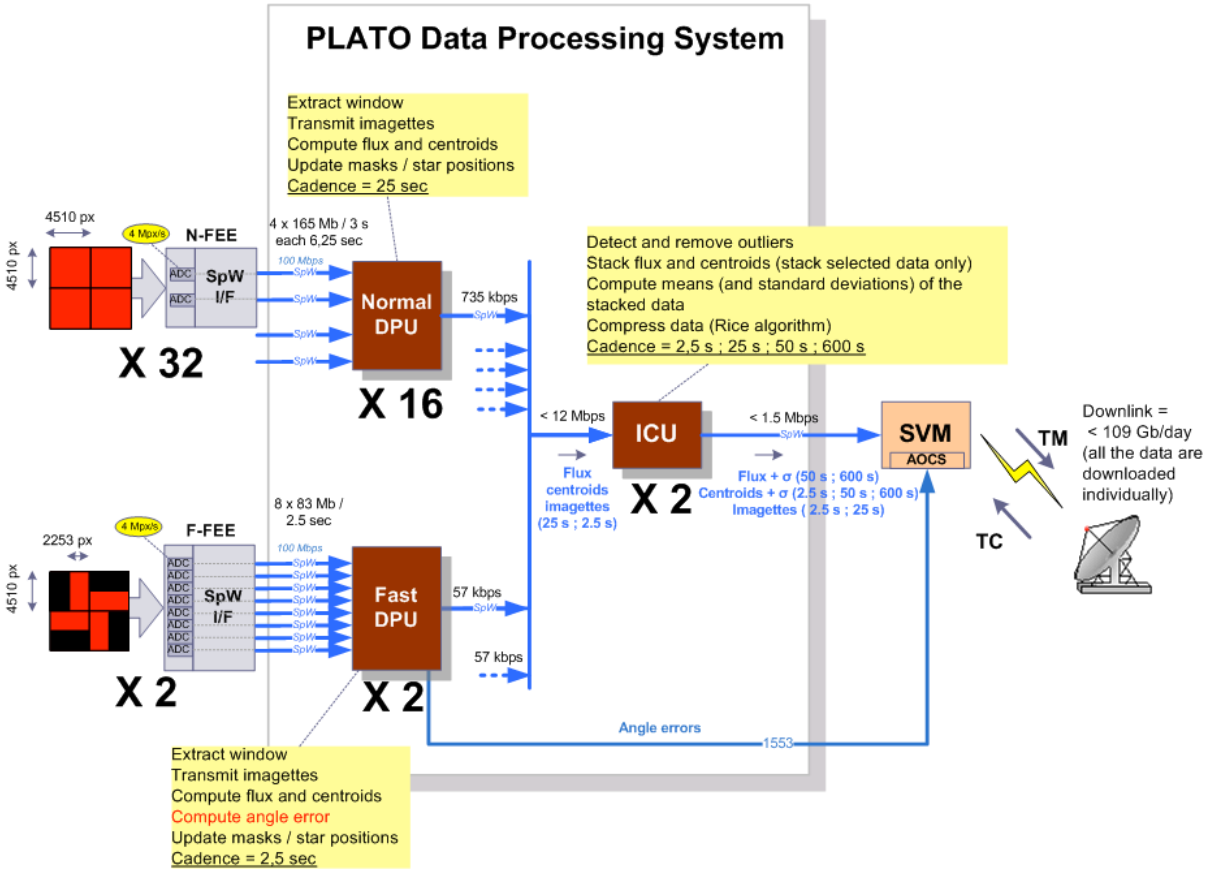

Figure 4.3: The PLATO onboard data treatment architecture

The general performances and parameters of the baseline optical configuration are reported in the table below.

Spectral range	500 – 1000 nm
Entrance Pupil Diameter	120 mm
Working f/#	2.06 @ 700 nm
Field of View	1151.5 degree^2
Image quality	90% Enclosed energy < 2×2 pixel^2 over 1108.3 degree^2
Maximum Field Distortion	5.043%
Plate scale	15 arcsec/pixel
Pixel size	Square, 18 microns
CCD format	4510×4510 (×4) pixel^2
FPA size	164.36 mm (2 mm CCDs gap)
Working Temperature	-80°C (at telescope TRP)
Working Pressure	0 atm

The optical configuration consists of 6 lenses, plus one window, placed at the entrance of the telescope, providing protection against radiation and thermal shocks. The first surface of the first lens contains even aspherical terms (K, a^4, a^6), while the second surface is flat in order to facilitate the interferometric surface measure during the aspheric manufacturing. All the other lenses are standard spherical surfaces. The first surface of the third lens is the optical system stop and guarantees a real entrance pupil diameter of 120 mm. A layout of the design is shown in figure 4.4.

This configuration provides a corrected field of view up to 13.7° (90% of encircled energy within less than 2x2 pixels), while the full field of view is up to 14.3°, accepting slightly degraded image quality, as well as a ~7% vignetting, in this small region at the edge of the field.

4.5.2 Mechanical design

The TOU main structure consists of a machined tube with all the interface planes, threads and holes necessary to mount the other components.

The heat dissipated by the CCD needs to be transported through the TOU structure, which therefore must be made of material with high thermal conductivity. In addition, the large temperature difference between integration and operation requires a design able to accommodate the dimensional changes of the assembled components without leading to unacceptable mechanical stresses.

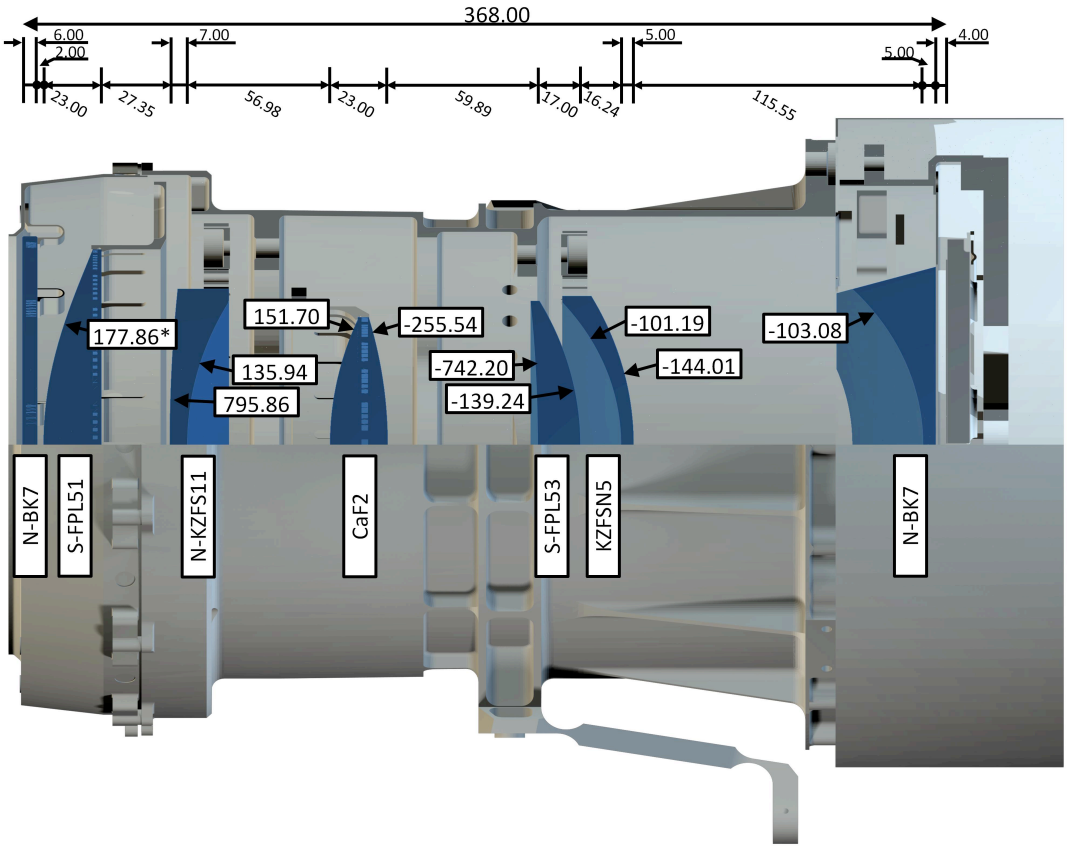

Figure 4.4: The baseline optical layout is shown together with a cross section of the mechanical envelope. One of the attachments point to the optical bench is visible in the lower part while the baffle is missing in this drawing. The structure of the focal plane assembly with the detectors is also seen (at the right side).

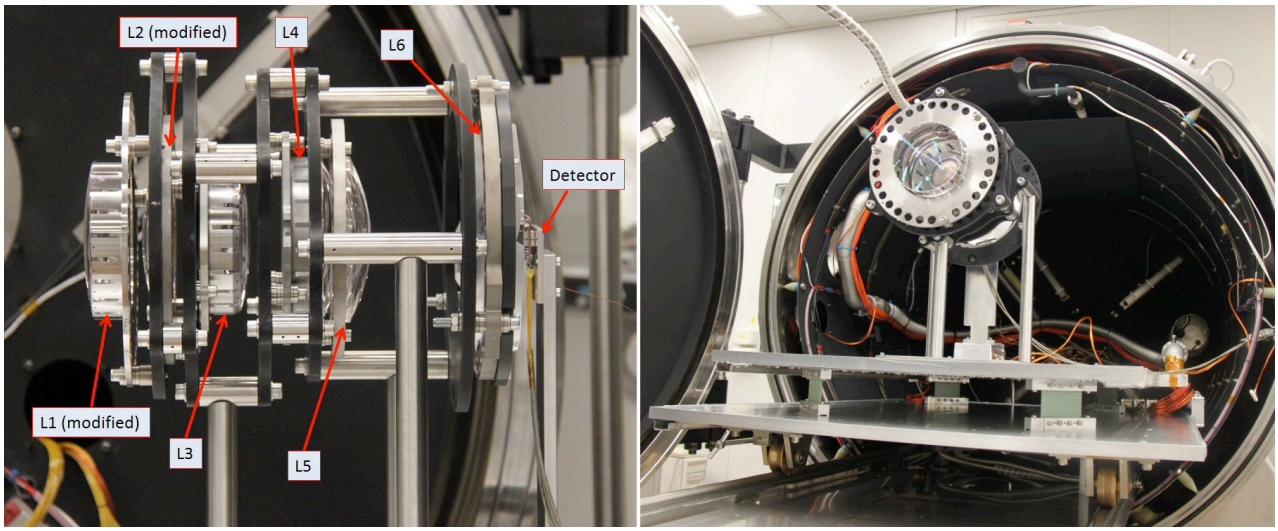

Figure 4.5: The TOU Breadboard (left) as shown on a side with indicated the lenses. Four out of six are nominal ones (including the pupil stop one in Calcium Fluoride) and (right) while entering the cryo-vacuum chamber for the alignment tests.

TOU integration and verification procedures have been defined and are being tested by breadboarding and prototyping activities. Currently a breadboard with 4 out of 6 lenses identical to the nominal ones (other than using the non radiation hardened glass) have been manufactured, integrated, aligned in the warm, measured the optical performances, and re-measured in a cryo-vacuum chamber under conditions very similar to the nominal ones (see also Fig. 4.5). Details can be found in PLATO-INAF-TOU-RP-0013 (issue 02). At the same time two blank in CaF2 with similar size of L3 has been mounted on the same current mechanical design of the holder foreseen in the TOU and subject to vibrational and thermal tests following the specifications given in the launcher manual with an uneventful result.

4.5.3 Thermal design

The thermal design of the TOUs is such that the mean temperature at TRP is -90°C ±1.5°C with the heaters switched off. The TRP location is at a distance of 244 mm from the CCD (near L3).

We must distinguish three cases, depending on the baffle cutting angle: N-TOU #1&4, N-TOU #2&3, F-TOU. Several solutions exist in these three cases, depending on the choice of conductivity between the baffle and the tube, baffle emissivity and presence of low emission filter on the entrance window.

4.6 Focal Plane Assembly

4.6.1 Detectors

The PLATO detector is a CCD with two separately connected sections to allow full frame (FF) or frame transfer (FT) modes. It is a back-illuminated, back-thinned device, non-inverted type (non-MPP), whose characteristics are summarized in the instrument fact sheet at the beginning of this chapter. An antireflection (AR) coating is required on its sensitive surface for quantum efficiency increase. Only one readout register with two outputs is required for both the FF and FT devices. The detector will work at a temperature lower than -65°C.

4.6.2 Focal Plane Assembly Structure

The Focal Plane Assembly structure itself supports the 4 CCDs via quasi-static mount on a support plate, ensuring a good planarity. The support plate is attached to the telescope structure by a stiff interface ring of

the same material as the TOU. It has the possibility to be adjusted in position (along Z_{CAM} and around camera transverse axes) by use of 3 shims located between FPA and telescope. It is electrically isolated from the telescope, and the thermal power dissipated at FPA level is evacuated by the mechanical interface with the telescope, the CCD packages being thermally connected to FPA-telescope interface via flexible thermal straps.

Figure 4.6 shows the CCD array configuration for both normal and fast cameras, while Fig. 4.7 depicts the Focal Plane Assembly.

The flexi-cables have a free length of ~80 mm (TBC) from the bottom of the FPA to the top of the FEE. The distance between FPA and FEE is limited to a nominal value of 65 mm to get slightly bended flexi-cables allowing small misalignments, displacements or rotations between them during AIT, launch.

Extensive analysis has been performed to guarantee PLATO FPA performances, in terms of vibration robustness, flatness, CCD temperature, while remaining within mass and power budget.

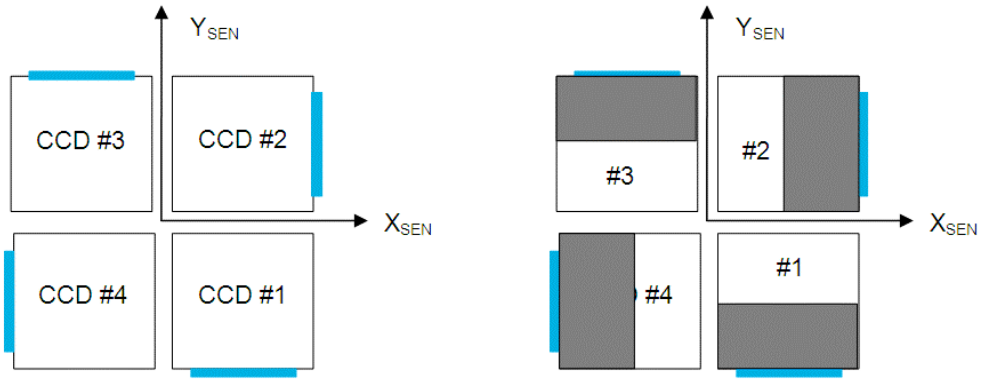

Figure 4.6: The CCD array configuration for normal cameras (left) and fast cameras (right).
Blue rectangles represent the flexi-cables. The shaded area in the fast cameras CCD corresponds to the frame transfer storage area, and is not light sensitive.

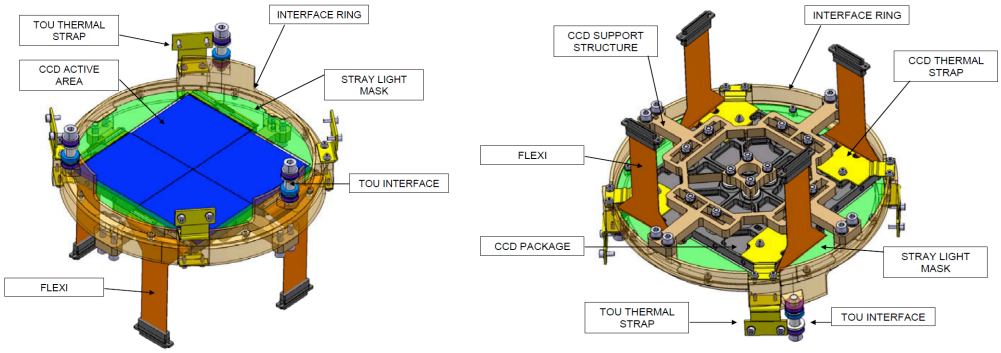

Figure 4.7: The Focal Plane Assembly seen from top (left) and from bottom (right.)

Finally integration and verification procedures for FPA have been defined and are being tested using a mock-up manufactured in Al with the current design (see figure 4.8)

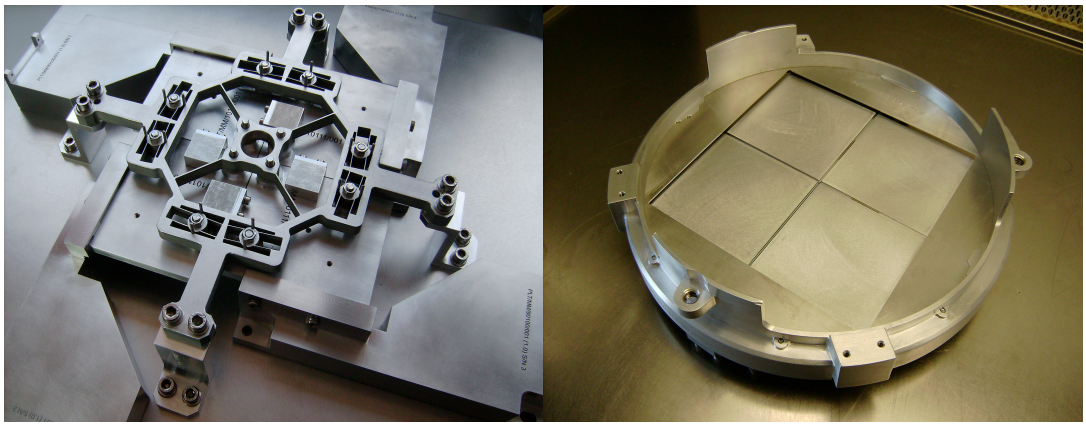

Figure 4.8: The Focal Plane Assembly mock-up. Left, CCD support structure; right, top view with 4 dummy CCD already integrated.

4.7 Front End Electronics (FEE)

4.7.1 Normal Front End Elelctronics (N-FEE)

The N-FEE operates the 4 CCDs of a normal camera, digitises the image data and transfers it to the DPU. Each CCD has an integration time of ~22 s and a readout time of ~3 s. The readouts are staggered at equal intervals of the 25 s period. The readout and data transfer to DPU are arranged so that the readout of one CCD is finished before the next begins, in order to minimise crosstalk and interference effects (see Fig. 4.9.

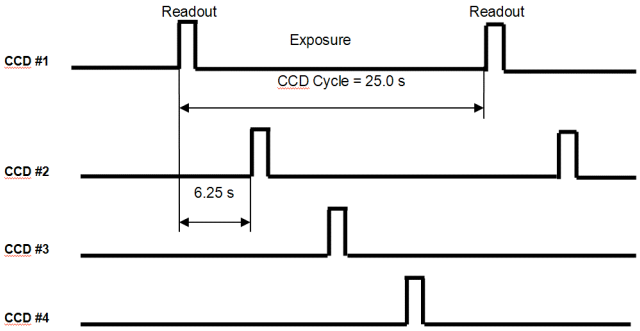

Figure 4.9: N-FEE block-timing diagram.

An FPGA is the core of the N-FEE, receiving command packets from the DPU and timing and synchronisation data from the AEU. It generates all the clocks necessary for driving the 4 CCDs and drives the DACs responsible for providing the bias voltages.

The interface between N-FEE and N-DPU is made by two SpaceWire links. The protocol used is RMAP in all cases, but the command interface is actually simulated RMAP with control registers, HK data, etc..., memory mapped for simple access.

4.7.2 Fast telescope Front End Electronics (F-FEE)

Many aspects are common for N-FEE and F-FEE: commanding, CCD bias supplies, clock waveforms, housekeeping. Other aspects are significantly different, due to the use of frame-transfer devices and shorter integration time: FPGA and programming, number of SpaceWire interfaces and data rate.

In fast cameras, the 4 CCDs are read out simultaneously every 2.5 seconds. Due to less critical noise requirement the F-FEE uses an integrated analogue front-end (AFE) electronics, instead of the non-integrated 16-bit AFE used by N-FEE. As for N-FEE, synchronisation of the two cameras is ensured by receiving from the associated F-AEU a high frequency signal (50 MHz) and a signal giving the information of 2.5 sec period beginning, also synchronised with the 25.0 sec period of the normal cameras.

4.7.3 Ancillary Electronics Unit (AEU)

The N- and F-AEU boxes are located in the SVM. There are 4 N-AEU boxes, one for each group of cameras. Each box contains 8 independent DC/DC converters, dedicated to one N-FEE. There is 1 F-AEU box for the 2 F-FEEs, containing 2 fully independent DC/DC converters, one for each F-FEE.

The N- and F-AEU receive from the SVM regulated 28V power lines, the master clock signal at 50 MHz, and synchronisation links at 1.25 s, and deliver to N- and F-FEE 6 DC voltages and a set of synchronisation signals, for CCD activity management. In addition, the N- and F-AEU receive from the ICU main and redundant SpaceWire links (2 for N-AEU, 4 for F-AEU), as well as discrete command lines.

4.8 Onboard Data Treatment Subsystem

4.8.1 Main Electronics Unit (MEU) and Normal Data Processing Unit (N-DPU)

Each Main Electronics Unit gathers in the same box:

- 4 N-DPU boards: each N-DPU board is responsible for handling two normal cameras.
- 2 SpaceWire routers: one main and one redundant.
- A Power Supply Unit that converts the primary voltage received from the SVM into the secondary voltages needed for powering the N-DPU boards and the routers.
- A Motherboard for internal connections.

Fig. 4.10 shows the MEU architecture.

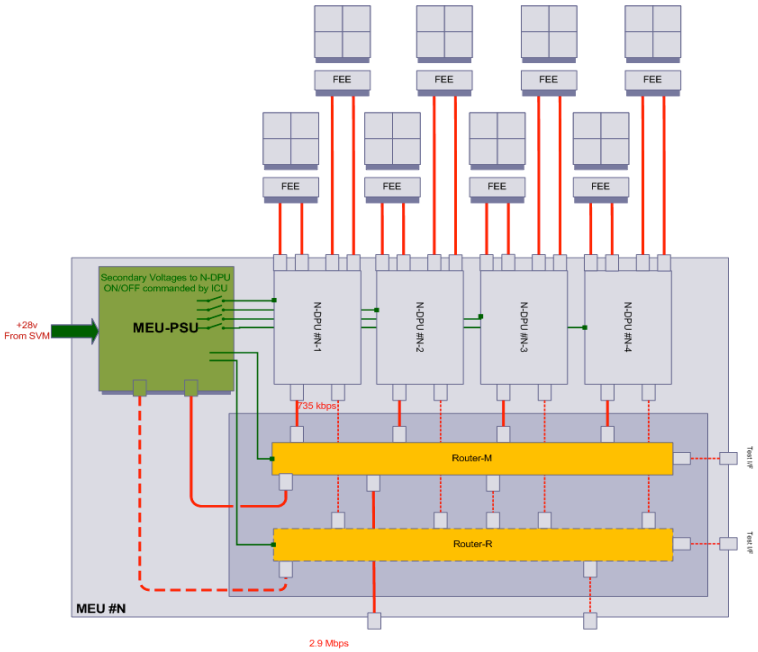

Figure 4.10: MEU box architecture.

Each N-DPU board is connected to 2 N-FEE thanks to 4 SpaceWire links configured to run at 100 Mbps (one SpaceWire link per CCD FEE readout output). Each N-DPU board is connected to the nominal router and to the redundant router. Nominally, both MEU routers are working in cold redundancy. However, to handle certain failure cases, both MEU routers can be switched on simultaneously and can work in hot redundancy.

The instantaneous data rate between 2 x N-FEE and N-DPU is: 2x2x4 Mpx/s x 1.25 = 4x80 = 320 Mbps. With two SpaceWire links between 1 N-FEE and 1 N-DPU, the instantaneous data rate over one link is 80 Mbps, compatible with a SpaceWire link configured to run at a bit rate of 100 Mbps. On the other end, the data rate towards the ICU includes a 50% margin on star count (accounting for the uncertainty on the star field content), the SpaceWire overhead and the packetization overhead. The data rate between one N-DPU and the MEU router is 735 kbps, corresponding to the transmission of about 21 packets per second. The full

data rate between one MEU and the active ICU is: 4x735 kbps = 2.9 Mbps, corresponding to the transmission of about 83 packets per second. The count of extracted windows for 4 CCDs is:

Sample P1	2 x 6720, with margin 50% = 2 x 10080
Sample P4	2 x 102200, with margin 50% = 2 x 153300
Background windows	2 x 400
Imagettes	up to 2 x 2000
Offset windows	2 x 2 x 4 offset windows (2255 pixels)
Smearing rows	2 x 4 x 10 over-scan rows

The application software running on each DPU performs the complete data reduction and photometrical extraction process, as explained in previous sections. It is triggered as soon as a set of windows extracted from a full-frame image is available.

The needed processing power has been estimated by prototyping the main algorithms in C language on a LEON2@100 MHz processor simulator. The measured CPU occupation rate is 37% (CPU load margin = 170%). The conclusion is that the normal N-DPU board can be implemented with one LEON AT697F processor working at 100 MHz. The CPU load margin can be used to improve the algorithms, to implement new algorithms, to process more targets, to update with a higher frequency the photometric masks or to reduce the processor frequency. The total memory required per N-DPU board will be 256 Mbytes, assuming +50% margin in the number of stars to be monitored per CCD.

4.8.2 FEU and F-DPU

The processing of each exposure is identical as that of the N-DPU, except that: (i) the cadence is 2.5 sec instead of 25 sec, (ii) pointing error measurements will be performed with an accuracy better than 0.032 arcsec/√Hz and transmitted to the AOCS (Fine Guidance System: FGS).

The distribution of the extracted windows is the following (counts for the 4 CCDs):

Stars	400
Background windows	100 (7x7 pixels)
Imagettes	40
Offset windows	2 x 4 offset windows (2255
Smearing rows	4 x 10 over-scan rows

The photometric algorithms will be based on the optimal mask method which gives the best results for the fast camera configuration (TBC). The FGS algorithms are based on an extended Kalman filter (EKF) used for recursive nonlinear optimization. Pixels will be digitized at a rate of 4 Mpixel/sec thus the max rate per half CCD is 64 Mbps. With 8 links (one per half CCD output), including the SpaceWire overhead, it gives 80 Mbps as a peak rate. In order to cope with this bit rate with margin, the link is configured at 100 Mbps for 8 links. The expected mean rate will be 1.25 (SpW overhead) x image size / 1.5 (readout time) so it is: 1.25x81 / 1.5 = 68 Mbps, leaving 30 % margin.

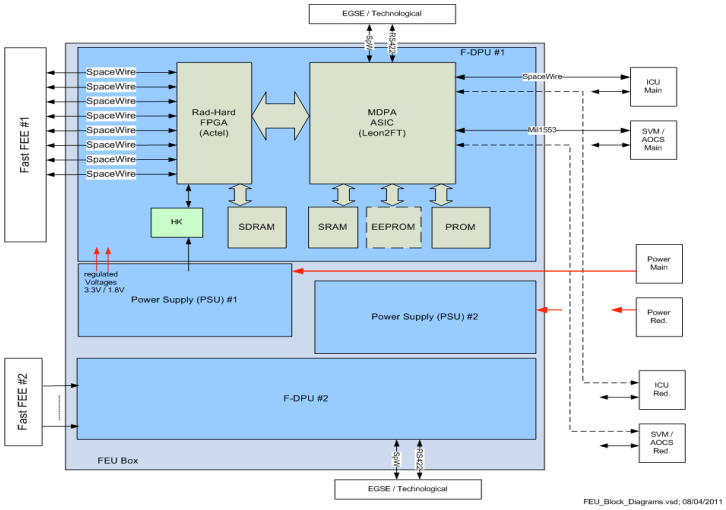

Figure 4.11: FEU Architecture Block Diagram

The CPU load needed by the data acquisition, correction and reduction process is about 40% with a MDPA LEON2 FT processor running at 80 MHz. In total 512 Mbytes of SDRAM will be needed per F-DPU. The FEU is an integrated electronics box, which consists of 2 data processing (F-DPU) boards (each within one module frame) and 2 power converters (PSU) integrated into a single frame. Fig. 4.11 shows the FEU architecture.

4.8.3 Instrument Control Unit (ICU)

Both ICUs (Main & Redundant) are gathered in a single box and work in cold redundancy. Each ICU shall implement the following common functions (non exhaustive list):

- Handle communications with spacecraft.
- Receive and process telecommands.
- Format and transmit cyclic and sporadic HK telemetry packets (HKTM).
- Format and transmit the scientific payload telemetry packets (PLTM).
- Manage the SpaceWire network: the ICU is a remote network manager (router configuration, router monitoring, router status reporting…).
- Receive the onboard time (Central Time Reference) from the S/C, handle the time stamping of the data transmitted in HKTM and forward the CTR to the DPUs.
- Receive a SpaceWire time code from the S/C and forward it to the DPUs.
- Produce state and diagnosis information (cyclic status, progress event).
- Schedule the DPU tasks (by the way of commands sent to the DPUs).
- Manage the data flow (especially in configuration mode).
- Manage the mode transitions.
- Manage the Software parameters.
- Manage the maintenance of the ICU software.
- Manage the maintenance of the N-DPU software.
- Manage the Star Catalogue.
- Compress the data using a lossless compression algorithm. A compression factor of at least 2.0 is required.
- Acquire and transmit to the S/C its own voltage and current consumptions.

Every 2.5 sec, the active ICU processes the data (flux, centroids and imagettes) sent by the F-DPUs. The imagettes are compressed before being transmitted to the SVM. The fluxes and centroids are stacked: N measurements are stacked for each F-DPU. Every 25 sec, the active ICU processes the data (flux, centroids and imagettes) sent by the N-DPUs.

The imagettes are compressed before being transmitted to the SVM. An outlier detection is performed on the fluxes and centroids by comparing the data corresponding to the same star as sent from N cameras (N=8, 16, 24 or 32). The selected measurements are stacked.

The active ICU performs a detection of the outliers on fluxes and centroids of stacked data. The mean of the valid stacked measurements (flux and centroids) are computed and bufferised waiting for compression and transmission to the SVM.

In configuration mode, the main functions of ICU are to transmit the star catalogues and all other configuration parameters to the DPUs, to compress full-frame images sent by the DPUs, to packetise and transfer to SVM all the data from DPUs necessary for subsequent validation of on-ground operations.

The expected data volume (adding 40% contingency) is roughly 212 Gb/day (imagettes, photometric data, centroid data, raw images, etc). Presently, the available TM rate is 106 Gb/day; therefore, ICU will compress data by a factor of 2 at least, without loss of information.

The ICU shall manage an input average data-rate from N-DPU and F-DPU of about 12 Mbps and an average output data-rate to the SVM of about 1.5 Mbps (16 x 735 kbps from the N-DPUs + 2 x 57 kbps from the F-DPUs). These average data-rates can be easily managed by the standard SpW link, running up to 100 Mbps.

The ICU shall be in charge of the in-flight maintenance of the N-DPU application software (scientific SW) and its own SW. The N-DPU and ICU application software shall be reconfigurable during the flight.

The ICU electronics architecture is shown in Fig. 4.12. It includes a Motherboard, 2 processor modules (AT697F - LEON2, SPARC V8), 2 I/O & Memory modules, and 2 Power supply modules.

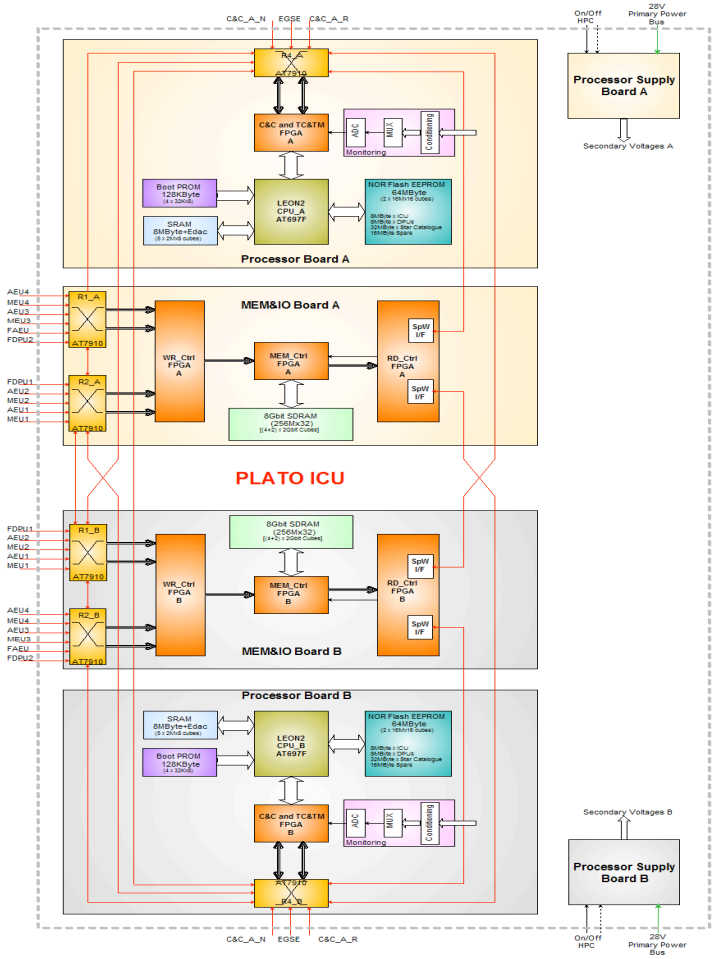

Figure 4.12: ICU overall architecture block diagram (Main and Redundant)

4.9 Payload Budgets

4.9.1 Payload mass budget

(in kg)	Per unit w/o uncert.	N unit	Total w/o uncert.	Total with 20% uncert.	Comments
Fast camera					
TOU w/o baffle	8.856		17.712		Good design maturity, lens thickness **TBC**
Baffle assembly	0.740		1.480		Good design maturity
Baffle cone	0.262		0.524		Size **TBC** with thermal I/F
FPA	1.320		2.640		Mass linked to power dissipated by FPA
I/F TOU-FPA	0.104		0.208		Good design maturity
Therm. equipment	0.400		0.800		Poor maturity, only first order estimate
Total w/o FEE	(11.682)		(23.364)		
F-FEE	1.400		2.800		Medium maturity, **TBC**
Total fast camera	**13.082**	**2**	**26.164**	**31.397**	
Norm. Camera 1&4					
TOU w/o baffle	8.856		141.696		Good design maturity, lens thickness **TBC**
Baffle assembly	0.740		11.840		Good design maturity
Baffle cone	0.320		5.120		Size **TBC** with thermal I/F
FPA	1.550		24.800		Mass linked to power dissipated by FPA
I/F TOU-FPA	0.104		1.664		Good design maturity
Therm. equipment	0.400		6.400		Poor maturity, only first order estimate
Total w/o FEE	(11.970)		(191.520)		
N-FEE	1.300		20.800		Medium maturity, **TBC**
Total norm. camera	**13.270**	**16**	**212.320**	**254.784**	
Norm. Camera 2&3					
TOU w/o baffle	8.856		141.696		Good design maturity, lens thickness **TBC**
Baffle assembly	0.740		11.840		Good design maturity
Baffle cone	0.234		3.744		Size **TBC** with thermal I/F
FPA	1.550		24.800		Mass linked to power dissipated by FPA (CCD dummy output use ?)
I/F TOU-FPA	0.104		1.664		Good design maturity
Therm. equipment	0.400		6.400		Poor maturity, only estimation
Total w/o FEE	(11.884)		(190.144)		
N-FEE	1.300		20.800		Medium maturity, **TBC**
Total norm. camera	**13.184**	**16**	**210.944**	**253.133**	
Electronics					
N-AEU	4.650	4	(18.6)	(2.3)	Poor maturity, **TBC**
F-AEU	2.300	1	(2.3)	(2.8)	Poor maturity, **TBC**
MEU	4.500	4	(18.0)	(21.6)	Medium maturity, **TBC**
FEU	4.500	1	(4.5)	(5.4)	Medium maturity, **TBC**
ICU	6.500	1	(6.5)	(7.8)	Medium maturity, **TBC**
Total electronics			**49.9**	**59.9**	
Total payload			**499.3**	**599.2**	

This mass budget is compliant with the allocated mass of 600.0 kg, including 20% uncertainties. Note that it is based on a design with good maturity, especially for the cameras which represent a large fraction of instrument mass.

4.9.2 Payload power budget

(in W)	Per unit	Number of box	Power w/o uncertainties	Power with 20% of uncertainties	Remarks
Camera					
Telescope thermal	2.0	34	68.0	81.6	2W shall be considered as the mean value per camera. It depends on location on the OB
Normal FPA	0.55	32	17.6	21.1	
Normal FEE	6.4	32	204.8	245.8	
Fast FPA	0.8	2	1.6	1.9	
Fast FEE	13.0	2	26.0	31.2	
Electronics boxes					
Normal AEU	28.0	4	112.0	134.4	
Fast AEU	19.0	1	19.0	22.8	
MEU (4 DPU)	43.8	4	175.2	210.2	
FEU (2 DPU)	20.0	1	20.0	24.0	
ICU	19.8	1	19.8	23.8	
Heating			**68.0**	**81.6**	
Others			**596.0**	**715.2**	
Total			**664.0**	**796.8**	

This budget is fully compliant to the allocated power consumption of 820 W including 20% uncertainties.

4.9.3 Telemetry data budget

Overall TM budget	
Daily volume for all normal cameras (science data)	97.6 Gb
Daily volume for all fast cameras (science data)	2.2 Gb
Daily for all cameras (with compression, without header)	99.8 Gb
CCSD packet header overhead	0.6%
Data auxiliary header overhead	2.5%
Total daily volume (with compression, with headers)	**103 Gb**
Available data rate	**109 Gb**
Margin	6 Gb (6%)
Instantaneous rate ICU → SVM	*1.19 Mbps*

4.10 Payload expected performance

Four major scientific performance indicators can be identified for the PLATO mission:

- The total number of stars that will be monitored for long intervals of time (2 to 3 years), down to a given photometric noise level. This performance indicator depends in a complex way on a combination of the field of view of each individual camera, the configuration of the cameras in the proposed overlapping-line-of-sight concept, the pupil size of each camera, and finally the total duration of the mission, i.e. the number of long monitoring phases that the mission can afford.
- The total number of stars that will be monitored for shorter intervals of time (2 to 5 months), down to a given photometric noise level. In addition to the characteristics listed in the previous item, this indicator also depends on the exact strategy of the step & stare phase.
- The total number of stars that will be monitored for long intervals of time (2 to 3 years), down to a given magnitude. This performance indicator depends on the global field of view of the instrument and on the total duration of the mission.
- The total number of stars that will be monitored for shorter intervals of time (2 to 5 months), down to a given magnitude. In addition to the characteristics listed in the previous item, this indicator also depends on the exact strategy of the step & stare phase.

It is clear from the list of indicators above, that in order to maximize the science impact of PLATO, we need to maximize at the same time:

- The total duration of the mission
- The field of view of each camera
- The global field of view of the instrument
- The pupil size of each camera
- The number of cameras
- The flexibility of the step & stare phase observation strategy

The current instrument and mission baseline represents one possible point in this complex multi-dimensional parameter space. The PLATO assessment study and the early phases of the definition study have shown that this point indeed corresponds to a globally optimized situation.

However, should some of the characteristics of the present baseline be descoped in future phases of the project, the impact of such potential descoping would have to be studied in detail, as descoping one of the above characteristics might be compensated by an upgrade in other characteristics. For instance the decrease in the number of cameras that was imposed at the time of the selection into definition phase was compensated by an upgrade of the individual field of view of the cameras.

Similar trade-offs for departures from the current baseline may be imposed in the future by technical, financial or programmatic considerations. In such circumstances, the PLATO Science Team, with the help of the PMC, will have to review and rank the scientific performance indicators listed above, in order to provide guidance to the PLATO mission management teams as to the best compromise for an updated baseline.

It is fortunate that PLATO, with its concept involving a set of identical instruments, and its observation strategy divided into long and short monitoring phases, is an extremely flexible mission, and certainly offers several satisfactory configurations.

In the rest of this section we describe the expected scientific performances of the current mission baseline. These estimates are based on the best knowledge of the instrument, of the characteristics of the fields and of the behaviour of the targets to be observed. Most of these performances are derived from models (e.g. star density in the observed fields) and from the instrument end-to-end simulator developed during the study and updated with the latest parameters of the instrument baseline.

The PLATO end-to-end simulator was used to generate simulated light curves for various sets of stars representing realistic portions of the fields to observe. All known sources of noise were introduced in these simulations, including photon noise, readout noise, jitter noise, background noise, etc. The simulations also

assume the standard on-board and on-ground data treatment system, including e.g. onboard weighted mask photometry, and on-ground a posteriori jitter correction.

The results of these simulations were used to validate simplified models of the instrument and data treatment system, with which extensive computations were performed in order to evaluate the global performance of the mission.

Some of these results are presented in Fig. 4.13, which corresponds to a simulation on a small sub-field with representative star densities. Shown on this figure is the noise level of every star in this test field, first without and then with a posteriori jitter correction, *à la CoRoT*. The results show that for the majority of targets down to at least m_V=11, the total noise level is close to the theoretical photon noise limit after jitter correction.

These results have been used to validate a simpler model of the overall noise performances of the instrument, which is shown in Fig. 4.14.

For each portion of the global field of view of the instrument, covered by either 8, 16, 24 or 32 normal cameras, the mean magnitude down to which various levels of noise are reached were computed using this model, then the star density model was used to derive the corresponding numbers of stars observable during the mission. Similar performance calculations were also performed for the two fast cameras.

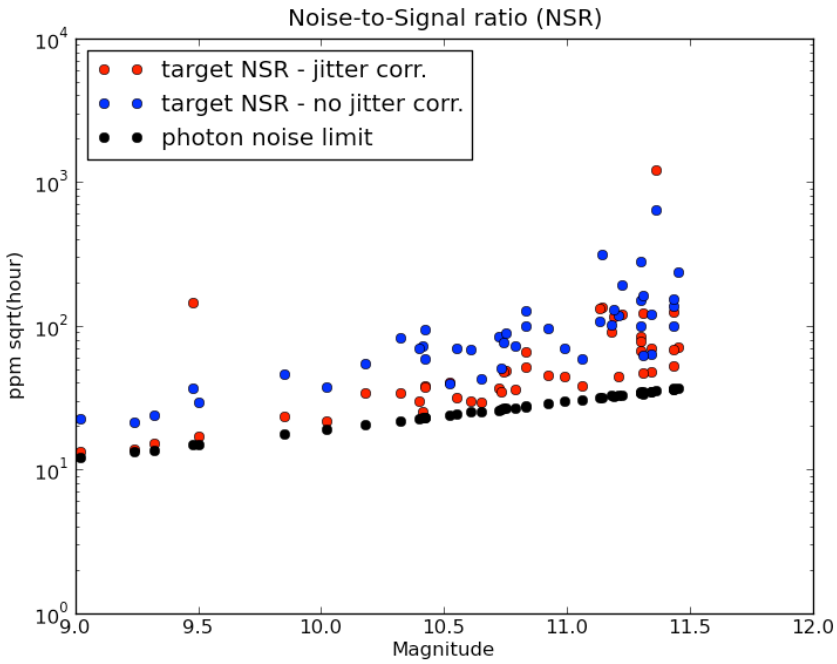

Figure 4.13: expected total noise level, without and with a posteriori jitter correction

The basic outcome of these performance evaluations is summarized in Table 4.2. For this evaluation, we have assumed two long runs of 2 years each, and a 2 year step & stare including the following successive runs: 3 x 5 months, 1 x 4 months, 1 x 3 months, 1 x 2 months.

As can be seen, all scientific requirements are well met, and some are significantly exceeded, in this evaluation of the performance of the instrument baseline. A more precise evaluation of the expected number of M dwarfs in the observed fields still needs to be performed.

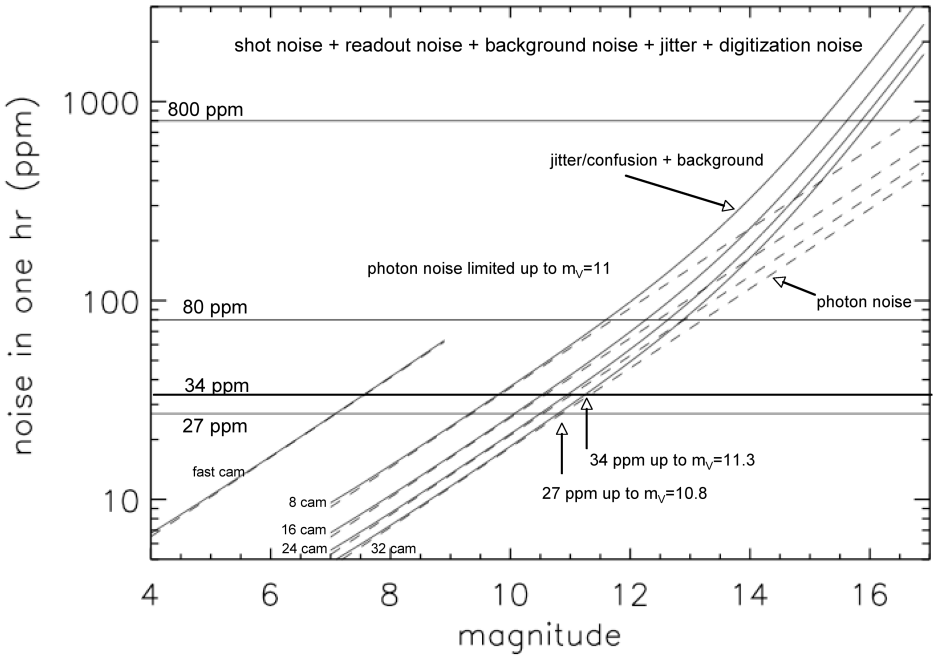

Figure 4.14: overall noise performances of the PLATO instrument, including jitter correction

PLATO star sample	# of stars			
	after two long monitoring phases 4,300 deg^2	science requirement	incl. step & stare phase 20,000 deg^2	science requirement
P1 : dwarfs/sub-giants later than F5, noise ≤34 ppm in 1 hr	21,300	20,000	85,000	n/a
P2, P3 : dwarfs/sub-giants later than F5, $m_V \leq 8$, noise ≤34 ppm in 1 hr	1,250	1,000	3,100 (≥ 5 months)	3,000
P4: M dwarfs, noise ≤800 ppm in 1 hr	>5,000 (TBC)	5,000	>5,000 (TBC)	5,000
P5 : dwarfs/sub-giants later than F5, noise ≤80 ppm in 1 hr	267,000	245,000	1,000,000	n/a
# dwarfs/sub-giants later than F5, $m_V \leq 11$	36,000	maximize	145,000	n/a

Table 4.2: *A summary of PLATO scientific performance evaluation*

4.10.1 Centroid precision of imagettes

Concerning centroid measurements, simulations have also shown that a noise level of the order of 1 mas in one hour can be achieved for more than 90% of the targets at m_V=11, and that the centroiding performance reaches 0.5 mas in one hour for more than 50% of the targets at m_V=11. These centroiding performances will allow us to perform a powerful check for false alarms due to variable neighbouring sources, such as background eclipsing binaries, in a similar way as what is being done in *Kepler*. The centroid displacement induced by a change in the intensity of a neighbouring faint source is approximately given by : $\delta c = \rho\, i/I\, \delta i/i$, where δc is the resulting centroid displacement in arcseconds, ρ is the separation between the target and the contaminating source in arcseconds, i is the intensity of the contaminant, I the intensity of the target and $\delta i/i$ is the relative variation of the contaminating source (0.5 for an eclipsing binary with two similar stellar components).

A background variable source with intensity i will mimic a transit with a depth d in front of a target star with intensity I if $i/I\ \delta i/i = d$. For a transit depth of 10^{-4} (earth-size planet) and a contaminating eclipsing binary ($\delta i/i$ =0.5), this corresponds to a magnitude difference with the target around 9. Applying the above approximate approach, we find that centroid measurements can identify false alarms due to background variable sources if $\delta c \leq \rho\ d$. For d=10^{-4} and δc=0.5mas, this gives $\rho \geq 5$ arcseconds. Thus centroid measurements at this level of accuracy will be sufficient to discard all occurrences of background eclipsing binaries down to 20th mag at more than 5 arcseconds from the target, which will account for the vast majority of cases. Only background EB closer than 5 arcseconds will remain undetected, but their probability of presence will be very small. The PLATO centroid data will therefore vastly simplify the ground-based follow-up by eliminating most of the false alarms.

5 MISSION DESIGN

5.1 Mission Implementation

PLATO will perform the scientific observations in an "operational orbit" around the Earth-Sun Lagrange Point 2 (L2). Such operational orbit is defined in as a free-insertion, large amplitude, **eclipse-free** libration orbit around L2. This orbit is unstable and shall be maintained by regular station-keeping manoeuvres every 30 days. The angular size of the libration orbit seen from the Earth is approximately 33° in the ecliptic plan e and 25° out of this plane. The launch window for reaching such an orbit opens every day for at least 45 minutes over a period of at least 2 weeks out of every 4 weeks. PLATO will be launched from Kourou by a Soyuz 2-1b rocket with Fregat upper stage into a direct transfer trajectory to the operational orbit. The transfer will last approximately 30 days. Trajectory correction manoeuvres (TCMs) shall be performed by the spacecraft 2, 5 and 20 days after the separation from the Fregat (occurring about 1500 s after lift-off) in order to remove the launcher dispersions and correct the perigee velocity.

The PLATO mission profile consists of the following phases:

- Pre-launch Phase, from launch campaign preparation to launch vehicle lift-off.
- Launch and Early Orbit Phase (LEOP), from lift-off to the completion of the first trajectory correction manoeuvre performed by the spacecraft on day 2 after the separation from the Fregat upper stage.
- Transfer Phase, from the end of the LEOP to the attainment of the operational orbit around L2.
- Commissioning Phase, starting during the Transfer Phase and running in parallel to it (and after if necessary) till the completion of the check-out of the spacecraft and of the check-out and calibration of the Payload with completion maximum 2 months after the arrival in the operational orbit.
- Nominal Science Operations Phase, starting at the end of the Commissioning, consisting of a *Long-Duration Observation Phase* and a *Step-and-Stare Observation Phase* lasting 6 years in total.

The *Long Duration Observation Phase* consists of the continuous observation of two wide sky regions: the first sky field will be observed for a minimum of 2 years up to a maximum of 3 years while the second sky field will be observed for 2 years.

The *Step-and-Stare Observation Phase* consists in the observation of several sky field and will last 1 to 2 years in total (depending on the overall duration of the Long Duration Observation Phase). Each sky field will be observed from a minimum of 2 months to a maximum of 5 months. This Phase is subject to the Sun is in "favourable direction", i.e. compatible with the Payload instruments protection from the solar radiation, power generation and the thermal control.

- Extended Science Operations Phase, starting at the completion of the Nominal Science Operations Phase and lasting up to 2 years.

5.2 Overall Configuration

The PLATO spacecraft is configured with three main modules that can be individually integrated and tested:

- **Payload Module** (PLM), the full set of Instruments as well as the optical bench, supporting structures and the hardware thermal control
- **Service Module** (SVM), the part of the Spacecraft that supports the PLM and Sunshield
- **Sunshield** (SSH), the part of the Spacecraft that shields the payload from the Sun, as well as generates power via body-mounted solar cells.

The top-level product tree of the PLATO spacecraft resulting from this system architecture and from the definition of the reference Payload is provided in Fig. 5.1. Within the PLM, the products under the

responsibility of the PLATO Payload Consortium (PMC) will be delivered to the industrial Prime Contractor as customer furnished equipments (CFE) by ESA for their integration in the spacecraft.

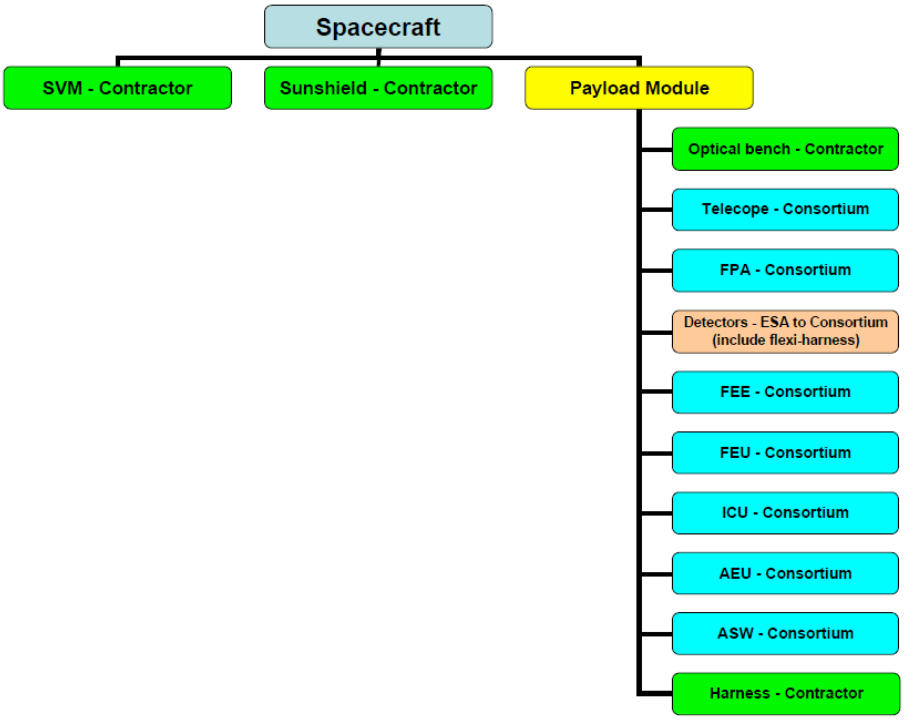

Figure 5.1 – The PLATO Product Tree

5.3 Launch and Operations

5.3.1 Launch Windows

The mission analysis has shown that the spacecraft can be launched in 2018 with limited constraints on the launch window as shown in Figure 5.2.

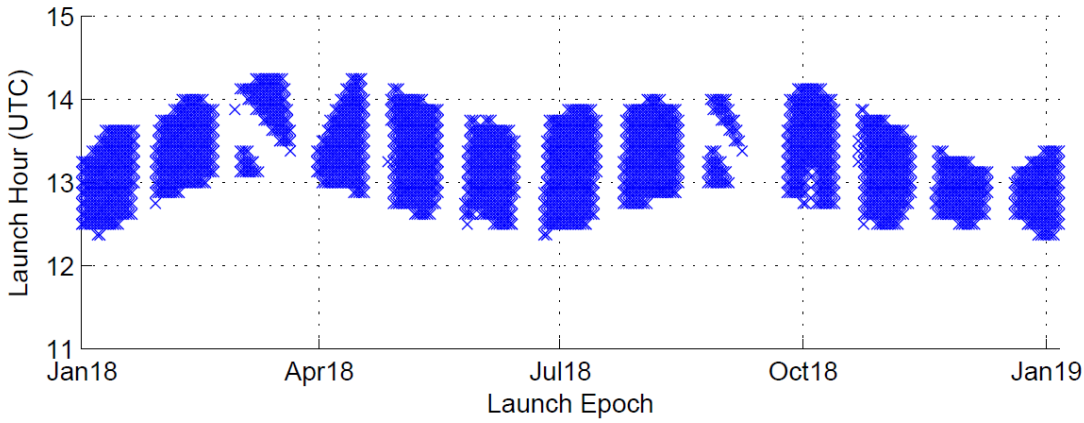

Figure 5.2: PLATO Launch windows in 2018

5.3.2 Orbit

PLATO shall orbit the Earth-Sun Lagrange Point 2 (L2). Such operational orbit is defined in as a free-insertion, large amplitude, **eclipse-free** libration orbit around L2 and is shown in Figure 5.3.

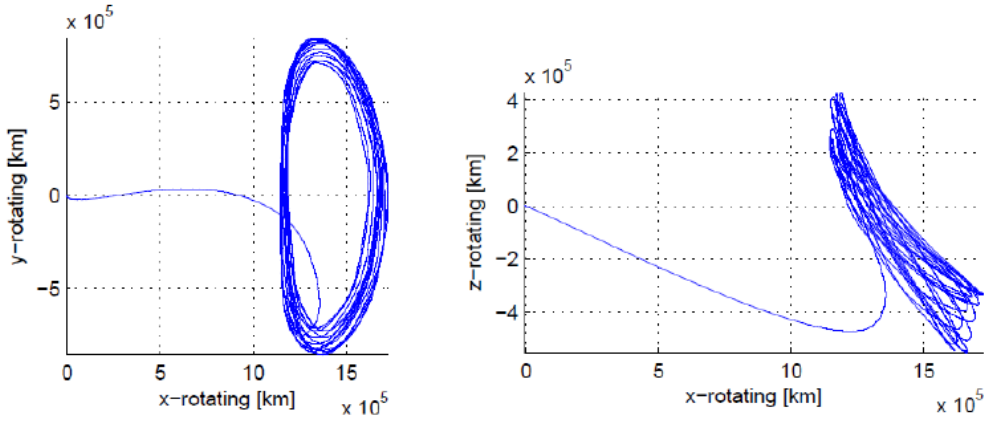

Figure 5.3: PLATO Orbit in L2

5.3.3 Mission Phases

From the duration and composition of the various phases and sub-phases, the overall mission timeline shown in Figure 5.4 has been obtained. From the end of the Transfer Phase to the completion of the Extended Science Operations Phase, PLATO will spend in total 8 years and 2 months around L2. In the same figure, the spacecraft orbits and the ground stations that will ensure the telecommunications coverage during the various phases are also indicated. During LEOP and the first day of the Transfer Phase, the ESA stations at Kourou (15-m), New Norcia (35-m) and Cebreros (35-m) will be used for contact with the spacecraft. After the first day of the Transfer Phase and till the end of the Extended Science Operations Phase, the ESA station at New Norcia (35-m) shall be used for contact with the spacecraft, with Cebreros (35-m) as backup and Kourou (15-m) as backup for critical/contingency operations. During the Nominal and Extended Science Operation Phases a 4 hour communication session per day with the ground station will be available: 0.5 hours allocated to communication setup and ranging and 3.5 hours to data transmission.

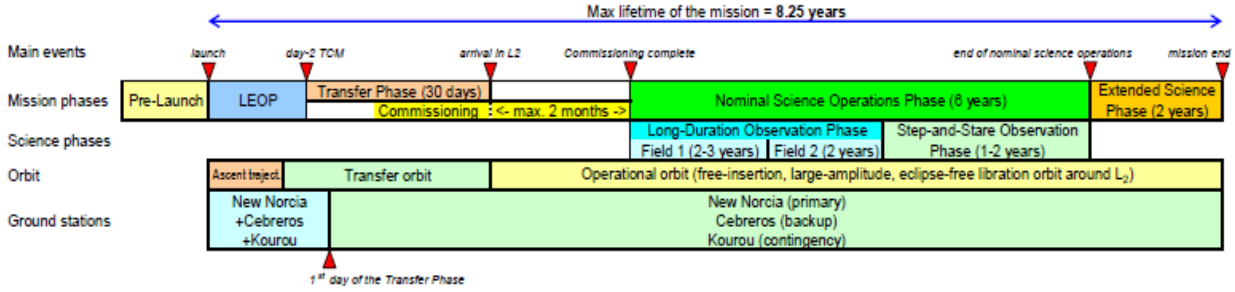

Figure 5.4: PLATO Mission Phases

5.3.4 Observation Strategy

Once in the operational orbit, the Spacecraft will conduct nominally two long-duration observations, each on a different sky field, for several years per field. This will be followed by a phase in which targets of specific interest will be observed for several months. During the long observations, the Spacecraft must maintain the same line-of-sight (LOS) towards one field for up to several years. However, the Spacecraft must be periodically re-pointed in order to ensure the solar arrays are pointed towards the Sun. This is achieved by rotating the Spacecraft around the LoS by 90° roughly every 3 months, as shown in Figure 5.5.

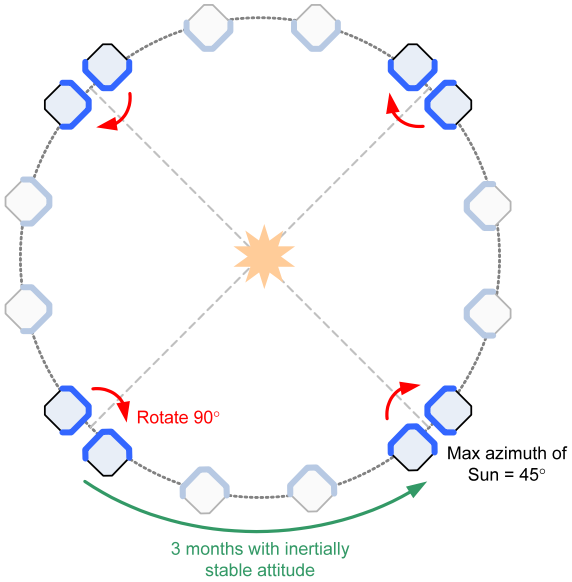

Figure 5.5: Spacecraft Rotation around Payload LOS during one Orbit

5.4 Concept A Design

5.4.1 Overall Configuration

The spacecraft is based on a prism-shaped structure with equilateral triangle basis (Fig. 5.6). Three main vertical panels of 2m x 5m constitute the all-CFRP main structure, together with closing panels and stiffening struts. The 34 instruments that constitute PLATO's payload are installed horizontally on one of the 3 vertical panels.

This vertical accommodation offers the best area for accommodation of the payload, while the load of the significant payload mass is directly carried by the main structure. In consequence the central main structure constitutes the optical bench, and together with cameras and electronics, they constitute the Payload Module (PLM). Cameras are attached through an individual camera support structure, and are installed in 34 holes on that panel. This design allows preserving a reasonable centring of the spacecraft Centre of Mass, and separates the Front-End Electronics from the main panel of the optical bench, offering a natural filtering of FEE dissipation noise onto Optical Bench thermo-elastic performances.

Furthermore the cameras are accommodated on the optical bench so that they fit both the organisation in "subgroups" – with 8 cameras belonging to a given subgroup (see Chapter 4) – and organised in "batches", connected to the same electronics boxes, which allow keeping the electronics directly facing their related cameras, and minimize payload harness mass.

In order to minimise disturbances towards PLM, in particular thermal and thermo-elastic disturbances, the SVM is made of several suspended backpacks. Up to 7 backpack panels are defined, each carrying a consistent set of equipment corresponding to each main functional chain of the Service Module (3 panels for PLM electronics, 1 panel for TT&C, 1 panel for Power, 1 panel for avionics, 1 panel for Reaction Control System, i.e. RCS or Propulsion). Each of them is simple in its design, with a simple plate, isostatically mounted on the main structure and are as much as possible thermally isolated from the main structure.

The Propulsion panel is nested within the main structure at the bottom of the satellite, while the 6 other backpacks are installed on one other of the 3 main structural panels, permanently facing the cold space.

The Sunshield is the last major element of the spacecraft. It has a double role: It shall protect payload and electronics from direct illumination by the Sun, and also serves as Solar Array for power generation. It is mainly based on a main flat panel of 3 x 5 m covered of solar cells facing the third structural panel, plus additional MLI on the top and bottom sides of the satellite.

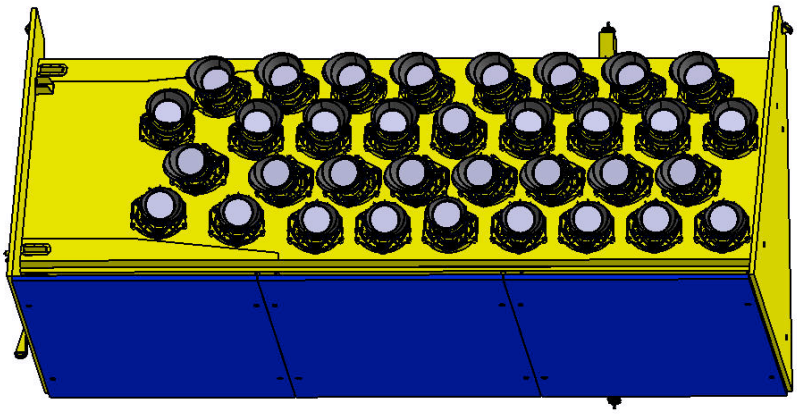

Figure 5.6: Concept A - General view showing the PLM side of the spacecraft .

The design is therefore based on an *inversion of the classical separation of SVM and PLM*, while the PLM constitutes the main satellite bus, and the SVM is mounted isostatically on it.

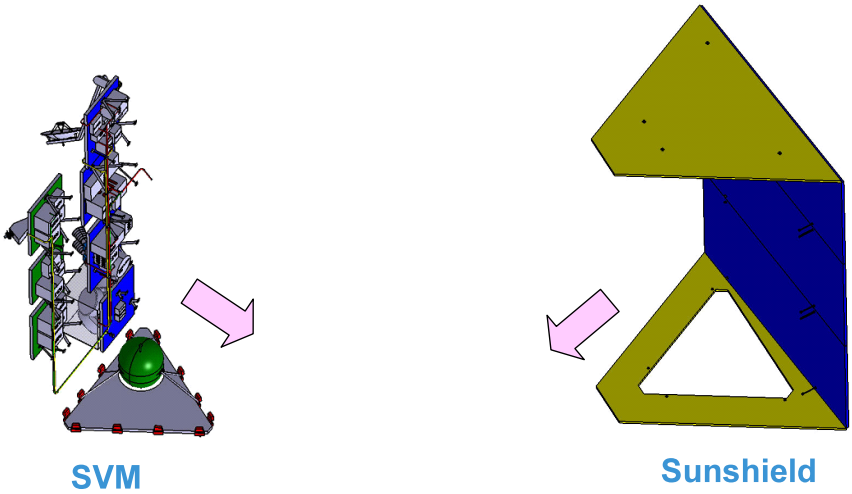

Figure 5.7: The spacecraft is organised in 3 main parts : Here the SVM and Sunshield sides of the spacecraft are shown.

The triangular shape of the spacecraft allows both the payload side and the SVM side to be permanently in the shade, once shielded by the Sunshield, for any ecliptic latitude of observation higher than 60° (in Northern or Southern hemisphere), as specified for the design-driving long-duration observation phase. The main panel of the sunshield provides 15 m² of surface potentially covered with solar cells, with a solar incidence that never falls below 51°, i.e. providing comfortable margins with respect to the spacecraft power needs.

The mass of the PLATO spacecraft is about 2,000 kg at launch, and uses about 1,6 kW of power in normal operations, all margins included. This allows a growth margin of nearly 5% in mass with respect to the Soyuz capacity, and a similar growth margin around 5% with respect to the maximum available area for the Solar Array.

5.4.2 Avionic Architecture

The main functional chains are:

- The payload functional chain made of the cameras and their electronics
- The On-Board Computer (OBC), Mass-Memory Unit (MMU), and Remote interface Unit
- The Power System, in charge of providing electrical power to all spacecraft equipment, thanks to Solar Array (formally falling into the "Sunshield" Subsystem), Power Control and Distribution Units, and battery. The entire spacecraft harness also falls into the perimeter of the power subsystem.
- The AOCS, based on Star Trackers and gyroscopes as sensors (with Sun sensors for safe mode), and 4 reaction wheels as actuators.
- The Reaction Control System, which is a mono-propellant propulsion system (hydrazine), with 2 redundant branches of 7 thrusters, spread on 4 separate pods.
- The Telemetry, Tracking and Command subsystem (TT&C), which is based on a X-band only, with 2 LGA for LEOP and contingency situations and a 2-axis-steerable High Gain Antenna of 50 cm of diameter for nominal communications.
- The Thermal Control System, composed of passive thermal items (MLI, radiators), and active control (thermistors and heaters).
- The structure system, made of primary and secondary structure parts. Structure and thermal are grouped into a single subsystem.

The spacecraft functional architecture matches well with the electrical architecture.

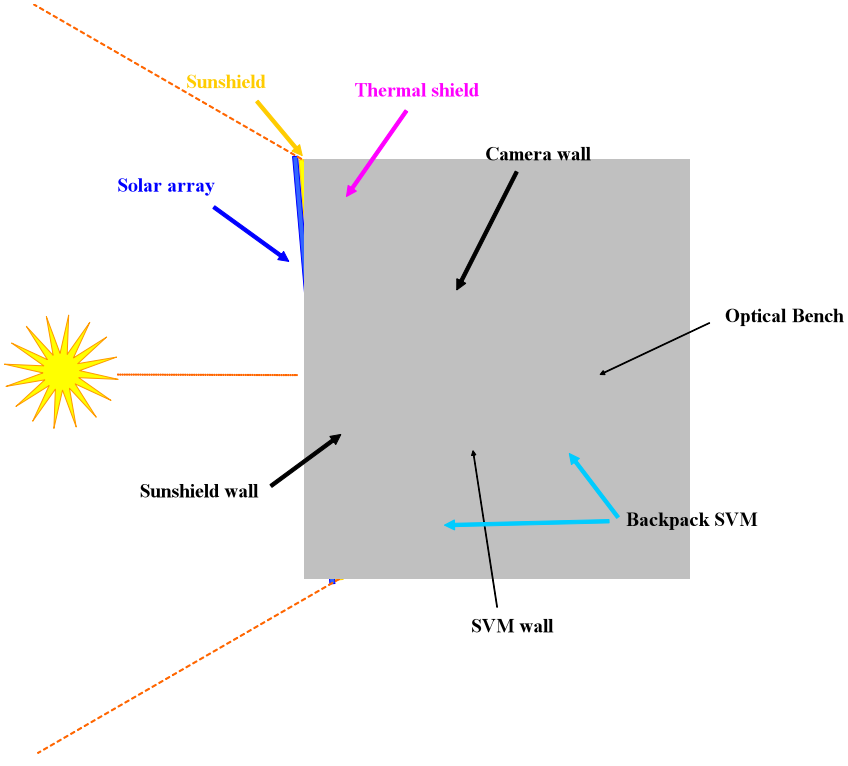

Figure 5.8: PLATO general concept with respect to Sun illumination

5.5 Concept B Design

5.5.1 Overall Configuration

The PLATO spacecraft is composed by three main modules that can be individually integrated and tested (Figure 5.9):

- **Payload Module** (PLM), that functionally includes the entire Payload (i.e. the items supplied as CFE), the Optical Bench (OB), the supporting and interface structures, the thermal control hardware and the harness interconnecting the P/L units among them and with the SVM.
- **Service Module** (SVM), that provides the spacecraft subsystems supporting the P/L functioning and operation, and provides the structural interfaces to the PLM, the Sunshield, and the launch vehicle. The SVM hosts also the P/L electronics boxes (MEU, FEU, N-AEU, F-AEU, ICU), which functionally belongs to the PLM.
- **Sunshield** (SSH), that shields the P/L instruments installed on the OB from the solar radiation and supports the Photovoltaic Assembly (PVA) that supplies electrical power to the whole spacecraft.

The SVM is octagonal-base prism built around a central cone that provides the interfaces with the launcher and with the Optical Bench of the PLM and hosts the propellant tanks. The lateral panels of the SVM accommodate the S/S equipments and the P/L electronics boxes.

The external lateral panels of the SVM accommodate the radiators and the insulators for the thermal control of the internal equipments. The following equipments are also installed outside the SVM:

- Two star trackers, placed on the upper platform, $-X_{SC}$ side, a position very close to the PLM optical bench.
- Four clusters of 4 thrusters each, utilized for the spacecraft attitude control, placed on the lower platform and protruding from the 45° tilted sides.
- Two clusters of 2 thrusters each, utilized for the orbital manoeuvres, placed on the lower and upper platforms and protruding from the $+X_{SC}$ and $-X_{SC}$ sides respectively.
- Two low-gain antennas (LGA), placed on the lower platform, $+X_{SC}$ and $-X_{SC}$ sides respectively.
- A high-gain antenna (HGA) with its deployment and pointing mechanism, placed under the lower platform so that it is deployed towards the $+X_{SC}$ side.

A cluster of 4 Fine Sun Sensors is accommodated on top of the $+X_{SC}$ side of the Sunshield.

In its deployed position, the HGA beam (cone with 5° half-angle at 20 dBi gain) is free to span the whole working range necessary to point the Earth in any S/C position on its libration orbit around L_2 and in any nominal attitude assumed during the Long-Duration Observation Phase: azimuth = ±85°, elevation = ±55°. The equipments inside the SVM are mounted on the lateral panels grouped per subsystems (Figure 5.10):

- TT&C subsystem equipments mounted on the $+X_{SC}+Y_{SC}$ panel.
- AOCS equipments mounted on the $+X_{SC}-Y_{SC}$ panel, with the exception of the ICU of the gyroscope, installed alone on the $-Y_{SC}$ panel for a better insulation and a more stable thermal environment.
- CDMU mounted on the $+Y_{SC}$ panel.
- EPS equipments mounted on the on the $-X_{SC}$ panel.
- P/L electronics boxes distributed on the $-X_{SC}+Y_{SC}$ and $-X_{SC}+Y_{SC}$ panels respectively.

Each lateral panel can be individually dismounted to facilitate the equipment integration. In particular, the P/L electronics panels can be installed on a suitable MGSE in proximity of the Optical Bench during the integration and functional verification of the PLM.

The Optical Bench is a step-based structure (each step bears a set of cameras) connected by an isostatic mount (formed by three bipods) to brackets installed on the upper edge of the central cone.

The Sunshield surrounds the Optical Bench following the octagonal shape of the SVM. The Sunshield has

been designed to keep the Optical Bench in shadow under Sun aspect angles that exceeds the values defined by the nominal sky observation strategy during the Long-Duration Observation Phase. The shading effect of the Sunshield is shown in Figure 5.11 for different values of the Sun azimuth and elevation angles, The Sunshield and the Optical Bench are designed also to avoid any vignetting of the camera UFOV (Figure 5.12).

The spacecraft dimensions are compatible with the Soyuz fairing envelope, considering a ST type fairing (Figure 5.13). The interface between the spacecraft and the launcher is implemented by a Standard 1666-SF type separation system.

5.5.2 Avionic Architecture

The services provided by the spacecraft avionics for the proper mission operation accomplishment are:

- Power conditioning and distribution to the spacecraft and payload units under a 28V regulated and protected form.
- Spacecraft data handling tasks:
  - reception via the X-Band receivers of ground telecommands;
  - collection and storage of science data and satellite housekeeping data for the 72 hours specified functional autonomy duration;
  - capability to store on board up to 72 hours Mission Timeline;
  - downlink of stored and real-time data using the X-Band transmitter;
  - spacecraft accurate time maintenance and distribution to instruments and AOCS;
- RF signal reception and demodulation for the uplink, modulation and transmission for the downlink.
- Thermal control of the spacecraft and FPA via temperature sensors-heaters loops.
- Spacecraft attitude and orbit control, including AOCS sensors acquisition and processing, actuators and thrusters commanding.
- Spacecraft failure detection isolation and recovery to satisfy fault protection and autonomy requirements.

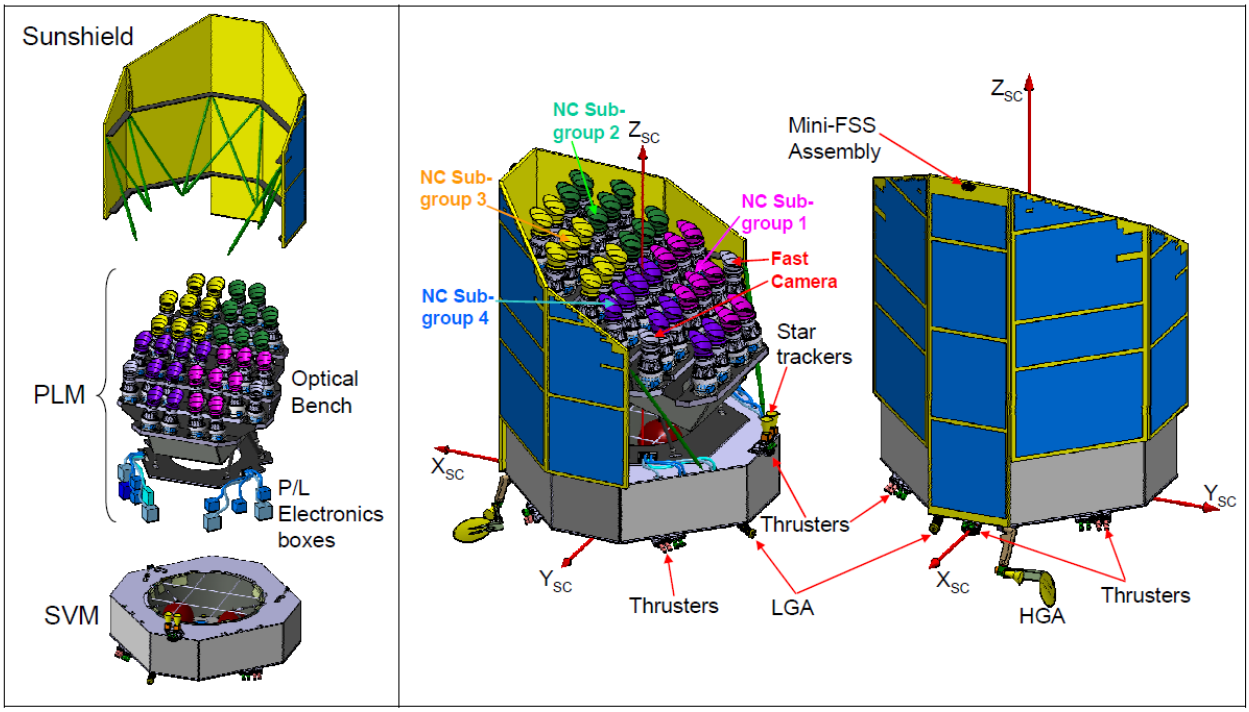

Figure 5.9: Concept B - PLATO spacecraft configuration and external equipment layout (X_{SC}, Y_{SC}, Z_{SC} = Spacecraft Reference Frame - SRF).

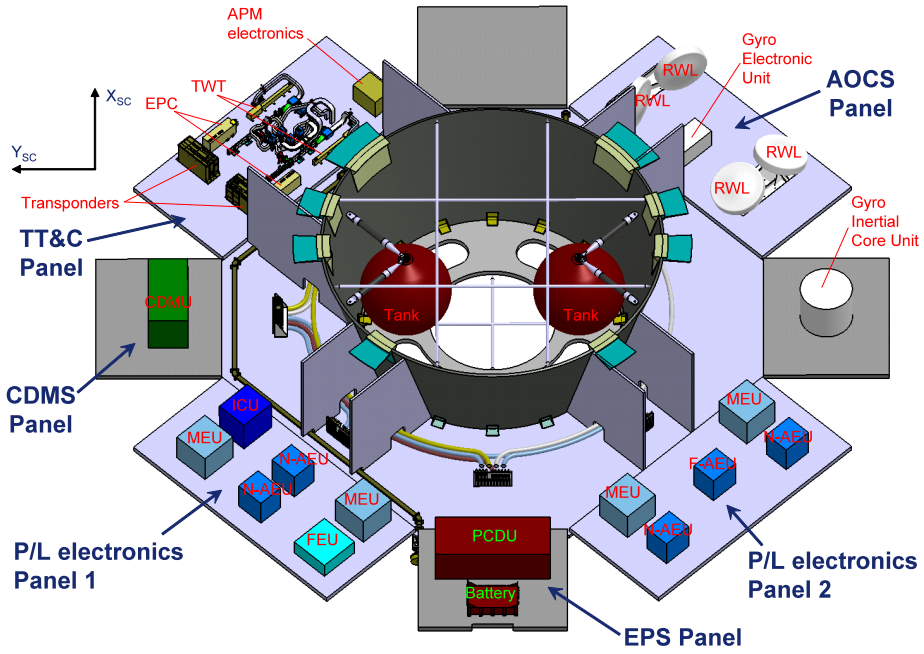

Figure 5.10: Concept B - Internal view of the SVM showing the equipments accommodation (the lateral panels have been rotated outwards by 90°).

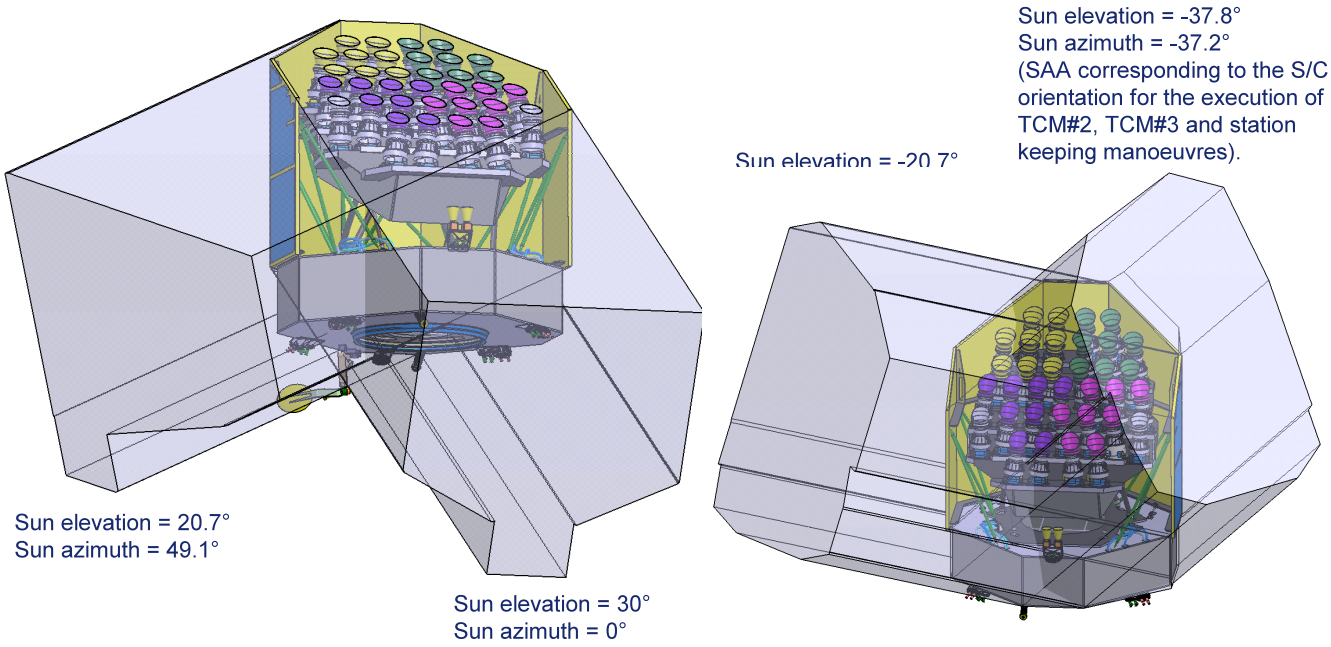

Figure 5.11: Concept B - Shading effect of the Sunshield for the limit values of the azimuth-elevation angles of the S/C-Sun vector in the SRF.

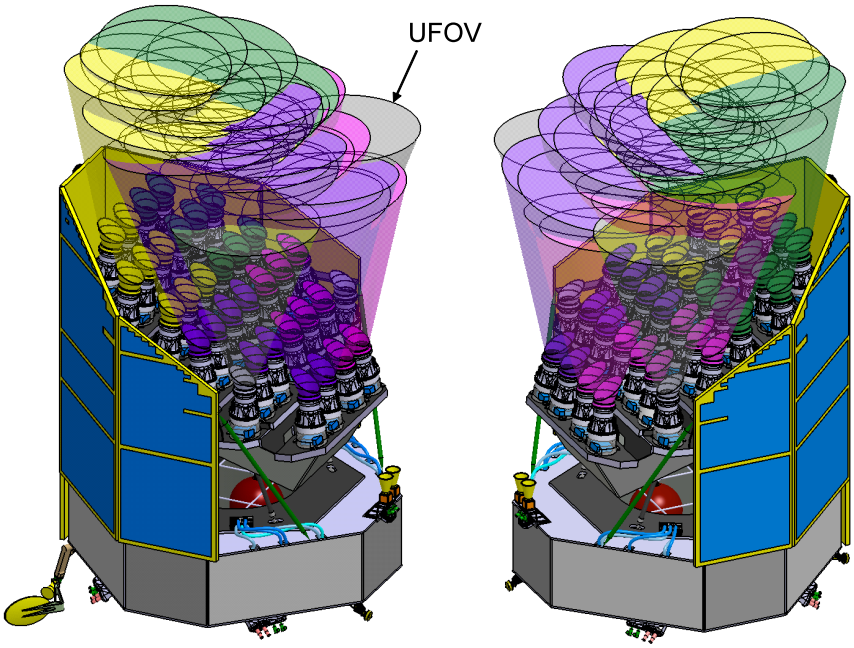

Figure 5.12: Concept B - Spacing between the cameras UFOV and the Sunshield.

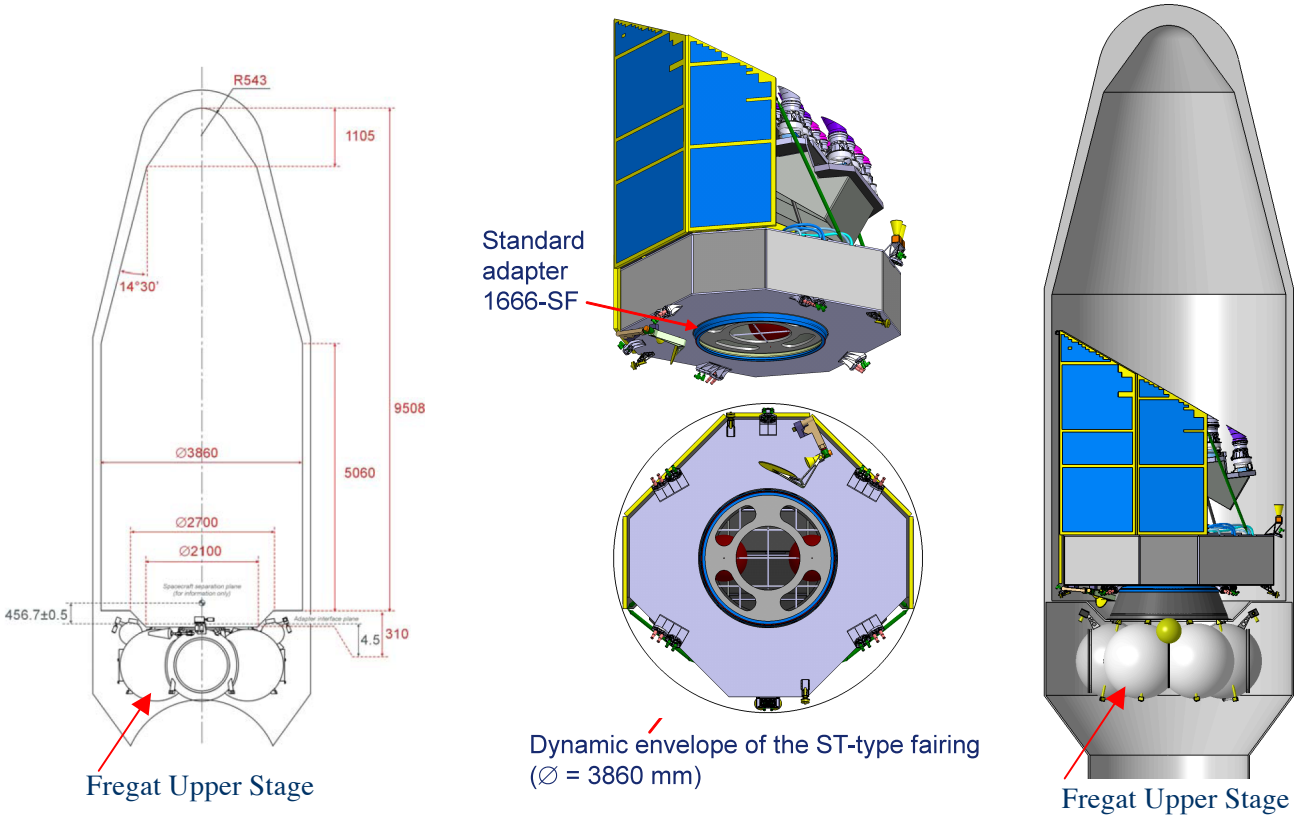

Figure 5.13: Concept B - Spacecraft launch configuration under the Soyuz ST-type fairing.

The above functions are implemented with the following main units:

- Centralized On-Board Computer (CDMU) providing science data storage, spacecraft and AOCS Command, Control and Data processing, It is based on modular unit including core standard boards, mass memory boards and dedicated I/O boards to interface AOCS and SC unit/devices. It interfaces

Instrument Control Unit with SpaceWire serial links and the other units by Mil-Std-1553 bus, serial lines, analogue and discrete interfaces.

- PCDU providing: SA regulation, bus regulation, power outlet protection and distribution. The regulated 28Vdc power bus will be distributed by independent outlets protected by LCLs/FCLs. The PCDU interfaces with the SA panels and the battery used to supply the Spacecraft during the LEOP phases, in case of attitude loss or whenever Solar Array power is not sufficient. The PCDU interfaces with CDMU for command and control via 1553 MIL bus.
- X-Band Transponders to handle the TLM downlink, ranging operations and TC uplink based on X-band communication capability. The Transponders are controlled by CDMU through 1553 bus.
- AOCS sensor and actuators for attitude commanding and control. All the AOCS items are interfaced with CDMU by 1553 Mil bus interfaces or by dedicated serial or discrete interfaces.
- Thermal Control. The thermal control is performed through acquisition of temperature sensors and actuation of heater lines. Thermal control maintains units within their proper operative temperature range and guarantees the necessary stability.
- Propulsion based on Hydrazine thrusters.

The spacecraft has a total dry mass of 1732.1 kg, without system margin. Including the propellant (80.8 kg) and an allocation of 5 kg for balancing mass, the launcher limit of 2100 kg is met with a system margin of 16.3% (282 kg).

The largest power consumption (1645 W, including 20% system margin) occurs in the P/L Observation Mode during the 4-hour daily telecommunication period for the transmission of the collected data to the ground station.

The battery (777 W capacity) supplies power to the load or complements the contribution of the solar array from pre Lift-off to fist Sun acquisition, during the orbital manoeuvres in which the S/C deviates significantly from the nominal attitude, and in case of loss of the nominal pointing following a failure.

The on-board mass memory (capacity = 512 Gbit) can store up to 3 days of science data collected by the P/L and 7 days of housekeeping data collected by the P/L and by the S/C subsystems, with a margin > 50%.
The X-band telecommunication system has a throughput of 8.718 Mbps in downlink, sufficient to transmit to the ground station in 3.5 hours all the science and housekeeping (P/L plus S/C) data stored in the previous 24 hours, plus the housekeeping data collected in real time during the telecommunication period.

6 PREPARATORY WORK & FOLLOW-UP OBSERVATIONS

6.1 Preparatory Work

In this chapter we will describe the role of available stellar catalogues and Gaia data to optimally prepare PLATO observations. The analysis of existing catalogues is used to evaluate the PLATO capabilities and to select the best two long-duration fields that satisfy the scientific requirements. Gaia results are used for stellar sample selection and characterization.

In particular, Gaia early releases will provide estimates of the radii of PLATO targets to within 10-20%, allowing us to distinguish dwarfs from giants and optimize target selection, which at the end should improve the percentage of successful detections of small-size planets. However, in the definition phase we have shown that existing catalogues are sufficient to select the main PLATO targets (samples P1, P2, P3, and P4).

Gaia data will also be extremely useful to precisely characterize the vicinity of each PLATO target, by identifying fainter neighbours and measuring their exact positions and magnitudes. This additional information will be used to finely tune on-board and on-ground data treatment, e.g. by optimizing photometric masks and jitter correction algorithms. It will be used also for optimizing the follow up analysis of false positives (see below). Thanks to Gaia, the preparation work of PLATO will therefore be much easier than that of previous missions such as CoRoT and *Kepler*.

The choice of the stellar samples is a key issue in order to define the best pointing of the instrument and hence to maximize the science return, because the number of transiting systems scales linearly with the number of cool dwarfs and sub-giants monitored. In the case of PLATO this is compounded by the need to focus on bright stars in order to guarantee an efficient follow-up of transiting candidates. This subject has been approached using either models of the Galaxy or star counts from available extensive photometric catalogues. The star count approach has the advantage that it is based on real data, but generally only gives approximate stellar parameters of the population. The model approach, based on average stellar populations in the Galaxy, has the weakness that local fluctuations such as spiral arms are effectively removed. However, by definition, models give a complete knowledge of the (modelled) stellar population in terms of mass, temperature, luminosity class, radius, metallicity etc., allowing us to derive a precise characterization of the sample. Here we initially adopt a star count approach which we then validate using models.

The star count method is based on the Ofek (2008) catalogue, which contains 1,560,980 stars and is built from the cross-correlation between Tycho2 and 2MASS catalogues. In particular it includes Tycho stars with $B_T \leq 13$ and $V_T \leq 12$ with only one 2MASS counterpart within 6 arcsec, which excludes stars with close objects that may contaminate the PLATO Point Spread Function. For each star in this catalogue, a fit to the Spectral Energy Distribution, using the Spectral Library of Pickles (1998), provides the spectral type and luminosity class. The simplified approach used by Ofek, ignoring interstellar reddening, has produced unphysically large numbers of K and M dwarfs in the solar neighbourhood. For a better identification of cool dwarfs and sub-giants, an additional criterion on the J-H colour was used: F5-M9 IV-V stars were counted only $0.10 \leq J\text{-}H \leq 0.65$. Moreover the Ofek catalogue includes only 62% of the Tycho2 catalogue, and is therefore incomplete, presumably in the most crowded regions, so the derived numbers are likely lower limits to the true star counts.

Using the above method, cool dwarf and sub-giant densities were estimated in a series of 550 deg^2 fields located in the continuous viewing zone of PLATO. The resulting maximum density of cool dwarfs and sub-giants later than spectral type F5 is 12.27 stars per deg^2 for stars with $m_V \leq 11$. A fit to the cool dwarf and sub-giant star counts gives a $log(N)$-m_V slope of 0.55, slightly lower than the 0.6 slope expected in spherical approximation, with absorption and scale effects as second order effects. These figures are very similar to those used for the payload studies, both in the industry and in the Payload Consortium, which were based on a preliminary estimate.

We have estimated the uncertainties of these numbers with different methods. First we critically analyzed Ofek's classification and made several small corrections (see Barbieri et al. 2011, for details), evaluating the impact of the overestimates of K and M giants mentioned above. Finally the 2MASS catalogue was used for

star counts at fainter magnitudes. Cool dwarfs and sub-giants are taken as the stars with $0.11 \leq$ J-H ≤ 0.62 and $0.01 \leq$ H-K $\leq .12$ and $1.45 \leq$ B-K ≤ 2.9, corresponding approximately to F5-K0 stars. These analyses show that the numbers derived with the Ofek catalogue are uncertain within a factor 25%. Furthermore the 2MASS analysis shows that the number of expected stars with $m_V \leq 13$ is ≈113 per deg^2.

We have further tested our results in an independent way using the Besançon model, bearing in mind the caveat stated earlier about the use of average densities in these modelling methods. Hence, we would expect the Besançon model to give lower star counts. This model is a synthesis of the stellar population in our Galaxy and includes dynamical and evolutionary aspects (Robin et al. 2003, Robin & Crézé, 1986). The Besançon model also includes some spatial structures such as the thin disc, thick disc, spheroid, and bulge. Each component has its own spatial distribution (scale height and density), IMF, evolutionary tracks and metallicity. The extinction is modelled by a diffuse thin disc. The model is reasonably complete but, of course, it predicts the average properties of the Galaxy and cannot account for local spatial fluctuations.

The output of the Besançon model is a catalogue of simulated stars, for which all the information is known: distance, mass, age, spectral type, luminosity class, metallicity, age, etc. Thanks to these capabilities it is possible to explore in detail the "average" properties of the stars in selected fields of view of PLATO. Note that the model accounts also for poissonian noise on stellar counts. We have simulated stars with visual magnitudes in the $m_V = 6\text{-}18$ range in a region in the $70^\circ \leq$ longitude $\leq 130^\circ$ and $0^\circ \leq$ latitude $\leq 60^\circ$ range, which is part of the visibility region of PLATO. We have used the Besançon model in its "grid" mode that allows us to take into account the variations of stellar density with the position in the Galaxy within the considered area, which is needed because of the large area that PLATO will observe.

As a further check we have used the Trilegal model (Girardi et al. 2005, http://stev.oapd.inaf.it/cgi-bin/trilegal). The counts from both models are within 25% of the counts derived from star count analysis.

6.1.1 PLATO Input Catalogue (PIC) and General Philosophy of Preparation

Telemetry limitations impose the pre-selection of PLATO targets for the detection of planets. The optimal field selection is closely related to the target selection. The success of the mission is related to our ability to select fields that maximize the number of F5 or later spectral type dwarfs and sub-giants for which we can have photometry with the required S/N, i.e. fields in which P1 to P5 targets are maximized. We need to prepare a PLATO input catalogue (PIC) which includes P1-P5 targets, and provide their main parameters.

A limited number of additional targets may be added to the PIC, to monitor special objects (e.g. in star formation regions or star clusters within the long monitoring fields) for the main and complementary science. Finally, the PIC will help us to assess the nature of the detected transiting bodies: a good knowledge of the central star will help to exclude false alarms and will trigger the most appropriate follow up strategy. It will also allow us to get a first estimate of the size of the planet. The PIC will be constantly updated, also during the operation and post-operation phase, with target parameters coming from astrometric, photometric, spectroscopic and stellar activity surveys (e.g. from Gaia intermediate and final release catalogues).

The PIC will serve to: 1) select the optimal PLATO Fields (PFs); 2) select all appropriate >F5 dwarf and sub-giants within them (samples P1-P5); 3) characterize as much as possible the selected targets, i.e. estimate their temperature, gravity, variability, metallicity, binarity, chromospheric activity; 4) provide a list of neighbours that contaminate the target star flux; 5) give a first estimate of the transit object radius; 6) optimize the follow-up strategy.

Pre-launch characterization of PLATO targets will provide us with the basis for a statistical analysis of planetary system properties on a large scale. The precise definition of the contents of the PIC is strongly dependent upon which input data will be available in the next few years.

The building of the PIC will require the assembly of information from very different input catalogues (broad- and medium-band photometry, spectroscopy, astrometry) on a wide range of targets (from mid-F to M-dwarfs). We will allow for redundancy to avoid single point failure, and to check the reliability of the PIC entries. To this purpose, the cross-identification of selected PIC targets (e.g. from the Gaia catalogue) and other databases (e.g. photometric, astrometric and spectroscopic surveys) will provide a robust estimate of the accuracy of the classification.

The main source for the PIC will be Gaia early, intermediate, and final release catalogues. A complementary survey of available photometric and spectroscopic catalogues will be carried out. This survey can also be used as back up for the PIC target selection and characterizations in the case of delays in the publication of Gaia catalogues. During the definition phase, we have demonstrated that available catalogues are sufficient to select the main PLATO targets (P1, P2, P3, and P4), and to provide us with their basic parameters, assuring the success of PLATO mission, independently from Gaia performances.

6.1.2 Statistical Analysis of Available Stellar Catalogues

6.1.2.1 Catalogue Analysis

A first approach to the target/field selection is the statistical analysis of the existing catalogues. For each star down to PLATO limiting magnitude (that is V~13.5 for the P5 sample, and even fainter for the P4 sample), we will collect all parameters needed for a complete stellar characterization (parallaxes, absolute magnitudes, $T_{\rm eff}$, log(g), metallicity, activity diagnostics, variability, binarity, etc.). No catalogues including all such information are available, at the moment.

For this analysis, we can take advantage of:

Existing catalogues of parallaxes, spectroscopic parameters or narrow-band photometry with a bright limiting magnitude (i.e. V<7.2 for the Hipparcos catalogues, V<8 for the MK/HD/Geneva-Copenhagen surveys) or limited to specific areas of the sky (i.e. RAVE for southern targets with $|b|$>20);

Catalogues derived from stellar classification techniques based upon broad-band infrared/visible colours and proper motions (see also "complementary target selection");

The latter are limited by the completeness, the magnitude range, and the accuracy of the source catalogues. The most used source catalogues are: Tycho-2 for proper motions and BV photometry, 2MASS for JHK infrared photometry, and UCAC3 for proper motions. No deep, all-sky source of precise (~0.01 mag) visible magnitudes is available so far, except for the space-based Tycho-2 which is complete down to V~11. In any case, we note here that the brightest PLATO stellar samples (P1, P2, P3) are the most scientifically relevant, and that the selection of the PLATO fields will be driven by the intent of maximizing the number and the photometric quality of these bright targets. This holds in particular for the P1 sample, due to its relevance for the mission.

As for the P2-P3 sample (very bright stars with V<8) the existing catalogues provide us with a nearly complete astrophysical characterization, based especially upon Hipparcos parallaxes and spectra/*uvby* Strömgren photometry from the Geneva-Copenhagen survey. These stars are very close to the Sun (<80 pc, which is the distance of a F5V star at V=8). They are nearly reddening-free and isotropically distributed over the sky. Indeed, the all-sky counts of suitable P2-P3 targets from the above-mentioned sources demonstrate that their angular density is nearly uniform, and that we met the scientific requirement of ~1,000 targets observed during the long-duration phase (that is, over two PLATO fields) in any directions.

Catalogues from broad-band classification techniques (e. g. Ammons et al. 2006) give us density maps for the P1 (bright stars with V<11) sample by selecting suitable targets in the ($T_{\rm eff}$, log g) plane (Fig. 6.1). The resulting star density is in agreement (within 20-30%) with the Galactic models, both in the number and spatial distribution of targets.

As for the P1 sample, we can make an alternative estimate of target density by using Galactic models. Synthetic fields from Trilegal and Besançon Galactic models, sampled at different Galactic latitudes b, show that the density of P1 targets lies in the range 5-8 stars per square degree, i.e. it changes only by a factor smaller than two, moving from the Galactic disc to the Galactic pole. This weak dependence is mainly due to the F star components of the sample, while the GK dwarfs are nearly isotropically distributed.

As for the P4 sample (M dwarfs down to V~15-16), by using the nearby luminosity function (LF) by Kroupa (2001) obtained by Hipparcos data for objects brighter than M_V=11 and from ground data for fainter objects, in the range 9<M_V<13 and for spectral type M1-M7, the number of M dwarf stars expected in the 1000 deg^2 is 2,795 for V<15 and 11,125 for V<16, well within the scientific requirements.

6.1.2.2 Contaminant Analysis

Astrophysical false alarms, mainly due to eclipsing binaries were shown to outnumber true transiting planets in ground-based and space-based photometric surveys for planets. In the case of PLATO, this problem is minimized, thanks to the brightness of the targets. Complementary techniques are also foreseen in the PLATO project to identify astrophysical false alarms like the analysis of light curve to identify e.g. V-shaped grazing eclipses, the analysis of centroids to identify blended eclipsing binaries, the comparison of transits at different colours from the FAST telescopes, as well as the photometric and spectroscopic ground-based follow-up observations.

In any case, we will do our best to minimize the number of astrophysical false alarms with an estimate of the various possible contaminants in the process of selection of the PLATO field.

For the estimate of the expected level of contaminants we employ binary population synthesis techniques. The binary population synthesis code BiSEPS (Willems & Kolb 2002, 2004, Willems et al 2006) is presently being expanded to address features of the light curve of eclipsing binaries, and to enhance the underlying Galactic structure and extinction model. Preliminary results allow us to estimate the probability of observing blends with relative apparent transit depth in the range between 10^{-4} and 10^{-3}, as a function of target star m_V, for different field locations. This is the most critical and frequent astrophysical false alarms. The probability of observing blended eclipsing binaries with apparent transit depth relevant for PLATO is a strong function of galactic latitude. Fig. 6.1 shows that moving from |b|=30 to |b|=20, the contaminants density almost double.

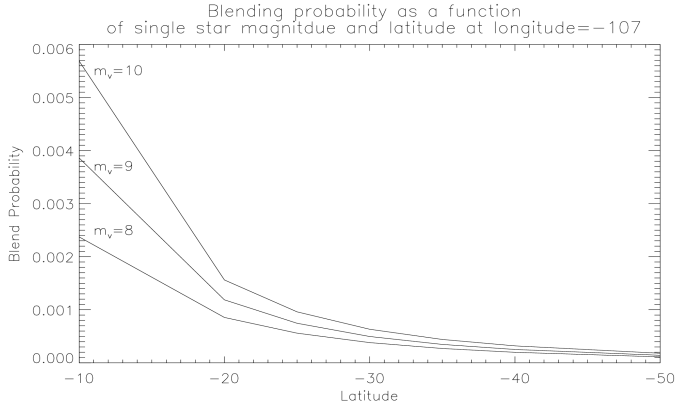

Figure 6.1: Blend probability versus Galactic latitude, for different target star magnitudes

6.1.2.3 Reddening Analysis

PLATO targets are located close to the Sun. At the limiting magnitude of sample P1 (V=11) we have that the brightest (F5) stars can be observed out to ~300pc (~200 pc for the G0 stars). For a magnitude limit at V=13 the limiting distances increase by a factor 2.5. It is very well known that the Sun is located in a local bubble, with a radius of about 150-200 pc (Lallement et al., 2003, Vergely et al., 2010) where the reddening is negligible. At increasing distances the reddening increases depending on the specific directions. An estimate of the reddening from the all sky survey of the Holmberg Geneva-Copenhagen Catalogue (2009) shows that it remains very low [E(B-V)<0.02 mag] up to 300-400 pc from the Sun. This distance includes basically all targets limited to V=11 and the influence of the distance from the Galactic plane is marginal.

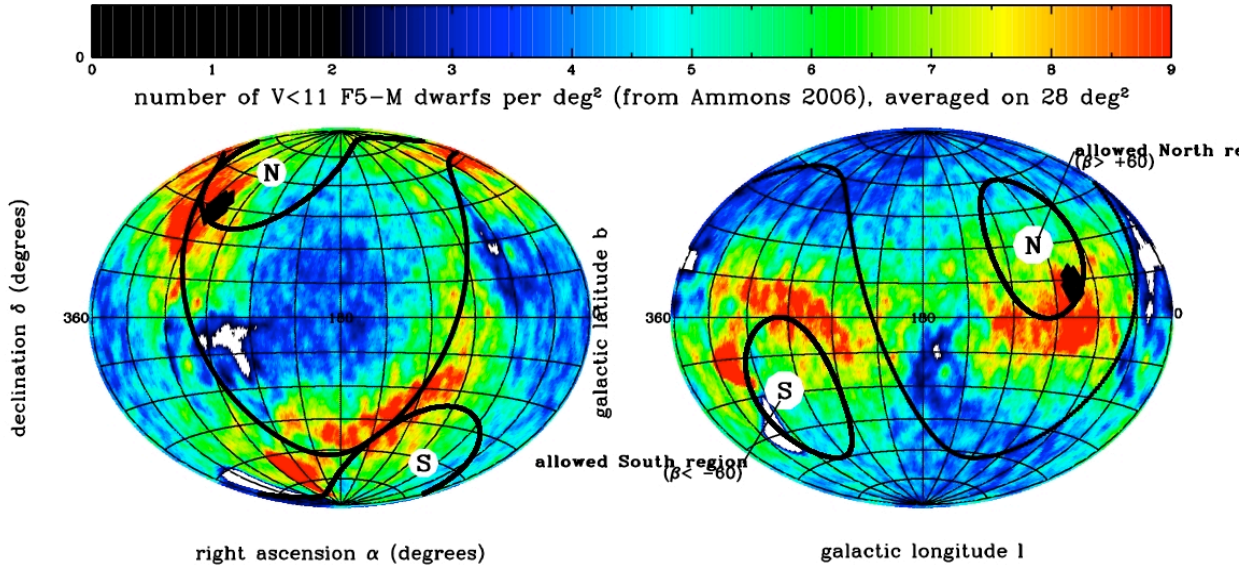

Figure 6.2: All-sky angular density of P1 targets as selected by Ammons et al. (2006), in equatorial (top panel) and galactic coordinates (bottom).

This guarantees that, even independently from Gaia, sample P1, P2, P3 can be selected from available catalogues with high completeness and a very low contamination level. The reddening between 400 and 800 pc (corresponding to the deeper P5 samples) can be determined from other distance limited maps of the reddening, typically obtained measuring individual bright stars, such as those published by Neckle and Klare (1980). These maps show that, in general, the reddening rapidly increases just before 1 kpc, in agreement with the average values obtained by infrared measurements of Marshall et al. (2006). A consequence of this analysis is that the rapid increase of the reddening beyond about 1 kpc can be used for a colour separation of much more distant, contaminating sources, such as bright giants, enabling us to select P1, P4, and P5 samples from available catalogues (UCAC3 and 2MASS).

6.1.3 Field Selection and field content

The two long-duration PLATO fields will represent the core of the mission. Their centres must stay within two regions imposed by observability constraints. These "allowed regions" are spherical caps defined by an ecliptic latitude $|\beta|>63$, and are located respectively in the southern and northern hemispheres, mostly at high declinations ($|\delta|>40$). The choice of the long-duration fields should be driven by 1) the fulfilment of the requirements concerning the number of observable targets for all five P1-P5 samples, and the maximization of the P1-P2 samples 2) the minimization rate of expected astrophysical false positives due to crowding, above all from blended eclipsing binaries. Both Galactic models and catalogues tell us that for every field choice, within the allowed southern and northern regions, the requirements for the P2 (>1000 targets summed on both fields) and the P1 (>20,000) samples are always met, with a large margin. The requirement for the P5 sample (>245,000) is conservatively met for fields centred at $|b|<40$. M-dwarfs with V<16 are a factor of 10 more numerous than the P4 requirements, and therefore are overabundant with respect to the science requirements. On the other hand, both the number of expected false positives and the number of nearby dust clouds rise steeply for $|b|<30$ (see Fig. 6.1). The best trade-off strategy is then to select fields centred at about $|b|\sim30$. As for the Galactic longitude, we note that the regions at low declination $|\delta|<60$ are on average less affected by interstellar extinction as visible on the dust maps. Also, low-declination regions have the advantage of a more efficient observability during the ground-based follow-up phase. A proposed conservative choice (to minimize contaminants, still satisfying the scientific requirements in terms of target numbers) for the field centres is (l=253, b=-30) for a Southern sky field and (l=65, b=30) for a Northern sky field. These fields are centred approximately on Pictor (South) and Lyra/Hercules (North) constellations. The

northern field includes the *Kepler* field on a corner. An additional, thorough study of the contaminant problem will allow us to verify whether the field centre can be moved to lower Galactic latitudes (|b|~25), thus increasing the number of targets.

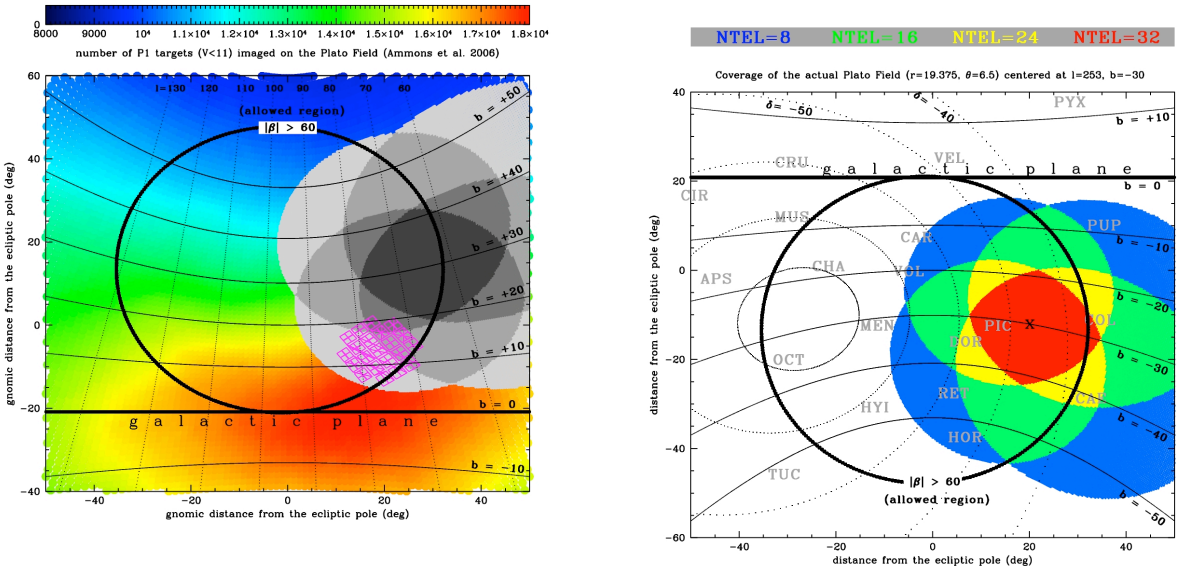

Figure 6.3: Left: Density of P1 targets for the northern region, averaged over the area of the PLATO Field, following Ammons et al. (2006). The preliminary long-duration PLATO Field is shown in gray. The Kepler field is indicated in pink colours. Right: The preliminary long-duration PLATO Field chosen for the southern allowed region, with the number of telescopes covering the single sub-regions indicated by different colours.

6.1.4 PIC Target Selection and Characterization from Gaia Catalogue

Gaia all-sky survey, due to launch in Spring 2013, will monitor astrometrically, photometrically, and, in part, spectroscopically, during its 5-yr nominal mission lifetime, all point sources with 6<V<20. A huge database, encompassing ~10^9 objects. Using the continuous scanning principle first adopted for Hipparcos, Gaia will determine the five basic astrometric parameters (two positional coordinates α and δ, two proper motion components μ_α and μ_δ, and the parallax π) for all objects, with end-of-mission precision between 7 μas (at V=6) and 200 μas (at V=20).

The precise determination of fundamental stellar parameters with Gaia will be instrumental in helping us to identify bright, nearby cool F-, G-, K-, M-dwarfs and sub-giants across the huge sky region (almost 50% of the sky) covered by the PLATO fields

6.1.4.1 Gaia Performance Estimates for PLATO Target Selection

During implementation phase, the first objective will be to coordinate the analysis of all available information (astrometric, photometric, and spectroscopic), initially from detailed simulations of Gaia observations, and then from Gaia early (and possibly intermediate) release catalogues, to provide a highly complete reservoir of well-classified nearby dwarf/sub-giant stars from which to choose, in order to populate the PIC, ahead of launch. To this end, a collaboration agreement has been established between the PLATO Consortium and the Data Processing & Analysis Consortium (DPAC) of Gaia mission (www.rssd.esa.int/gaia/dpac), responsible for the preparation of the data analysis algorithms to reduce the astrometric, photometric, and spectroscopic data. DPAC's Coordination Unit 2 (CU2) operates the GOG (Gaia Object Generator) software tool to obtain simulated early release catalogue (ca 2015) astrometric, photometric, and spectroscopic data from the Gaia satellite, based on specific simulation requirements (e.g., focusing on long- and short-term PLATO fields). Analysis of the first simulations, provided by CU2 during definition phase, indicates that a 'clean' sample of main-sequence dwarfs later than F5, with only a few percent 'contamination' from cool giants, could be easily selected with simple cut-offs in distance and reddening-corrected absolute magnitude in the Gaia main photometric pass-band MG, thanks to the exquisite precision estimates of Gaia parallaxes (<<1% for all potential PLATO PIC targets), based on detailed error

models, taking into account the selection of specific gate schemes in order to avoid saturation on bright (V<13) stars. The contaminants can be reduced to a negligible fraction (<1%) using the information on effective temperature T_{eff} and surface gravity log(g) from Gaia spectro-photometry, which will be accurate to ~200-300 K and 0.2-0.3 dex, respectively, for bright stars (V<14).

Upon release of the Gaia early release catalogue, in-depth investigations of the quality of Gaia astro-spectro-photometric measurements will be carried out for both 'primary' stars included in the core data analysis (processed by CU3) as well as for stars showing hints of variability (processed by other CUs). The re-assessment of Gaia performance in astrometry, photometry, and spectroscopy on bright stars will continue into PLATO mission operations phase, until the publication of the final Gaia catalogue (ca. 2021).

6.1.5 Complementary target selection for PIC

The advent of accurate all-sky catalogues such as Hipparcos, Tycho-2, and 2MASS made the extraction of stellar main parameters from wide-band photometry and proper motions possible (Ammons et al. 2006, Belikov & Roeser 2008, Ofek 2008, Bilir et al. 2006, Pickles & Depagne 2010). These authors defined the main techniques we can use to extract P1 sample targets (P2 and P3 samples will be available mainly from Hipparcos and MK/HD/Geneva-Copenhagen surveys).

Most of these works employ similar input catalogues, usually Tycho-2 and 2MASS magnitudes, as they provide uniform, precise all-sky photometry over passbands that contain useful information on [M/H] and log(*g*). Proper motions, when used, are extracted also from Tycho-2. During the definition phase, we carried out an external validation of these techniques by selecting stars with "photometric" ($T_{\rm eff}$, log(*g*)) suitable for the inclusion in the P1 sample, and then checking how many of them are confirmed as P1 targets by the spectroscopic parameters from RAVE DR3 (Siebert et al. 2011). We find on average <20% of contaminating giants in such a selected sample, which is still acceptable (but shall be reduced during the implementation phase) as PLATO telemetry will allow us to monitor more P1 targets than the 20,000 stated by the scientific requirements. Further contaminants can be identified by on-board photometry and discarded afterwards.

Unfortunately, most photometric classifications are limited to about V<11 (and therefore to the PLATO stellar samples P1-P3) by the completeness limit of Tycho-2. Though 2MASS provides very good photometry (σ<0.05 mag) down to V~15 and Tycho-2 proper motions are also well complemented by UCAC3 for stars brighter than V~15, no reliable source of visual magnitudes is available for V>11 on the whole sky, making stellar classification more difficult (i.e. affected by a larger contamination level), with the only exception of M-dwarfs (P4). However, once full-coverage catalogues from APASS and SkyMapper will be released, it will be possible to extend photometric spectral and luminosity classification of stars to fill P5 target requirements. Meanwhile, we note that "reduced proper motion" (RPM) techniques from UCAC3 proper motions coupled with 2MASS *JHK* colours are already able to perform an acceptable selection of M-dwarfs (which, by far, outnumber the minimal P4 science requirement) and a minimal giant/dwarf separation for the P5 sample. Preliminary estimates done on RAVE dr3 entries with UCAC3/2MASS data show that it is possible to perform a P4 target selection with >60% efficiency, and <30% contamination, and a P5 target selection with <30% contamination and >80% completeness. This implies that we will be able to prepare the PIC even in case of failure or reduced performances by Gaia.

6.1.6 PIC Target Characterization

After field selection and the identification of the targets to be observed with PLATO we will focus our attention on the determination of the target properties. A thorough astrophysical characterization of the PIC target stars will help, for example, minimizing false positives, and the optimization of expensive, time-consuming follow-up work. The target characterization will normally involve the determination of a complete set of stellar parameters (e.g., distance, proper motion, magnitudes, Teff, surface gravity log(g), metallicity [M/H], extinction, stellar activity, age indicators, etc.) for each PIC entry. This, combined with information on binarity/multiplicity and/or the presence of planetary-mass companions (likely available at the level of intermediate data releases), will also allow for detailed prioritization of the PIC targets.

The list of relevant astrophysical parameters to be included in the PIC, and their priority will be collected taking into account the requirements of the various PSPM Work Packages.

The principal source of target parameters will be Gaia catalogues (see below). Cross-matching of other catalogues will help to complete target characterization, and will be performed at ASI Data centre. The level of magnetic activity will be collected from available catalogues in the literature and archives (e.g., X-rays, UV emission lines, Ca II H&K indexes, H-alpha EWs) in order to define subsamples of stars with different activity levels. Recalling that high magnetic activity is an indicator of youth, choosing stars having different activity levels will allow us to investigate the properties of planetary systems in an evolutionary contest. Archival spectra of PLATO targets will also be used for characterization,

Dedicated surveys for further characterization are also been considered. Super-WASP telescopes equipped with suitable narrow-band filters might provide reliable temperature and gravity for PLATO targets in a limited amount of time. Observations of the PLATO field using a dedicated 0.8m robotic telescope at Cerro Amazones (to be operated by AIP) might provide information on stellar content around PLATO targets at 1 arcsec spatial resolution, very useful to evaluate blend scenarios, as well as temperature and activity characterization of PLATO targets (including the P5 sample) by means of narrow-band observations. An extension of the RAVE survey devoted to PLATO targets is also being considered.

6.1.7 Gaia Parameters Extraction and Target Characterization

We expect that the bright PLATO stellar sample (V<11) will have distance, proper motion, magnitudes, T_{eff}, surface gravity log(g), metallicity [M/H], extinction A_V, stellar activity and age indicators provided with high precision by Gaia, even at the time of an early data release. During the Implementation phase, the astrometric, spectroscopic, and photometric parameters from the Gaia early/intermediate data releases will be defined and prioritized for the purpose of the definition of the PIC entries, for the optimization of the PLATO fields of view, and for the characterization/prioritization of potential PLATO targets. Dedicated algorithms will be created, implemented and tested for cross-examination of the Gaia astrometric, spectroscopic, and photometric information for the definition and prioritization of the set of parameters utilized for the selection of PIC targets, based on extensive simulations of the PLATO fields, and the completeness assessment described above. The algorithms will be adapted for ingestion, and extraction of the relevant parameters from Gaia early as well as intermediate release data. During operations, the algorithms will be utilized to derive a finalized and prioritized list of stellar parameters from Gaia astrometry, photometry, and spectroscopy at the time of publication of the final Gaia catalogue. All activities will be carried out in close collaboration with and with the technical support of the PLATO Data Centre (PDC). Formal interaction mechanisms with the Gaia DPAC, if needed with ESA's direct mediation, will allow us to guarantee that all stellar parameters deemed necessary for selection, characterization, and prioritization of dwarf stars for the PIC shall be included into Gaia catalogues since the first, early data release.

6.2 PLATO follow-up observations

The prime science product of PLATO consists in a sample of fully characterized planets of various masses, sizes, temperatures, and ages, with a special emphasis on terrestrial planets in the habitable zone of their parent stars. To reach this ambitious goal, in addition to the space-based photometric transit detections and asteroseismic characterization, a ground-based support is absolutely required, mostly for the follow-up of planetary system candidates.

The role of the follow-up is multiple. We first need to discard false positive configurations leading to photometric signatures similar to the ones induced by planetary transits. Then, complementary observations provide information on the planet properties not available from the light curves, the most important among them being the planet masses derived from radial velocities. Taking advantage of the expertise gained with the successful ground-based transit search surveys, and with the CoRoT and *Kepler* space missions, a battery of diagnostics has been developed to detect some of the most common false positive configurations directly from the photometric observations. The most efficient surveys on the ground still have 5 to 10 times more false positives than real planets in their candidate list. From the *Kepler* experience, we are learning that this ratio seems to get more favourable in space with high quality photometric data but the false positive will nevertheless be non negligible. **The final performance of the PLATO space-based transit search program is thus ultimately determined by the associated follow-up capabilities**. It is therefore particularly important to include these considerations in the planning of the mission. An important part of the

preparatory work for the mission includes estimates of the expected planet yield and false-positive rate in order to estimate, plan, and organize in an optimum way the ground-based telescope observations.

6.2.1 False positive estimate

The main types of false positives include grazing eclipsing binaries [GEB], transits by planetary-size stars (*e.g.* late M dwarfs for giant planets, or white dwarfs for terrestrial planets), M dwarfs or brown dwarfs eclipsing giant stars [MEG], background eclipsing binaries [BGEB] diluted by a physical or optical bright stellar companion (inside the photometric window), sometime unresolved [BEB]. In the same way, a background star with a transiting giant planet diluted by a brighter companion [BGPT] will mimic a small-size planet transit. All these astrophysical scenarios masquerade as transiting planets of various types. Some of them can be solved directly from the PLATO high-precision photometry and astrometry, or from the comprehensive information in the Input Catalogue. The expected rate of remaining false positives should be estimated to define and estimate the need of ground-based follow-up, in addition to planet characterization.

For the CoRoT space mission, the false-positive rate, estimated from the follow-up effort made during the past three years, is up to 70% (Moutou et al. 2009, Cabrera et al. 2009). For the *Kepler* space mission, the false-positive rate is not yet completely determined. Borucki et al. (2011) estimate that about 20 to 40% of the recently announced 1200 candidates might be false positives. The main difference with CoRoT comes from the capability of *Kepler* to determine the relative position of the image centroid during and outside of the transit epoch (Bryson et al. 2011).

For PLATO, we may reasonably consider that all GEB's and MEG's will be identified from PLATO photometry and Input Catalogue (mainly Gaia database). The BGEB's inside the PLATO window, and as close as few arcsec from the target star, will be identified by the image centroid motion. This technique was found to be especially efficient for the *Kepler* candidates. The PLATO PSF surface is larger than for *Kepler* but this is in great part compensated by targets 3.5 magnitude brighter, which suffer less contamination by companions at a given contrast level. Additional ground-based high-resolution and high-contrast imaging will be required to exclude contaminants and background eclipsing binaries within a few arcsec of the main target. Resolving the bright star from the BGEB will allow us to determine, from *on-off* photometry, which of them is hosting the transit. This approach is also efficient for BGPT's. The corresponding need in follow-up resources will depend on the rate of contaminants and the capability of PLATO to measure the image centroid motion, but we may expect that it will concern between 5 and 10% of PLATO candidates. For still unresolved BEB's, like physical triple system, the bisector span diagnostic from radial velocity follow-up will permit to identify this scenario which is expected to concern less than 20% of PLATO candidates.

To conclude, from the experience of CoRoT and *Kepler*, we may reasonably assume that the rate of false-positives will be less than 30%. These false-positives, mainly BGEB's and BEB's, will require high-resolution and high-contrast imaging facilities as well as high-resolution and high-precision radial velocity facilities.

6.3 Optimization of the radial velocity follow-up

The planet minimum mass estimated from Doppler measurements is directly proportional to the amplitude of the reflex motion of the primary star. The characterization of the lowest possible mass planets detected with PLATO will then be intimately linked to the ultimate long-term precision achieved on the radial velocity (RV) measurements of the star.

6.3.1 Limitations to precise radial velocity follow-up measurements

Looking for the highest RV precision, several sources of uncertainty have to be considered. They can be classified into several broad categories: photon count, technical, and astrophysical. Each of these sources is essentially independent from the others and thus the actual precision eventually obtained on the measurements will be a quadratic combination of the different contributions.

Instrumental requirements: The exciting results obtained with the ESO HARPS spectrograph demonstrating sub-m/s long-term RV precision (typically 80 cm/s for published planetary systems) have motivated new studies to push down the limits of Doppler spectroscopy. From the instrumental perspective, reaching a

precision level of a few cm/s should be possible with especially-designed spectrographs, provided that a special care is put in some very important aspects (Pepe & Lovis 2008): spectrograph stability, high spectral resolution to resolve the spectral lines, adequate sampling, precise wavelength reference, efficient image scrambling, and precise guiding and centring. The ESO ESPRESSO/VLT and CODEX/E-ELT projects materialize the efforts in this direction. New spectrographs designed as well according to the requirements set for high-precision RV's and pushing in the IR domain are also in development (Spirou/CFHT, Carmenes/Calar-Alto).

Photon noise: The uncertainty on the RV's associated with photon noise roughly scales with the measurement signal-to-noise ratio (S/N) of the spectra, i.e. with the square root of the flux, or also with the telescope diameter. With HARPS, a photon noise level of 1 m/s is achieved in 1 min for a V=7 K dwarf. This precision corresponds to an exposure time of close to 4 hours for a V=13 star. Assuming a similar spectral window (0.38-0.68μm), considering an expected efficiency about 4 times better for ESPRESSO (from phase A study), and taking into account the difference in collecting areas, we estimate that with ESPRESSO on the VLT we will reach 10 c/m in 15 min for a V=8 star, or 20 cm/s in 1 hour for a V=11 star, These estimates demonstrate the need for bright stars and large collecting areas when considering the radial velocity follow-up of very low-mass planet candidates.

Contamination effects: the contamination of the target spectrum by an external source is also a potential limitation for the precision of the RV measurements. The most disturbing cases are the *light from a close-by object* and the *Moonlight*. The light of faint objects close to the science target may fall on the spectrograph fibre and contaminate the science target spectrum. This is in particular the case for transit false-positive detections due to triple-star blends. High-resolution, high-contrast follow-up observations with instruments equipped with AO capabilities will be required to point out visible companion of any magnitude closer than typically 3 arcsec from the science target. In the same way, we have to avoid as much as possible that direct or indirect sunlight reaches the detector with a contrast magnitude compared to the science target smaller than ~8-10 for the highest RV precision.

Stellar jitter: Besides instrumental, environmental and photon-noise limitations, other phenomena intrinsic to stellar atmospheres, which we call "stellar noise" or "stellar jitter", have to be taken into account. They cover different timescale intervals depending on their origin.

- *p-mode oscillations:* The solar-like oscillations induced in stars with convective envelopes have typical periods of a few minutes in solar-type stars and typical amplitudes per mode of a few tens of cm/s in radial velocity (Kjeldsen et al. 2005). The observed integrated signal is then the superposition of a large number of these modes, possibly adding up to several m/s. Amplitudes of the RV variation become larger for early-type and evolved stars. Low mass, non-evolved solar-type stars are therefore easier targets for planet searches. However, even in the most favourable cases, it remains necessary to average out this signal if aiming at the highest RV precision (see below).

- *Granulation and super-granulation:* Granulation is the photospheric signature of the large-scale convective motions in the outer layers of stars with convective envelopes. The granulation pattern is made of a large number of cells with upward and downward motions tracing hot matter coming from deeper layers and matter having cooled down at the surface. On the Sun, the typical velocities of these convective motions are 1-2 km/s in the vertical direction. However, the large number of granules on the visible stellar surface (~10^6) efficiently averages out these velocity fields, leaving some remaining jitter at the m/s level for the Sun, probably less for K dwarfs (*e.g.* Palle et al. 1995, Dravins 1990). The typical timescale for granule evolution is about 10 minutes for the Sun. On timescales of a few hours to about one day, evolution of larger convective structures in the photosphere may induce additional stellar noise, similar in amplitude to granulation itself. We talk about meso- and super-granulation. Overall, granulation-related phenomena likely represent a significant noise source when aiming at sub-m/s RV precision. Observing strategies to minimize their impact have been simulated (see below).

- *Magnetic activity:* Magnetic phenomena at the surface of solar-type stars induce radial-velocity variations through the temporal and spatial evolution of spots, plages, and convective inhomogeneities (Saar & Donahue 1997; Saar et al. 1998). When the star-spot pattern is long-lived, induced variations in the spectral line asymmetry are modulated by the rotational period of the star and can mimic a planetary signal (*e.g.* Queloz et al. 2001; Bonfils et al. 2007). When the star is observed longer than the typical lifetime of star

spots, the signal becomes incoherent, potentially inhibiting the detection of planetary signals of lower amplitude. Granulation is also damped within the spots, changing for spotted stars the balance of granulation effect over the surface. Stellar jitter depends on effective temperature, stellar activity, and projected rotational velocity (*e.g.* Wright et al. 2004). Typical values are below 1 m/s for slowly rotating, chromospherically quiet G-K dwarfs (Mayor et al. 2009b). To quantify the activity level of their targets, Doppler planet searches traditionally use the R_{HK} indicator representing the fraction of a star's bolometric flux emitted by the chromosphere in the Ca II H and K lines (Noyes et al. 1984). Since this chromospheric emission is closely related to the surface magnetic flux, a high value of R_{HK} is an indication that a star may exhibit significant activity-related velocity variations. The bottom level of the stellar-induced velocity jitter for the quietest stars is not known yet.

- *Magnetic cycles:* Longer-term change in the spot coverage of the stellar surface (over several years) often referred to as the star magnetic cycle (11-year cycle for the Sun) is also inducing a slow low-amplitude variation of the observed RV's. This effect can fortunately be tracked and corrected with activity-indicator monitoring (as e.g. the R_{HK}; Lovis et al., in prep).

6.3.2 Stellar intrinsic variation and optimal observing strategy

Although stellar noise is a major limitation on very high precision Doppler measurements, adequate observing strategies help diminish its effect. The strategy adopted to minimize the stellar oscillation noise consists in integrating over a few typical oscillation periods. Estimates based on HARPS observations and asteroseismology models show that, for quiet stars, an exposure time of 15 minutes is sufficient to average out the "perturbing" signal well below 1 m/s, and the noise even get down below 10 cm/s in about 20-30 minutes (Eggenberger P., private comm). On intermediate and long timescales, Doppler measurements are affected by stellar granulation and stellar activity, respectively. A strategy aiming at statistically averaging the perturbing effects is possible with enough observations covering a span larger than the typical timescale of the effects (hours to stellar rotation periods).

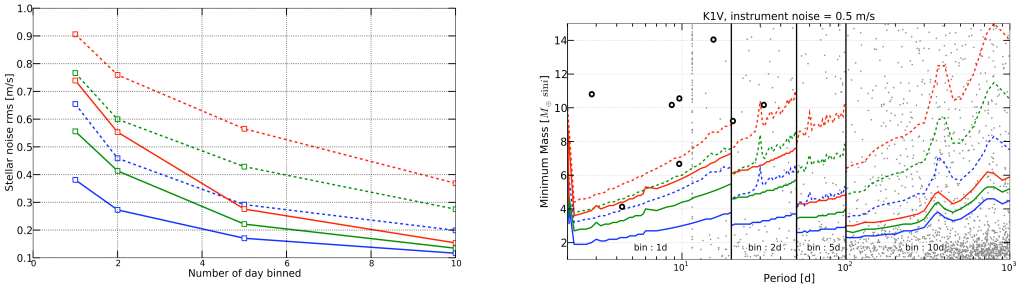

Figure 6.4: Left: Estimate of stellar noise effect on radial-velocity rms as a function of the binning of the measurements for Alpha Cen B (K1V). The 2 line types correspond to different observing strategies: dashed for the actual strategy presently used for the HARPS-GTO high-precision program (1 measure per night of 15 minutes, on 10 consecutive nights each month); continuous lines for a more efficient strategy with 3 measures per night of 10 minutes each, 2 hours apart, every 3 nights. The different colours correspond to different stellar activity levels: blue for log(R'HK)=-5.0, green for log(R'HK)=-4.9, and red for log(R'HK)=-4.8. Right: Corresponding limits of planet mass detection as a function of orbital period derived from Monte-Carlo simulations. The open circles represent small-mass planets found with HARPS around G and K dwarfs, and the lighter dots correspond to the expected planets from the Bern population synthesis models (Mordasini et al. 2009). Line types and colours have the same meaning for the left panel. The diagram is separated in 4 period regimes, each one using a different binning, well adapted to the corresponding period range.

Simulations have been performed to quantify the amount of observations required to reach a given level of precision, taking into account oscillations, granulations and activity-related effects (Dumusque et al. 2011a, 2011b):

1. First, from publicly available HARPS asteroseismology radial-velocity measurements for six stars, synthetic high-frequency observations were generated from corresponding models of the stellar noise in Fourier space, including oscillation and granulation effects. The rms of the synthetic velocities binned according to different observing strategies was then calculated for stars with

different spectral types in our sample. These cases correspond to spotless stars.

2. In a second step, in order to take into account activity-related phenomena, families of spots were generated in a realistic way, and estimate of the radial-velocity effect induced by the spots were derived. The spots appearance law, number, lifetime, and corresponding filling factors, for different activity levels, were calibrated from actual data of the Sun.
3. Finally, these simulations allowed the authors to derive, through a Monte Carlo approach, the detection limits in the mass-separation plane expected for each of the considered strategies.

The combined effect of the different stellar noises is presented in Fig. 6.4 for the star Alpha Cen B (K1V), for different activity levels and observing strategies. Although decreasing less rapidly than the best "statistical" case (i.e., as the square root of the number of measurements), the improvement of the measured rms is very encouraging and demonstrates the pertinence of the approach. Proceeding in this way, an *equivalent* precision of 35 cm/s has already been obtained on the 3-Neptune host HD 69830 (Lovis et al. 2006). Very interesting detection limits are obtained in the case of a realistic strategy (optimized precision versus cost in observation time) consisting in three 10-minutes observations per night, individually separated by 2 hours. A binning over several days can then be applied when looking for longer period planets (Fig. 6.4, right). The interesting point to note here is that, for a given planet mass, the detection limit is weakly depending on the period. Indeed, the lower amplitude of the signal is then compensated by the larger temporal bins considered for the average. The estimated yield of the PLATO survey presented in the next section is using results of these simulations to realistically take into account limitations set by stellar noise for the radial velocity follow-up. Over the past few years, 10 quiet stars have been monitored with HARPS following the proposed optimum strategy. Three of them are already found to host planetary systems (Pepe et al. 2011), two with detected RV amplitudes in the 50 to 90 cm/s range. The third system, HD 192310 (K3V), hosts a Neptune beyond the habitable zone of the star (P=526d), demonstrating the efficiency of the approach for the characterization of PLATO low-mass candidates. These early results are still including HARPS instrumental limitations (with centring and guiding effects) and a contribution from photon noise. Improvements are then expected with more stable instruments as ESPRESSO/VLT and longer exposure times to better average the stellar oscillations.

Another promising approach to better characterize stellar noise will be to simultaneously monitor activity indicators at the same time as the velocity observations and then use correlation between the velocity and the indicators to correct the velocity from the stellar intrinsic contribution. Studies are being conducted in this direction using photometric, activity indicators, and line-shape measurements (Lovis et al. 2011, to be submitted).

6.4 Expected number of characterized planets

The impact of PLATO on exoplanet science will be directly related to the number of exoplanets of different masses, radii, and densities that can be detected and fully characterized by the mission. In this respect, we note that PLATO will provide a far better coverage of the parameter space than *Kepler*, thanks to its extended surveyed area (~4'000 deg^2 for the long runs, compared to 100 deg^2 for *Kepler*), allowing the mission to concentrate on the brightest stars ($m_V < 11$). Bright stars are a key asset of PLATO as they will enable an asteroseismic analysis to determine the mass and age of the planet-host stars, as well as a fast and efficient radial velocity follow-up from the ground, presently the strongest limitation for the characterization of *Kepler* candidates. The PLATO follow-up will also benefit from improved radial-velocity performances of the next generation of instruments as e.g. ESPRESSO on the VLT in the southern sky, or Spirou/CFHT and Carmenes/Calar-Alto for the north.

The expected number of PLATO detectable (photometric detections) and characterisable (RV follow-up) planets as a function of their masses and orbital separations have been estimated through numerical simulations, taking into account i) the latest results of the high-precision RV planet-search surveys (Lovis et al. 2009, Mayor et al. 2011, Howard et al. 2010), as well as the preliminary *Kepler* findings (Borucki et al. 2011), and ii) simulations of strategies to average down the effect of stellar intrinsic phenomena (Dumusque et al. 2011ab).

Figure 6.5 illustrates the results of these simulations for both PLATO and *Kepler*. The simulation simply takes as starting point the star sample observable by each one of the missions. The displayed numbers are those of the expected characterized planets by PLATO, while the sizes of the coloured regions show the

respective discovery potential of both missions (blue: PLATO and green: *Kepler*). Note that there is no underlying planet formation model.

1. In a first step, a probability of detection and characterization was estimated for different cells of a grid covering the planetary mass-separation parameter space, assuming that each star of the sample is actually hosting a planet in each of the cells. A planet is considered as detectable if it can be seen in transit by the satellite and confirmed by follow-up radial velocity measurements with a reasonable amount of telescope time. Such a scheme could consist of a 1h observation each night, every 3 nights over a month (10 nights in total), repeating this sequence every month for the visibility period of the star during a couple of orbital revolutions.
2. The obtained probability of detection & characterization is applied to the number of stars in the sample to give the numbers in the blue circles in the figure.
3. In a second step, to obtain the fraction of stars that actually host a planet in a considered cell of the grid, we have to apply onto the grid the 2D distribution of planet occurrence in function of planet mass and planet-star separation, following the description in points 4) And 5) hereafter. We obtain so the red numbers in each grid cell of Fig. 6.5, corresponding to the expected planet yield of the mission.
4. For the separation distribution, relying on the fact that 80% or more of small-mass planets are found in multi-planet systems and that these systems appear to be "packed" i.e. filling up with planets all the available space (Lovis et al. 2011 for HARPS results, Lissauer et al. 2011 for *Kepler* multi-transiting systems), we considered that stars hosting planets will have 1 planet in each of the four defined cells along the separation axis.
5. For the mass distribution, the HARPS and Keck high-precision RV surveys find a distribution rising towards low masses. This result is confirmed by the *Kepler* distribution of planet sizes rising towards the smallest objects as well. For the mass distribution, we then use the distribution proposed by Howard et al. (2010) or obtained from the HARPS results (Mayor et al., in prep). The two estimates lead to the two red numbers per cell in the figure.
6. The expected results depicted in Fig. 6.5 have been obtained as realistically as possible, taking into account all sources of noise for the radial velocity follow-up (oscillation, granulation, activity level), and limiting the required observing time to reasonable values. The estimate can even be considered as conservative, as for especially interesting cases more observing time can be dedicated to the follow-up. Future developments in our understanding of the interplay between activity level and induced RV jitter might help correct for the spurious effect and further improve our characterization ability.
7. The more valuable candidates are the low masses and long periods (in the habitable zone). Their number is small (a few tens) whereas short-period planets (especially if heavier than ~10 Earth masses will be numerous, very probably outnumbering the possibilities of the follow-up. We thus plan to limit the follow-up of short-period planets to 300 per defined separation cell for low-mass planets requiring 4m-clas telescopes (1-3 m/s precision) and to 500 for intermediate-mass planets requiring 2m-class telescopes (5-10 m/s precision). These numbers represent a trade-off between the need for a good statistics to cover the variety of exoplanet characteristics and telescope costs. These numbers are first estimates and can be adjusted in the course of the mission if necessary.

From the derived planet yield (including limit numbers for short-period planets), and assuming that 20 observations per planet (i.e. 80 observations per star, if the 4 planets spread over the separation range orbit the same star) are adequate to characterize the candidates, we estimate that each class of telescopes are requiring the following amount of observing time for the radial-velocity follow-up:

- 1-2m class telescopes (3-10 m/s precision): 1750 planets (giant planets on short/medium orbits) requiring 900 nights = 50 nights/year x 6 years x 3 telescopes
- 4m-class telescopes (1-3 m/s precision): 1400 planets (giant planets on long orbits and super-Earth on short/medium orbits) requiring 700 nights = 40 nights/year x 6 years x 3 telescopes
- 8m-class telescopes (10-20 cm/s precision): 550 planets (super-Earths on long orbit, earths on short to medium periods, Earths on long orbits for the brightest stars (m_V<10) requiring 240 nights = 40 nights/year x 6 years x 1 telescope

These estimates of telescope time can be pushed up or down, depending on the limit number of observations we are ready to dedicate to a given candidate (planets orbiting more active stars can be characterized at the expense of observing time, see CoRoT-7b for an example, Queloz et al. 2009) and on the maximum number of candidates we will monitor in the PLATO follow-up program.

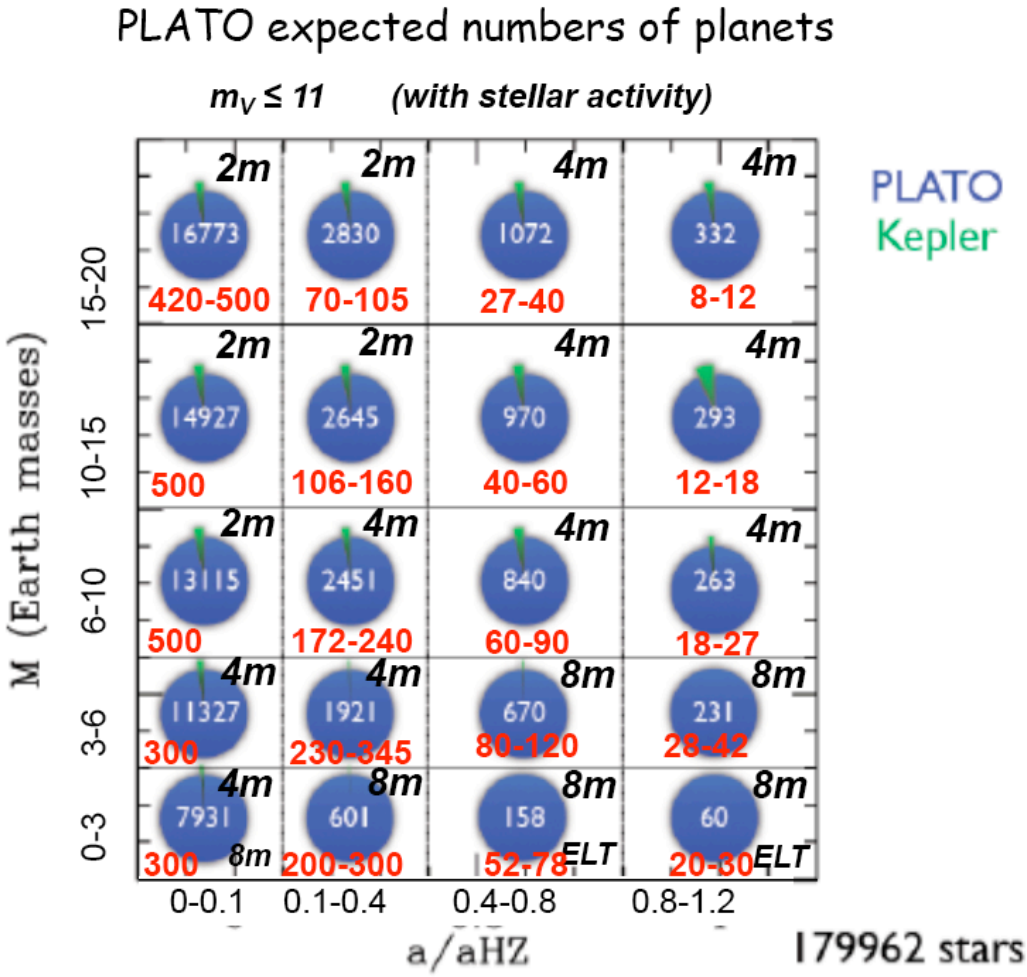

Figure 6.5: Estimated total numbers of detected transiting planets, which can be confirmed and characterized by ground-based radial-velocity observations, for PLATO (blue) and Kepler (green; see text for details). Note that a large fraction of the mass-separation space, not covered by Kepler, can be explored by PLATO. The separation axis is given in unit of habitable zone distance to take into account the spread in stellar masses of the targets in a typical PLATO field. The red numbers represent the estimated PLATO planet yield. The type of telescopes foreseen for the follow-up of each planet type is indicated as well.

6.5 Organization of the follow-up

The main aspect of the ground-based follow-up of PLATO transit candidates will reside in the basic planet characterization through radial velocity measurements. As seen in previous paragraphs, the same level of precision cannot be reached for all stars due to various sources of stellar intrinsic limitations: spectral type, luminosity class, activity level, star brightness. In particular, photon-noise limitations and activity-related jitter require a large amount of telescope time in order to detect the lower-mass planets.

False positives related to stellar diluted blends will usually not display large radial velocity variations. Due to the PLATO large pixel size on the sky, the situation will appear often. It is thus important to point out these cases before spending expensive time on large telescopes. As mentioned previously, many cases will be discarded from the light curve analysis (shape of the transit curve), from correlations between light curve and centroid curve from PLATO data alone, or from moderate-precision spectroscopic observations (variation of

the shape of spectral lines through bisector measurements). For the remaining cases, it will be important to check that the low-depth transit is not due to a deeper eclipse of a fainter star very close to the primary target. This can be achieved at higher spatial resolution, checking for transits on the neighbouring stars. The radial velocity follow-up coupled with the high-angular confirmation that the transit is indeed taking place on the primary target should be sufficient to safely characterize the planet candidates.

Due to the number of expected PLATO candidates, a systematic observation of all detected transits with large telescopes will be unfeasible and an optimized follow-up scheme has to be organized. Facilities of given precision should be mainly used for the characterization of planets accessible to that precision. In practice for the characterization follow-up, a multi-step approach going from moderate- to high-precision instruments is already successfully used in most of the on-going surveys. It will also nicely apply to PLATO candidates. It is sketched in Fig. 6.6.

1. The candidate list has to be cleaned as much as possible from false positives by diagnoses applied directly on the high-precision PLATO light curves, as described above.
2. Small telescopes will be used for a first screening of the remaining transit candidates, rapidly discarding unrecognized binaries from the list. As PLATO prime targets consist in bright stars, low- to intermediate-precision instruments (similar to FEROS on the ESO 2.2-m telescope, CORALIE on the 1.2m Swiss telescope at La Silla, or ELODIE on the 1.93-m telescope at OHP) will be perfectly suited for this part of the follow-up.
3. Given that the host star's brightness and activity level will define the expected ultimately achievable radial velocity precision, this will dictate which telescope+spectrograph facility has to be used for the planet characterization.
4. HARPS on the ESO 3.6-m telescope at La Silla or similar instruments in development (Spirou/CFHT, Carmenes/Calar-Alto) will be the working horses for planets with masses down to the super-Earth regime not too far from their central stars, as well as for the most active part of the sample (anyway limited by stellar noise to a level comparable to the instrument precision).
5. Finally the most interesting and demanding lower-mass, longer-period planets will require the best possible radial velocity precision that should be available with ESPRESSO on the VLT (foreseen on the sky in 2014) and possibly with a super stable spectrograph (CODEX) on the E-ELT for the southern sky. HARPS-N to be installed on the Italian TNG at La Palma (Canary Islands) in April 2012 is for the moment the best instrument available in the northern hemisphere.
6. A very important amount of telescope time will be required for the PLATO follow-up. It is the duty of the PLATO Consortium through its *mission lead* and *follow-up scientist* and/or of ESA to discuss with the owner institutes of the observing facilities on a scheme for obtaining the amounts of time required to observe the candidates. This has to be a global effort of the community, in the line of the open data property policy of ESA.
7. On the instrument development side, important progress has been made with the decision by the ESO council to build ESPRESSO for the VLT, and by the important advancement of the Spirou/CFHT and Carmenes/Calar-Alto projects. The entrance of Brazil as a new member of ESO is also opening the possibility to develop a Brazilian-led high-precision radial-velocity instrument in the southern hemisphere.

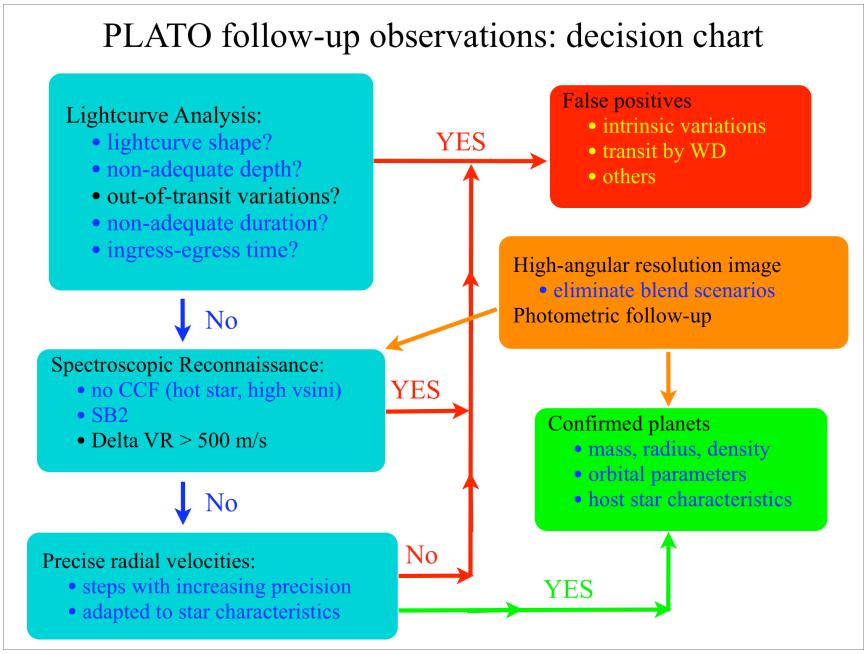

Figure 6.6: PLATO follow-up organization describing the different steps making use in an optimum way of the different observing facilities. WD is a white Dwarf, CCF is the Cross Correlation Function used in radial velocity (RV) observations, SB2 stands for a type of Spectroscopic Binary that can mimic an exoplanet.

7 PLATO GROUND SEGMENT AND OPERATIONS

7.1 Concept

The ultimate goal of the PLATO Ground Segment is to deliver a list of confirmed planetary systems, which will be fully characterized by combining information from the planetary transits, the seismology of the planet-host stars, and the follow-up observations. The major part of the PLATO data will become publicly available as soon as it is reduced.

The PLATO Ground Segment consists of 4 components: The Mission Operations Centre (MOC), the Science Operations Centre (SOC), the PLATO Data Centre (PDC), and the PLATO Science Preparation Management group (PSPM). Of these, the PDC and PSPM are part of the PLATO Mission Consortium (PMC) while the MOC and SOC are under ESA responsibility.

The SOC and the PDC/PSPM are jointly responsible for preparing and carrying out the science operation phases as regards use of the instrument to achieve the science objectives defined in the SMP. This will involve provision of the input catalogue to the MOC for uplink to the spacecraft, processing of the dumped data from the instrument, performing quality control of the dumped data and generating level 0, 1 and 2 products to be placed into the PLATO Archive at SOC for access (according to the expiry of the relevant proprietary periods) by the PLATO scientific community.

The PDC will provide support for the validation, calibration, and processing of the PLATO observations in order to deliver the PLATO science Data Products. The PSPM will provide the scientific specification of the high-level scientific algorithms implemented in the PDC, coordinate the ground-based follow-up and scientific community activities, and evaluate the scientific performance of the PLATO data chain.

7.2 PLATO Science Data Products

The baseline science telemetry budget yields a daily uncompressed data volume of 109 Gb. Over a nominal 6 year mission the total science telemetry down-linked will therefore be around 30 TB uncompressed data. The raw telemetry will be reformatted into a standard self-describing format in common use by the astronomical community (FITS).

The three data product levels to be generated from the PLATO mission are as follows:

Level 0

- The validated light curves and centroid curves for all individual telescopes. These are all the downloaded light curves (one each from each star and from each telescope) as well as the centroid curves and validated by assessing the quality and integrity of the data.
- Housekeeping data
- Auxiliary data, e.g. pointing

Level 1

- The calibrated light curves and centroid curves for each star and corrected for instrumental effects e.g. jitter. For all stars, the L1 calibrated data is the basic science-ready PLATO data. For the normal telescopes and for each star, the L1 light curves and centroid curves are (suitably) averaged, and an associated error is provided. The stars for which imagettes are available undergo a specific treatment.
- Auxiliary data, e.g. pointing, Time Correlation
- Associated calibration data

Level 2

- The planetary transit candidates and their parameters with formal uncertainties.

- The asteroseismic mode parameters with formal uncertainties.
- The stellar rotation periods and stellar activity models inferred from activity-related periodicities in the light curves, with formal uncertainties.
- The seismically-determined stellar masses and ages of stars, (and their formal errors), obtained from stellar model fits to the frequencies of oscillations
- The list of confirmed planetary systems, which will be fully characterized by combining information from the planetary transits, the seismology of the planet-host stars, and the follow-up observations. This represents the most important PLATO (the final and highest level PLATO science) deliverable. The parameters of the confirmed planets will be the orbital parameters, planet size, mass, and age (from the seismology of central stars). Any additional characterization of the properties of the planetary systems from the long duration PLATO light curves (e.g. secondary transits) and from specific ground-based observations (e.g. planetary atmospheres, imaging, etc) will also be included.

Within the PMC, these three data processing levels are thus organized according to specific PLATO Data Products, from DP0 to DP6, with DP0 and DP1 corresponding to Level 0 and Level 1 data respectively. The Level 2 data comprise DP2 to DP6, listed in Table 8.1 below.

Calibrated light curves and centroid curves	**DP1**	**L1**
Planetary candidate transits and their parameters	**DP2**	**L2**
Asteroseismic mode parameters	**DP3**	**L2**
Stellar rotation and activity	**DP4**	**L2**
Stellar masses and ages	**DP5**	**L2**
Confirmed planetary systems and their characteristics	**DP6**	**L2**

Table 7.1: PLATO science Data Products

All Level 2 sublevel products will be delivered for ingestion into the archive within 3 months of reception of the data at the PDC. These will be identified as proprietary data. The final Level 2 product, DP6, will take significantly more time to be delivered to the SOC for ingestion into the PLATO Archive due to the links such product generation has in follow-up observations etc. Upon ingestion of the DP6 products into the archive, the full level 2 product data set will be made public.

7.3 Observation Phases

The 6-years nominal duration of the scientific exploitation phase consists of three parts: two long-duration observations (up to 3 years), each focusing on a particular part of the sky with a high density of F, G and K dwarf stars, plus a one or two year long step-and-stare phase where a small number of selected fields will be monitored for one to up to a few months each. A mission extension of one (or more) years is possible.

7.3.1 Long-duration Observation Phase

Each of the long-duration observations will monitor a separate field in the sky that together will be encompassing a minimum of 20 000 dwarf and sub-giant stars of spectral type later than F5, each sufficiently bright to reach a photometric accuracy $\leq 3.4 \times 10^{-5}$, in one hour.
The photometric precision required by the mission puts stringent requirements on the pointing stability and accuracy of the s/c that must reach 0.2 arcsec per $Hz^{1/2}$ (Relative Pointing Error) over time scales of 25 seconds to 14 hours.

7.3.2 Step-and-Stare Phase

The step-and-stare phase will consist of a series of separate observations each lasting up to 5 months. The rationale is to extend the surveyed area of the sky and to further characterise planetary candidates that were

found to present a specific interest during the long monitoring phases (e.g. long period candidates that have shown only two transits).

7.4 Calibration Activities

7.4.1 On-ground calibration operations (Payload)

The PMC shall support the SOC in the production of the L1 data by performing the task of calibration of scientific data. This includes the definition of a calibration plan, the specification of observations or payload configurations required to gather calibration data, the derivation of the calibration parameters and their delivery to the SOC for implementation into the L1 processing pipeline.

Specific calibration data will be collected during the development phase on sub-system to instrument levels, either as initial estimates for the CPV and operational phases or to aid calibration model development.

All calibration data collected on-ground as well as in-orbit shall be stored in the Mission Archive for use in the L1 processing. Further information can be found in the "Instrument calibration plan" (Document 8 of the IPRR data pack).

7.4.2 In-Orbit calibration operations

In-orbit calibrations will be carried out during in-flight commissioning and performance verification; during normal operations, using the science & HK data; by observing specific calibration fields, generally combined with the ongoing long observation campaign.

The in-orbit calibration procedures will be performed throughout the mission, with certain activities specifically tailored to the performance verification (PV) phase, and also carried out on normal science data throughout the operations phase, with SGS tasks oriented to identifying calibration sources and extracting the calibration parameters. Note that most of the procedures permit several calibrations to be carried out.

During the Development & Operation phases, the PDC shall deliver to the SOC the calibration data and instrument parameter data sets to support quick look assessment and real time analysis of data. In addition, calibration data to support processing of Level 0 and Level 1 data sets shall also be provided for importing into the Archive. Finally, calibration algorithms and procedures shall be delivered to SOC.

7.5 Structure of the PLATO Science Ground Segment

The PLATO Ground Segment covers the in-flight operations of the satellite, such that the mission objectives can be met. The PLATO Operations Ground Segment consists of the Ground Station Facilities and the Mission Operations Centre (MOC), which operates the spacecraft and creates the telemetry and flight dynamics products. The PLATO Science Ground Segment (PSGS) consists of the ESA provided PLATO SOC and the PLATO Mission Consortium provided science ground segment components. The Science Ground Segment is responsible for mission planning and the end-to-end handling of the PLATO data and production of the PLATO Mission Products. The PMC part of the SGS consists of a Plato Data Centre (PDC) and the Plato Science Preparatory Management (PSPM) group.

The roles and responsibilities of the PDC and PSPM are distinct and complementary. During the development phase, they are organized according to the following guidelines: 1) PSPM provides the scientific specifications of the software, 2) PDC translates the scientific specifications into technical specifications, 3) PDC implements the technical specifications, 4) PSPM checks that the PDC software is consistent with the initial scientific specifications; this validation by PSPM occurs within the PDC – a normal part of the development QA process.

Apart from the SOC, the instrument operations dependent section of the Science Ground Segment is composed of the PMC Instrument team who are responsible for: contribution to end-to-end testing, maintenance of the instruments, payload monitoring and control specifications, instrument trend analysis, instrument calibration, second-level quality control (on calibrated data). This team will be set-up during the

pre-launch phase taking advantage of the experience gathered in previous missions and during the development of PLATO instruments and GSEs.

7.6 PLATO Operations Ground Segment

ESA is responsible for the readiness of the ground station facilities. The ESA Deep Space station at Cebreros is baselined as the primary ground station for PLATO operations and is equipped with K (26 GHz) and X band facilities.

MOC is responsible for the availability and operations during the operations phase. Data transfer and supporting infrastructure within the operations ground segment is managed by MOC. The MOC is in charge of the following tasks:

- Monitoring spacecraft health and safety
- Monitoring the payload safety and reacting to contingencies and anomalies according to procedures provided by the PLATO consortium.
- Alerting the SGS of all significant anomalies or deviations from nominal behaviour of the satellite
- Executing predetermined procedures to safeguard the spacecraft and payload, and preserve data integrity
- The uplink of the satellite and payload telecommands
- The maintenance of the satellite's on-board software
- The uplink of payload on-board SW executables as generated, validated and delivered by the PDC via the SOC.
- The flight dynamics support including determination and control of the satellite's orbit and attitude
- Handling and provision of the telemetry to the SOC
- Production and provision of auxiliary data to the SOC (e.g. orbit files, pointing information)

MOC will keep an archive of the housekeeping telemetry, the telecommand history and other auxiliary mission operations data for up to 6 months from the end of mission (depending on the volume of science data only short term storage of science data may be provided with long term storage at the SOC) and will keep on hard copy (e.g. DVD or similar) an off-line archive in a secure location for up to 5 years after the end of the operations.

7.7 PLATO Science Operations Centre

7.7.1 SOC Responsibilities

The ESA Project Manager delegates to the Science Operations Department of the Science and Robotic Exploration Directorate based at the European Space Astronomy Centre (ESAC) the design, development, validation, and operation of the SOC. The SOC is the only interface to the MOC during routine operations. Within the overall ESA responsibility for the PLATO SGS, the SOC coordinates the overall design, implementation and operation of the PLATO Science Ground Segment with the PMC. It is specifically responsible for:

- Acquisition and distribution of spacecraft telemetry from MOC
- Acting as interface between the PDC and the MOC for payload operations and for all files and procedures required for optimizing the quality of the data and safeguarding of the payload
- The SOC is responsible for the planning, co-ordination & support of a number of calls for proposals, including one taking place 2 years before launch
- Scientific mission planning based on input from the PDC after endorsement by the PST. In particular, Provision to the MOC of all parameters for each sequence of observations: at each rotation of the

satellite (every 3 months), and at each field re-pointing (every 2 or 3 years for the long sequences, every few months for the step & stare phase), the full list of targets with their expected location on the focal planes, and the full list of parameters for each star (essentially photometric mask parameters)

- Quality control: Monitoring of data integrity and quality
- Fine tuning of on-board software, parameters and payload configuration, based on quick look data
- Ground support for onboard processing. The SOC issues payload configuration change requests to the MOC as appropriate to optimize the quality of the PLATO data. In particular, the SOC provides support to the on-board processing through parallel running on-board algorithms on the down-linked imagettes and provision of updated optimized parameters to the MOC for uplink
- Support the PDC in the design, development, testing and maintenance of the modules in the data analysis system required for the quick-look assessment and the validation of L0 data
- Support the PDC in the design, development, testing and maintenance of the data analysis modules required for the generation of the L1 data
- Archiving of all PLATO data products, HK data, Auxiliary data and Science ancillary data
- Distribution of the data products to the scientific community
- Providing support to the general scientific community, including helpdesk support – especially in the context of the calls for proposals
- Post-operations activities. The SOC will remain active until three years after the end of operations to continue data processing, the product validation and the ingestion of the final L2 data products into the archive

In addition to the above, the SOC will also provide support in the coordination of payload health and maintenance activities which will be done in conjunction with the PMC instrument team based on the regular instrument health reports and quality check during the L1 processing

7.7.2 SOC Operational Activities – Uplink, Downlink & Interface to the Community

The planning of science operations will be performed at the SOC based upon input from the PDC endorsed by the PLATO Science team. These will be checked at the SOC and then forwarded to the MOC where they are to be uplinked and executed on board.

Every 24 hours during the 4 hour DTCP, the data will be acquired via the ground station and delivered to the MOC. The SOC shall retrieve this Level 0 data and perform a quick look assessment & validate this data through the running of quality control. The data will be placed in the SOC archive after which the standard pipeline generation process will be executed whereby the level 0 data will pass through a pipeline thus generating level 1 products, again being placed into the archive. Further quality control checks will be performed by the SOC of this data set to confirm correct integrity and scientific merit before it is made public in the archive.

The SOC will be the main interface point between the PDC and the MOC as regards payload operations in particular relating to safeguarding the payload and optimising the quality of the data set. Such interactions will also include the fine tuning of on-board software, parameters and payload configuration as a result of the quick look data checks of the L0 products.

The PDC data base will access the archive and retrieve L0, L1 and other data sets at which point it will make it available to the centres within the PLATO Consortium to produce the L2 data set. Upon generation of the L2 data set, these will be provided back to the SOC and ingested into the archive.

7.8 PLATO Data Centre

7.8.1 PDC Responsibilities

The PLATO Data Centre is under the responsibility of the PLATO Mission Consortium. The PDC supports the SOC in the production of the L1 data by carrying out the following tasks:

- Calibration of the scientific data, based on the calibration procedure and calibration data provided by the instrument team, for implementation into the L1 processing pipeline.
- Definition of algorithms and support to the implementation of modules to monitor the scientific integrity and health of the observations.
- Definition of algorithms and support to the implementation of modules in the data analysis system for the removal of instrumental effects and generation of L1 data.
- Provision of input to the scientific quality control software and procedures.
- Provision of the necessary algorithms and tools for the optimization of the onboard processing
- Provision of tools and support to simulate, test and validate the L0 to L1 processing pipeline.

The PDC implements, tests and maintains the data analysis tools needed to generate the Level 2 data and higher level scientific products, which include catalogues, list of planets, their parameters and additional characterisation information.

The PDC supports the spacecraft operations by providing input to the procedures needed for payload operation and for scientific mission planning.

The PDC is responsible for the development and maintenance of all systems required to process the final PLATO mission products and for the computing infrastructure required to deliver the PLATO Level 2 scientific data products. Specifically:

- The PDC technically designs, implements, tests and maintains the data analysis tools needed to generate the (exoplanet and stellar) Level 2 data and higher level scientific products, which include catalogues, list of planets, their parameters and additional characterisation information. The scientific validation of the data analysis tools will occur within the PDC based upon PSPM specifications and with PSPM involvement.
- The PDC shall develop and maintain a main PDC Data Base (PDC-DB) which will acquire, from the SOC, the L0 and L1 data, and other data. The PDC-DB shall make the data available to the PDC Data Processing Centres (PDPCs) to produce the L2 data products. The validated L2 data products, will then be provided back to the SOC. The PDC-DB shall be a central hub for the exchange and maintenance of data within the PDC.
- The PDC provides the PLATO Input Catalogue to the SOC for the scientific mission planning.
- The PDC is responsible for the management of the database that assembles all follow-up observations on PLATO targets, plus ancillary data extracted from various existing catalogues and databases, and places them in the PDC Data Base at the disposal of the PLATO Mission Consortium.
- Provision of data analysis support tools to assist the science team to inspect and to scientifically validate the PLATO data products within the PDC. In particular, these tools will assist the PST & the PSPM to update the ranking of planetary candidates and to confirm planetary systems.

7.8.2 PDC Development

The software and hardware technologies available today would suffice to build a successful PDC. The complexity of the PDC lies mostly in the management, integration, and validation of its many hardware and software components.

The PDC will adopt a well defined cyclical development schedule (6 month cycles). Software developed in the PDC will be released at the end of each cycle, with this being integrated into an end-of-cycle system. Over the development lifetime, there will always be a working system, with this working system increasing

in functionality over time, such that by the system readiness review prior to launch, the processing system has fully met the requirements.

This approach ensures that work developed over many sites is integrated on a frequent timescale – ensuring that any interface issues are resolved at an early stage. It enables end-to-end testing to commence at an early stage – thus facilitating the 'smooth transition' of a system handling test data to one handling real instrument data (from the lab during development) to one handling real data from the S/C during flight operations.

A key part of the development process will be access to simulation data, required to test all software components. This data will simulate the PLATO telemetry stream, PLATO pixel level data and PLATO catalogue level data. Simulation data will be released ahead of each cycle to allow for testing of the following cycle release. The simulation data is provided to the PDC-DB and is then available through the PDC-DB interface to all PDPCs.

The PDC shall remain operational for at least three years after the end of the PLATO space operations phase to enable the confirmation of planets with periods of up to three years.

7.8.3 PDC facilities

The PDC will encompass several facilities in Europe. The PDC-DB at MPSSR (Germany) will hold the PLATO scientific data products, the input catalogue, and all the ancillary data on the PLATO targets that are required for the processing of the L2 data products, in particular specifically acquired ground-based follow-up observations. Computing resources will be distributed among five Data Processing Centres: PDPC-C at IoA-Cambridge (UK) for the Exoplanet Analysis System, PDPC-I at IAS (France) for the Stellar Analysis System, PDPC-A at ASI (Italy) for the Input Catalogue, PDPC-L at LAM (France) for the Ancillary Data Management, and PDPC-M at MPSSR (Germany) for the running of the data analysis support tools. The PDC activities through all phases of the mission will be funded through institutional and national agencies.

7.9 PLATO Science Preparation Management

7.9.1 PSPM Responsibilities

The PLATO Science Preparatory Management Group (PSPM) is under the responsibility of the PLATO Mission Consortium. In particular, the PSPM has the following responsibilities :

- The PSPM is responsible for carrying out preparatory activities ensuring the scientific results of the mission. It provides the PDC with the specifications and inputs required to implement optimized methods and tools for PLATO data exploitation.
- The PSPM is responsible for the overall coordination of the Scientific preparation, for coordinating the scientific community activities and for PMC public relations and outreach.
- The PSPM is responsible for the scientific specification of the required elements for the detection of exoplanetary transits and the determination of exo-planetary parameters that are the main product of the PLATO mission.
- Likewise, the PSPM is responsible for the scientific specification of the required elements for carrying out the stellar physics part of the mission. Specifically as what concerns the detection of oscillation modes, stellar evolution models and the determination of fundamental stellar parameters.
- For both elements, the PSPM will provide the resulting scientific specifications to the PDC.
- The PSPM is also responsible for the Target/Field characterisation and thus the preparation of the PLATO input catalogue and the preparation of Target/Field selection.
- The PSPM is also responsible for the organisation, of the required (ground- and space-based) follow-up observations.
- The PSPM is responsible for the development and implementation of the End-to-End Simulator (PLATO Data Simulator).
- Finally the PSPM is also responsible for the preparation of the complementary science program.

- In the operation and exploitation phase the PSPM (then PSM) is responsible for providing input and support to the PDC and scientifically validate the L2 data products.
- In the operation and exploitation phase the PSM is responsible to coordinate planet detection, ranking, rejection, and the required follow-up observations.
- In the operation and post-operation phases the PSM is responsible to evaluate the scientific performance of the PLATO data chain and specify upgrades of scientific algorithms and tools.
- In the operation and post-operation phases the PSM is responsible to continue Target/Field selection and characterisation and update the PIC.
- The PSM is also responsible to continue coordination of the Scientific preparation, for coordinating the scientific community activities and for PMC public relations and outreach until end of the post-operation phase.

7.9.2 PSPM Facilities and Resources

The PSPM consists of sub-groups totalling more than 100, mainly European, experts who provide the needed state-of-the art scientific know-how, including in particular expertise from previous space missions like CoRoT and *Kepler* and expertise in ground-based follow-up observations for planet confirmation. This expertise is specially required to set-up an efficient scheme for planet detection, ranking and organisation of resource efficient follow-up observations. This is a lessons-learned from the ongoing transit search space missions. The PSPM also provides the expertise for target field selection and characterization and the specification of the PLATO Input Catalogue. Experts in the PSPM will provide updated stellar models to optimize the determination of stellar parameters. The CCD Simulator will make realistic simulated data available. The additional (complementary) science task in the PSPM includes experts from various scientific fields, but mainly on different aspects of stellar science not covered in the core program. These experts will help maximizing the scientific return of the mission by expanding its science exploitation. The PSPM will fund its activities through all phases of the mission by institutional and agency funding, depending on the national and institutional environments of the participants.

7.10 Level 2 Data Processing

With Level 0 and Level 1 data products existing in the PLATO Archive, the PDC can retrieve them. The current envisaged mechanism is for the PDC to retrieve the FITS format products from the archive via the Bulk Product Transfer Mechanism. This will be running at the PDC on an automatic basis and will retrieve products from the archive that have been updated or changed since its last retrieval.

The products (including associated auxiliary products) will be placed into the PDC main database (PDC-DB), as can be seen in figure 7.1 below. Access to the PDC-DB is possible by all the sub-centres of the PDC to allow the Level 2 generation process to be started. After acquisition of the L1 data from the PDC-DB by the stellar PDPC, the PLATO light curves are Fourier transformed and power spectra are analysed to provide the oscillation mode parameters DP3. In parallel, analyses of the light curves provide the stellar rotation and activity information DP4. Finally, DP3 and DP4 are used together with the science ancillary and catalogue data, which are stored and managed in the PDC, for producing the DP5. The exoplanet PDPC processing of the L1 data, for the production of the L2 products, is based on a ca. two week cycle. This cycle will allow an update of DP2 providing a ranked list of candidate planet systems. False positive modelling is undertaken to refine the estimate of probable planet systems, using follow up information when available. The ca. two weekly cycle allows for triggering of the ground based follow-up of objects which pass a certain threshold of interest and enables triggering of imagettes of planet candidates. Successive updates are applied over a three-month main processing cycle, corresponding to the period between PLATO satellite field rotations. At the close of the three month period, a full update of the L2 parameters for the objects observed by PLATO will be made to the PDC-DB.

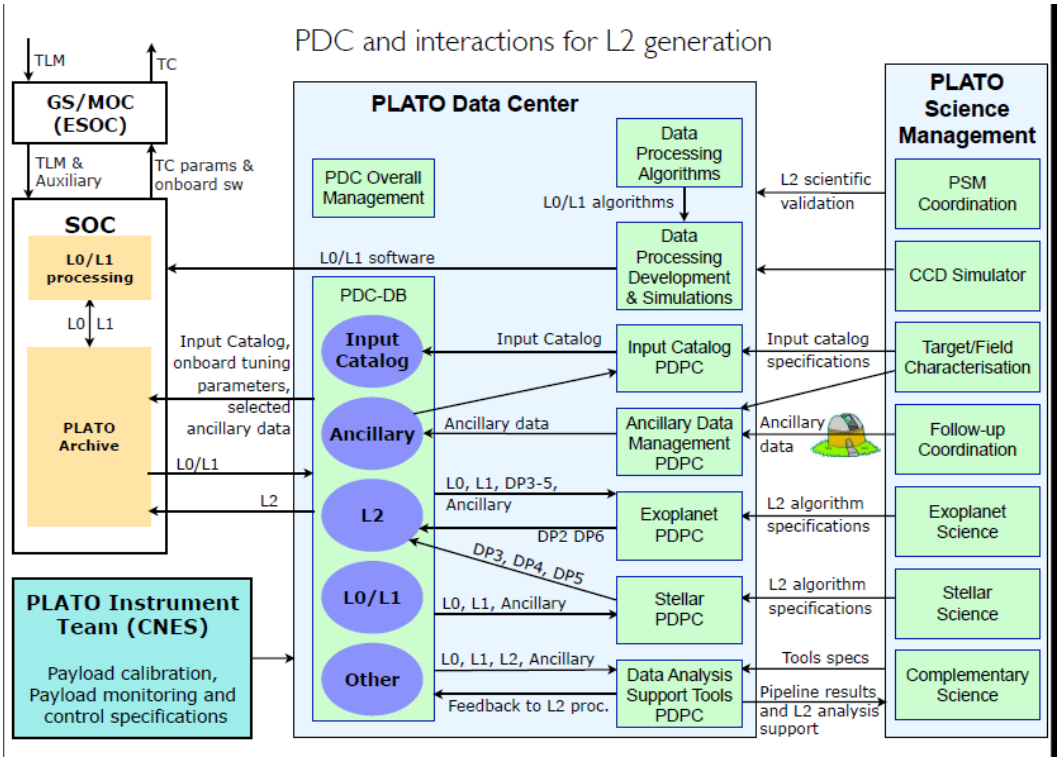

Figure 7.1: PLATO Data Centre with its main elements and main interactions with the SOC, Payload Team and PSM for L2 generation during operations. The PDPC represent the different PLATO Data Processing Centres.

The PSPM group will access the L2 pipeline products, and level 0 and 1 data as needed, via the data analysis support tools in the PDC. The PSPM will in particular evaluate the planet ranking and organise the required ground-based follow-up campaigns, including confirmation of planet candidates by radial-velocity follow-up. The PSPM will scientifically validate L2 data to finally obtain DP6 level products.

The PSPM group will furthermore evaluate the scientific performance of the L2 pipeline on real data in the operation phase and provide updated scientific specifications to the PDC data processing as needed.

The PDC shall deliver L2 data, corresponding to DP2-DP5 data levels, for each target to the SOC (for eventual incorporation into the PLATO Archive) within 3 months of reception of the L1 data of that target at the PDC. This data will be given a proprietary status in the archive.

The PDC shall deliver the final scientifically validated L2 data (corresponding to level DP6) for each target to the SOC (for eventual incorporation into the PLATO Archive) not later than at the time of the first publication of that target.

Upon delivery to the SOC, the Level 2 (DP6) data products will be placed into the archive and shall then be made public to the scientific community.

Large external datasets (science ancillary data, including follow up data) will be generated around each of the target level 2 data sets and these will be also fed back to the SOC and the PLATO Archive.

8 MANAGEMENT

This chapter gives an overview of the management approach of the PLATO mission as currently foreseen.

In February 2010, PLATO was selected by the Science Programme Committee (SPC) to enter a competitive Definition Phase as an M-class mission candidate for the 2017/2018 M1/M2 launch opportunities of the Cosmic Vision 2015-2025 Plan. At the end of this Definition Phase (A/B1) all interfaces and allocated resources are frozen in order to be prepared for a possible implementation phase. In October 2011, the Science Programme Committee (SPC) will select two of the three M1/M2 candidate missions. The successful candidates will move into the Implementation Phase (Phase B2/C/D/E1) and a Prime industry contract will be selected via a further ITT for start in 2012.

8.1 Responsibilities

The overarching responsibility for all aspects of the PLATO mission rests with the ESA Directorate of Science and Robotic Exploration and its Director (D/SRE). The overall project organization of PLATO envisages three major organizations: ESA, the PLATO Mission Consortium (PMC) and the Industrial Contractor with responsibilities in the Implementation Phase, defined as follows:

- ESA has the overall responsibility for the PLATO mission design and Implementation. ESA is also responsible for the development and procurement of the Charge Coupled Devices (CCDs).
- The Industrial Contractor is responsible for the development, procurement, manufacturing, assembly, integration, test, verification and timely delivery of a fully integrated spacecraft capable of accommodating the defined payload elements, fulfilling the established mission requirements and achieving the mission objectives.
- The PMC develops, procures and timely delivers the full set of payload (cameras and warm electronic units) fully verified and calibrated for later integration into the PLATO spacecraft by industry through the delivery via ESA of related units and sub-assemblies.
- The PLATO Mission Consortium Science Ground Segment (PMC SGS) in charge of processing all data from beyond Level 1 and transferring them to the ESA SOC for archival and distribution. The PMC also provides the organisation and leadership of associated ground based observations required by the mission.

The Contractor and the Consortium report individually to ESA via related management.

In addition, ESA would be responsible for:

- Spacecraft Launcher procurement and launch (Soyuz operated by Arianespace)
- Spacecraft Operations (ESOC and ESAC)
- Acquisition and distribution of data to the Payload Data Centre (ESOC and ESAC)

8.2 Preliminary Procurement Approach

This section gives an overview of the procurement philosophy for PLATO.

8.2.1 Procurement of spacecraft, Industrial Contractors and organisation

After a possible down-selection of the PLATO mission in October 2011 and related adoption by the SPC in February 2012, an Invitation to Tender (ITT) for the Implementation Phase (B2/C/D/E1) will be released in early 2012. The scope of this contract would be to implement all industrial activities leading to a launch and commissioning of PLATO in the requested timeframe. The successful bidder will be appointed as Prime Contractor in charge, amongst other items, of system engineering and management of the sub-contractors.

The final industrial organization will be completed only in Phase B2, mostly through a process of competitive selection and according to the ESA Best Practices for subcontractor selection, by taking into account geographical distribution requirements.

It is currently foreseen that the industrial prime contractor would design, manufacture and test the Service Module. The industrial prime contractor would also be in charge of the global assembly, integration and testing of the whole PLATO spacecraft (SVM and PLM).

Industrial contracts would be funded and placed by ESA. The responsibility for control and monitoring of the contracts and provision for liaison between partners, contractors and outside scientists would be with the ESA project team. Ground segment, Launcher and Mission and Science Operations are the responsibility of ESA.

The following list is a summary of the elements of the preliminary organisation, in which ESA would be responsible:

- The overall mission design and provision of Service Module (through industrial contract)
- Global Assembly/Integration/Testing and Verification of SVM and PLM (through industrial contract)
- Spacecraft Launch and Operations (Arianespace, ESOC and ESAC)
- Acquisition and distribution of data to the Science Data Centre (ESOC, ESAC)

8.2.2 Payload Procurement

The PLATO payload (PLM) is provided by the PLATO Mission Consortium which is financed by the national agencies.

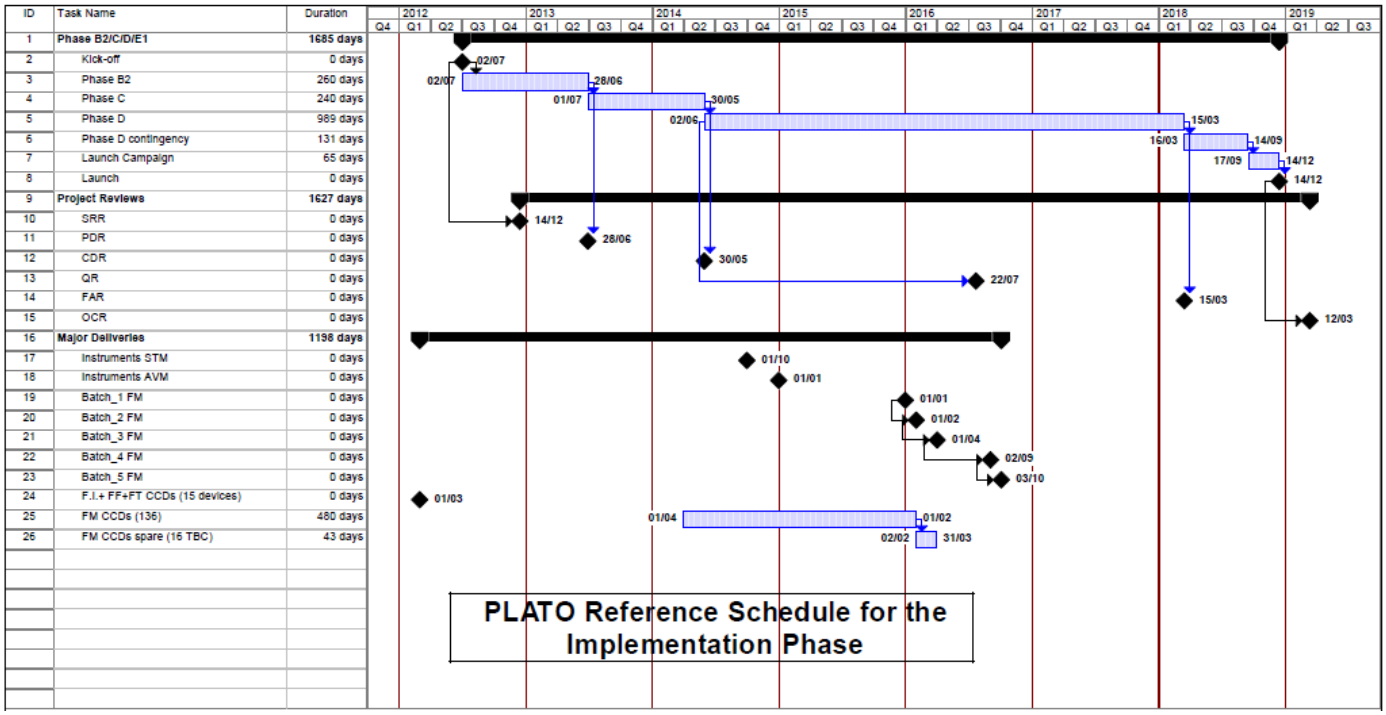

Figure 8.1. Reference schedule of the PLATO mission.

During the definition phase, the PMC have submitted a proposal for a payload concept in response to an AO and to a further solicitation proposal (spring 2011) updating the former. This proposal contains the payload technical description, budget provisions (mass, power, data rates, physical sizes etc.), schedule, payload interface parameters, and deliverable output. The proposal also contains a description of the organisation of the consortium and the contribution of each participating institute/organisation, providing a clear management structure regarding the scientific, technical and data analysis areas. Also included, is an estimated cost and the funding from participating national agencies. The proposal contains reference to and is consistent with a number of ESA provided documents including the Science Management Plan, the Mission Requirements Document (MRD), the Payload Definition Document (PDD), the Science

Requirements Document (SciRD) and the Mission Assumptions Document (MAD), all of which were updated with the results of the assessment phase.

The PMC was selected in February 2011 for the duration of the Definition phase. If PLATO is selected in October 2011, the SPC would decide on the confirmation of the PMC in early 2012, which would lead to phase (B2/C/D/E1) for the payload provision.

8.3 PLATO Schedule

The Implementation Phase (B2/C/D/E1) system study is expected to start in mid-2012 (T0) with the objective to launch in 2018. It will include 6 major reviews:

- The System Requirements Review (SRR, T0 + 6 months),
- The Preliminary Design Review (PDR, T0 + 12 months),
- The Critical Design Review (CDR, T0 + 24 months),
- The Qualification Review (QR, T0 + 48 months),
- The Flight Acceptance Review (FAR, T0 + 68 months),
- The In-Orbit Commissioning Review (IOCR, Launch+ 3 months),

The Technology Development Activities for the development of the Charge Coupled Devices (CCDs) have been initiated and are conducted partially in parallel with the Definition Phase with a expected completion in quarter 3 2012. The intermediate results will be fed into the System Study as necessary. At the ESA Preliminary Requirements Review (PRR), the mission baseline has been established and documented. A Baseline Configuration Design Review will close the Definition Phase by consolidating the overall mission concept for enabling an efficient start of the Implementation Phase, should the mission be finally endorsed. A reference schedule for the Implementation Phase is shown in Fig. 8.

8.4 Science Management

8.4.1 ESA Project Scientist (PS)

The PLATO Project Scientist (PS) is the ESA interface to the PMC and to the general scientific community for scientific matters related to the mission. The PS chairs the PLATO Science Team and coordinates its activities

8.4.2 PLATO Science Team (PST)

The PLATO Science Team (PST) supports the PS in monitoring the correct implementation of the scientific objectives of the mission and maximising its scientific return. The PST is formed with the selection of the PMC and remains in place until the end of the active archive phase. In addition to the ESA PS who chairs it, the PST is composed of 10 members as follows:

- Two Programme Scientists,
- A Calibration Scientist
- A Follow-up Scientist
- Two Data Processing Scientists
- A Stellar Physics Scientist,
- A Target Selection Scientist
- Two Independent Legacy Scientists, who will give advice on the support to the community in the usage and availability of the PLATO data

8.5 PLATO Mission Consortium (PMC) Proposed structure

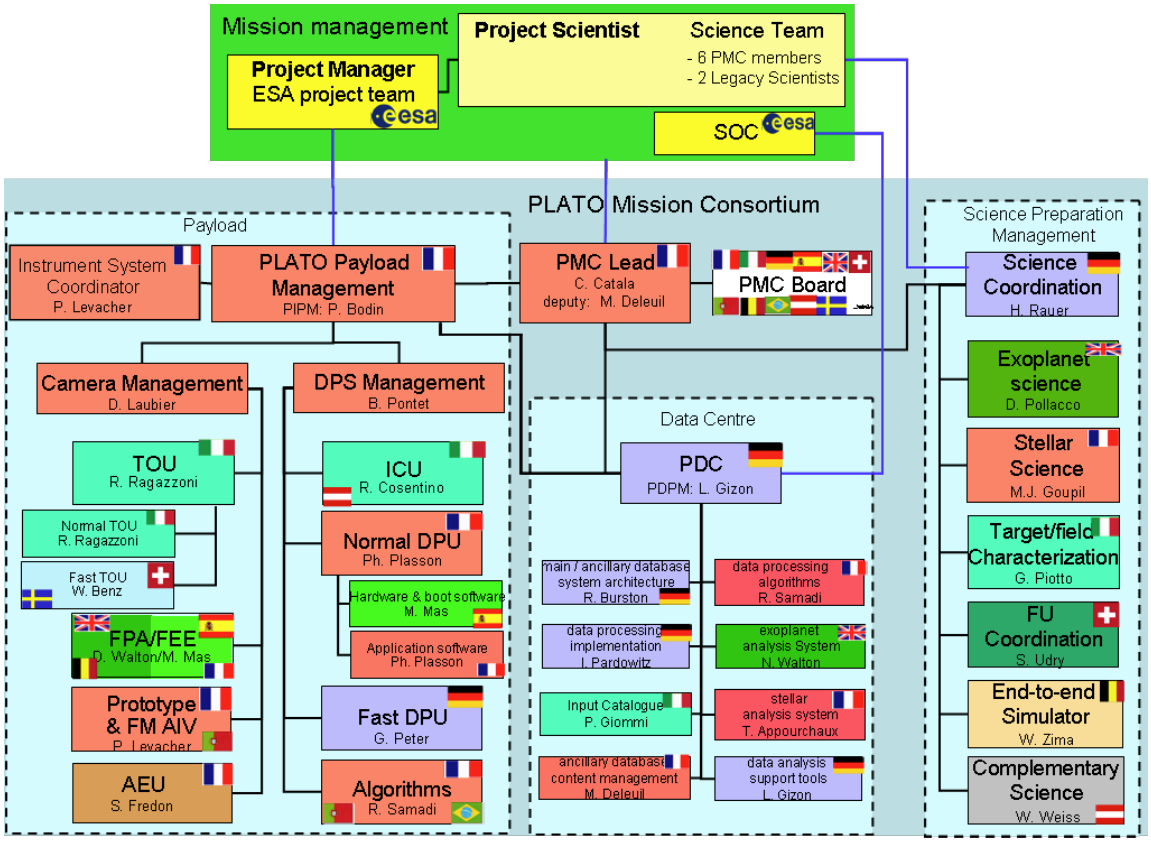

Figure 8.2 Structure of the PLATO Mission Consortium (PMC) with key elements, proposed national responsibilities and key personnel identified

The overall structure of the PMC is shown in the diagram in Fig. 8.2 and briefly described in the following text.

The PMC is placed under the overall responsibility of a PMC Lead (PCL). The PCL constitutes the formal interface of the consortium to ESA. The PCL ensures that the performances of the mission meet the science requirements set by the Science Team. The PCL also constitutes the main scientific interface of all consortium sub-structures with ESA and the PST. The PMC Lead is one of the six members of the Science Team nominated by the PMC.

A Steering Committee established through a Multi-Lateral Agreement between ESA and the national agencies supporting the partners of the PMC, is providing an overall supervision of the PMC and monitors potential future evolutions of the Consortium structure, e.g. the introduction of new partners, and makes all decisions concerning this matter.

All consortium activities will be monitored by the PMC Board, which will serve as interface between the consortium on one hand, and the national agencies and institutes involved in the consortium on the other hand. The PMC Board addresses problems concerning the procurement of the PMC elements of the mission, either payload, ground segment or science preparation activities, before they eventually reach the Steering Committee level. The PMC Board is chaired by the PCL, and is constituted by members of the Consortium. The PMC Board includes two representatives of each one of the main countries involved in the mission (France, Italy, Germany, Spain, UK and Switzerland) and one representative of all other contributors (Belgium, Portugal, Brazil, Austria, Sweden, Denmark, Hungary). The PIPM (see below) is a full member of the PMC Board. The board meets at least once a year. The chair is responsible for the organization of these meetings. The PCL may decide to hold additional meetings, as needed.

The PLATO Payload is managed by CNES. The corresponding activities are placed under global management of a CNES-appointed PLATO Instrument Project Manager, (PIPM), who acts as a support for

the PCL on all technical and managerial aspects of the Payload development. The hierarchical structure is shown in Fig. 8.2

The Instrument Management structure is supported by two System Teams, one for the Cameras and one for the DPS, staffed by involved French laboratories and CNES, under global coordination by the System Coordinator. The detailed structure is further elaborated in Figure 8.2.

The onboard Data Processing System (DPS) will be developed under management of the CNES appointed DPS manager.

The PLATO Data Centre (PDC) is the PMC contribution to the Science Ground Segment, which also includes the Science Operation Centre (SOC) under ESA responsibility, and the PSPM (see Chapter 7 for details). The PDC is led by the PLATO Data Processing Manager (PDPM).

8.6 Data policy

Data are proprietary from the moment of acquisition until they are publicly released. The general data policy is, however, to make the PLATO L1 data publicly available as soon as they are validated by the SOC, following a procedure defined by the PST (based on current best knowledge this time ranges ~ a few months in the early phases of the mission to days later on).

The L2 data, which depend also on additional observations, will be made publicly available in a timely manner, and no later than the acceptance for publication of the first refereed papers based on them.

However, among the several hundreds of thousands of targets, the data from a certain number (not exceeding 2000 in total, the exact number will be defined and agreed by the PST), are exclusively available to the PLATO-involved scientists for a period of one year after the corresponding L1 data have been validated and made available to them by the SOC. In this context, PLATO-involved scientists are considered to be members of the PMC, members of the PST, as well as ESA scientists involved in the mission. The distribution of reserved targets (or an equivalent metrics agreed by the PST) is such that 5% is assigned to the ESA scientists.

The list of proprietary targets is established at least 6 months prior to each phase of the mission (one phase being defined as one long run or the step & stare phase), as the outcome of a call for proposals aimed at PLATO-involved scientists. In response to such a call, PLATO-involved scientists will submit proposals for a limited number of identified targets, specifying the scientific use they propose to make of these proprietary data, as well as the preparation work that they have performed or intend to perform, detailing the organisation of their teams toward these goals. The PST will review the proposals and come up with a final selection of proprietary targets that will then be distributed among PLATO-involved scientists. All L1 data distributed under this procedure will become public after one year of proprietary period.

A call for proposals directed at the general scientific community is to be issued before launch and after the outcome of the call for proprietary data. More open calls may be issued during the mission to the discretion of ESA, following the advice from the PST. The open calls will ask for complementary science programmes not covered by the PLATO core science objectives. Complementary science programmes will focus on additional objects found within the field of view of each core programme pointing. They will not require re-pointing of the spacecraft or exclusively dedicated observing time. Proposers will be requested to describe the science objectives, specify the requirements on PLATO data acquisition and calibration to achieve the science goals, and provide a plan for the associated data processing. The proposals will be selected by a committee of experts formed under the supervision of the AWG. The SOC will provide dedicated support to the successful proposers. When an open call programme contains targets that are part of the proprietary target list, access to the associated data may be granted also to this programme, with the condition that the observations are exclusively used in relation with the science objectives of the proposal, and the same proprietary period will apply. For the remaining targets in the programme, no proprietary period will be assigned and the L1 data will be publicly available as soon as they are validated by the SOC.

8.7 Technological readiness of mission

The Service Module and sunshield of the proposed PLATO Spacecraft are heavily based on current technology and heritage from other missions. The AOCS and propulsion subsystems can use off-the-shelf equipment with no development required. Data handling and communications equipment can be performed with current technology, and proposals from industrial contractors are based on modifications of units used in current missions.

The SVM and Sunshield structures will use either qualified- or soon-to-be-qualified materials. There is one mechanism on the spacecraft (2-DOF high-gain antenna pointing mechanism), which at most will require a minor modification to accommodate the large azimuth and elevation range of the Earth as seen by the Spacecraft. All platform units TRL is 5 and above. In the payload design there are no show stoppers. Critical aspects exists (e.g. the CCD full well capacity, the telescope focusing via thermal control, the complexity of the overall data processing architecture) but all is in reach of the available technology and the areas requiring development attention are identified. Demonstration of TRL 5 and above is planned in the frame of the Phase B1.

References

Aerts C., 2008, "Core Overshoot and Nonrigid Internal Rotation of Massive Stars: Current Status from Asteroseismology", IAU Symposium, 250, 237

Aerts C., Christensen-Dalsgaard J., Kurtz D. W., 2009, "Asteroseismology", Springer-Verlag, Heidelberg

Aigrain S., Pont F., Fressin F., et al. 2009, A&A, 506, 425A

Aigrain S., Collier Cameron A., Ollivier M., et al. 2008, A&A, 488, L43

Alapini A., Aigrain S., 2009, A&A, MNRAS, 397, 1591A

Alibert A., Mordasini C., Benz W., 2004, A&A, 417, L25

Alibert A., Mordasini C., Benz W., Winisdoerffer C., 2005, A&A, 434, 343

Almenara J.M., Deeg H.J., Aigrain, S., et al., 2009, A&A, 506, 337A

Alonso R., et al 2007, ''The Transatlantic Exoplanet Survey (TrES): A Review'',
Transiting Extrapolar Planets Workshop ASP Conference Series, Vol. 366, 13. Edited by C. Afonso, D. Weldrake, and Th. Henning. San Francisco: Astronomical Society of the Pacific.

Alonso R, Alapini A, Aigrain S et al., 2009a, A&A, 506, 353

Alonso R., Guillot T., Mazeh T., et al. 2009b, A&A, 501, L23

Ammons, S.M., Robinson, S.E., Strader, J., Laughlin, G., et al., 2006, ApJ, 638, 1004

Appourchaux T., Michel E., Auvergne M., et al. 2008, A&A, 488, 705

Auvergne M, Bodin, P., Boisnard, L., et al. 2009, A&A, 506, 411A

Bakos, G., Noyes, R. W., Kovács, G., Stanek, K. Z., Sasselov, D.D., & Domsa I., 2004, PASP, 116, 266

Bakos G., Torres W., Pal A., et al 2010, Ap.J., 710, 1724B

Ballot, J., Gizon, L., Samadi, R., et al., 2011, A&A, 530, A97

Barbieri, M., et al., 2011, in preparation

Barge P., Baglin A., Auvergne M., et al. 2008, A&A, 482, L17

Barnes J. W., Fortney J.J., 2003, ApJ, 588, 545

Barnes S.A., 2007, ApJ, 669, 1167

Batalha N.M., Borucki W.J., Bryson S.T., et al. 2011a, ApJ, 729, 27

Batalha N.M., Borucki W.J., Koch, D.G., et al 2011b, Ap.J., 713, L109

Bazot M., Vauclair S., 2004, A&A, 427, 965

Beaulieu, J.-P., Bennett D., Fouqué P., et al. 2006, Nature, 439, 437

Bedding T.R., Mosser B., Huber D., et al., 2011, Nature, 471, 608

Belikov, A.N, Roeser, S., 2008, A&A, 489, 1107

Bilir, S., Karaali, S., Guever, T., et al., 2006, AN, 327, 72

Belu A.R., Selsis F., Morales J.-C., et al., 2011, A&A, 525, A83

Bennett D.P., Bond I.A., Udalski A., et al. 2008, ApJ, 684, 663

Benomar O, Baudin F., Marques J.P., et al., 2010, AN, 331, 956

Bonfils X., Mayor M., Delfosse X., et al. 2007, A&A, 474, 293

Borucki W.J., Koch D., Basri G., et al. 2010, Science, 327, 977

Borucki W.J., Koch D.G., Basri G., et al., 2011, ApJ, 728, 117B

Bouchy F., Mayor M., Lovis C., et al. 2009, A&A, 496, 527

Brown T. M., Christensen-Dalsgaard J., Mihalas B., Gilliland R., 1994, ApJ, 427, 1013

Bryson S., Jenkins J., Gilliland R., et al., 2011, ApJ, submitted

Burrows A., Heng K, Nampaisarn T., 2011 accepted to the ApJ

Burrows A., Hubeny I., Budaj J., Hubbard W.B., 2007, ApJ, 661, 502

Butler, R.P., Marcy, G.W, 1996, Ap.J., 464, L153

Cabrera J., Fridlund M., Ollivier M., et al., 2009, A&A, 506, 501

Carrier F., Eggenberger P., Bouchy F., 2005, A&A, 434, 1085

Casertano S., Latanzi, M.G., Sozetti, A., et al., 2008. A&A, 482, 699

Chabrier G., Gallardo J., Baraffe I., 2007, A&A, 472, L17

Chaplin W. J., Appourchaux T., Arentoft T., et al., 2008, Astronomische Nachrichten, 329, 549

Charbonneau D., Berta Z.K., Irwin J., et al. 2009, Nature, 462, 891

Charbonneau D., Brown T.M., Noyes R.W., Gilliland R.L., 2002, ApJ, 568, 377

Charbonneau D., Knutson H., Barman T., et al. 2008, ApJ, 686, 1341

Charbonneau, D., Brown, T.M., Latham, D.W., Mayor, M., 2000, ApJ, 529, 45

Chauvin G., Lagrange A.-M., Dumas C., et al., 2004, A&A, 425, L29

Christensen-Dalsgaard J., 1988, "A Hertzsprung-Russell diagram for stellar oscillations", Proc. IAU Symposium No 123, Advances in helio- and asteroseismology, Eds Christensen-Dalsgaard, J., Frandsen, S., Reidel, Dordrecht, 295

Christensen-Dalsgaard J., 2008, Ap&SS, 316,13

Christensen-Dalsgaard J., Kjeldsen H., Brown T.M., et al., 2010, ApJL, 713, L164

Claret A., 2007, A&A, 475, 1019

Clementini G., Gratton R., 2002, European Review, 10, 237

Crossfield I.J.M., Hansen B.M.S., Harrington J., et al., 2010, ApJ, 723, 1436

Czesla S., Huber K.F., Wolter U., et al., 2009, A&A, 505, 1277

Deheuvels S., Brunt H., Michel E., et al., 2010, A&A, 515, A87

Deheuvels, S., et al., 2011, in preparation

Deleuil M., Deeg H.J., Alonso R., et al., 2008, A&A, 491, 889

Demory B.-O., Gillon M., Deming D., et al., 2011, submitted to A&A

Dravins D., 1990, A&A, 228, 218

Dumusque X., Udry S., Lovis C., Santos N.C., Monteiro M.J.P., 2011a, A&A, 525, 140

Dumusque X., Santos N.C., Udry S., et al., 2011b, A&A, 527, A82

Fabrycky D., Tremaine S., 2007, ApJ, 669, 1298

Fortney J., Marley M.S., Barnes J.W., 2007, ApJ, 659, 1661

Fossey S., Waldmann I.P., Kipping D.M., 2009, MNRAS, 396, L16

Garcia, R.A., Regulo, C., Samadi, R., et al., 2009, A&A, 506, 41

Gardner J.P., Proceedings of the Eighteenth International Symposium on Space Terahertz Technology, held March 21-23, 2007, at California Institute of Technology, Pasadena, CA USA. Edited by Karpov, A., 237

Gaulme P., Deheuvels S., Weiss W.W., et al., 2010, A&A, 524, A47

Gillon M., Lanotte A.A., Barman T., et al.,2010, A&A,511, A3

Girardi, L., Groenewegen, M.A.T., Hatziminaoglou, E., da Costa, L., 2005, A&A, 436, 895

Gough D.O., 1990, Progress of Seismology of the Sun and Stars, 367, 283

Grasset O., Schneider J., Sotin C., 2009, ApJ, 693, 722

Grillmair C.J., Burrows A., Charbonneau D., 2008, Nature, 456, 767

Guillot T., 2005 Annual Review of Earth and Planetary Sciences, 33, 493

Guillot T., 2008, Physica Scripta, 130, 014023

Guillot T., Havel M., 2011, A&A, 527, A20

Guillot T., Santos N.C., Pont F., et al., 2006, A&A, 453, L21

Harrington J., Hansen B.M., Luszcz S.H., et al., 2006, 314, 623

Hatzes, A.P., Fridlund, M., Nachmani, G. et al., 2011, ApJ, submitted

Howard A., Marcy G., Johnson J., et al., 2010, Science, 330, 653

Hu Y., Ding F, 2011, A&A,, 526, A135

Hu Y., Yang D., Yang J., 2008, Geophysical Research Letters, 35, L19818

Ibgui L., Spiegel D.S., Burrows A., 2011, ApJ, 727, 75

Ida S., Lin D.N.C., 2004, ApJ, 616, 567

Ida S., Lin D.N.C., 2005, ApJ, 626, 1045

Ida S., Lin D.N.C., 2010, ApJ, 719, 810

Ikoma M., Guillot T., Genda H., et al., 2006, ApJ, 650, 1150

Irwin J., Charbonneau D., Nutzman P, et al., 2008, ApJ, 681, 636

Kalas P., Graham J.R., Clampin M., 2005, Nature, 435, 1067

Kaltenegger L., Segura A., Mohanty S., 2011, ApJ, 733, 35

Kasper M., Beuzit J.-L., Verinaud C., et al., 2010, Ground-based and Airborne Instrumentation for Astronomy III. Edited by McLean, I.S., Ramsay, S.K., Takami, H.. Proceedings of the SPIE, 7735, 77352E

Kirsh D.R., Duncan M., Brasser R., Levison H.F., 2009, Icarus, 199, 197

Kjeldsen H., Bedding T.R., 1995 A&A, 293, 87

Kjeldsen H., Bedding T. R., Butler R., 2005, ApJ, 635, 1281

Kjeldsen H., Bedding T. R., Christensen-Dalsgaard J.C., 2008, ApJ, 683, L175

Knutson H.A., Charbonneau D., Allen L.E., et al., 2007, Nature, 447, 183

Knutson, H.A., Charbonneau, D., Cowan, N.B., et al., 2009, ApJ, 703, 769

Krauss L.M., Chaboyer B., 2003, Science 299, 65

Kroupa, P., 2001, ASPC, 228, 187

Kulikov Y.N., Lammer H., Lichtenegger H., et al. 2006, Planetary and Space Science, 54, 1425

Kulikov Y.N., Lammer H., Lichtenegger H., et al. 2007, Space Science Reviews, 129, 207

Lagrange A.-M., Bonnefoy M., Chauvin G., et al., 2010, Science, 329, 57

Lallement, R., Welsh, B.Y., Vergely, J.L., et al., 2003, A&A, 411, 447

Lammer H., Bredehöft J.H., Coustenis A., et al 2009, A&A Rev., 17, 181

Lammer H., Eybl V., Kislyakova K.G., Weingrill J., et al., 2011a, accepted to Astrophysics and Space Science

Lammer H., Kasting J., Caussefière E., et al. 2008, Space Science Reviews, 139, 399

Lammer H., Kislyakova K.G., Holmström M., et al., 2011b, accepted to Astrophysics and Space Science

Latham D.W., Rowe J.F., Quinn S.N., Batalha, N.M., et al., 2011, ApJL, 732, L24

Latham, D.W., Stefanik, R.P.; Mazeh, T., et al., 1989, Nature, 339, 38

Laughlin G., Crismani M., Adams F.C., 2011, ApJL, 729, L7

Lebreton Y., 2008, "Stars in the age of micro-arc-second astrometry 2008, A Giant Step: from Milli- to Micro-arcsecond Astrometry", Proceedings of the International Astronomical Union, IAU Symposium, 248, 411

Léger A., Rouan D., Schneider J., Barge P., Fridlund M., et al., 2009, A&A, 506, 287

Lecavelier des Etangs A., Vidal Madjar A., McConnell J.C., Hebrard G., 2004, A&A, 418, L1

Linsky J.L., Yang H., France K., 2010, ApJ, 717, 1291

Lissauer J., Rogozzine D., Fabrycky D., et al., 2011, ApJ, submitted

Liu X., Burrows A., Ibgui L., 2008, ApJ, 687, 1191

Lovis C., Fischer D., 2010, Exoplanets, edited by Seager S., Tucson, AZ: University of Arizona Press, 27

Lovis C., Mayor M., Bouchy F., et al. 2008, IAU Symp, 253, 502

Lovis C., Mayor M., Pepe F., et al. 2006, Nature, 441, 305

Lovis C., Segransan D., Mayor M., Udry S., Benz W., et al., 2011, A&A, 528, 112

Lovis, C., Mayor, M., Bouchy, F., et al., 2009, IAUS, 253, 502

Machalek P., McCullough P.R., Burke C.J., et al., 2008, ApJ, 684, 1427

Madhusudhan N., Seager S., 2009, ApJ, 707, 24

Marcy, G.W, Butler, R.P., 1996, Ap.J., 464, L147

Marois C., Macintosh B., Barman T., et al., 2008, Science, 322, 1348

Marshall, D.J., Robin, A.C., Reyle, C., et al., 2006, A&A, 453, 635

Mathur S., Handberg R., Campante T.L., 2011, ApJ, 733, 95

Mayor M., Queloz D., 1995, Nature, 378, 355

Mayor M., Bonfils X., Forveille T., et al., 2009a, A&A, 507, 487

Mayor M., Udry S., Lovis C., et al. 2009b, A&A, 493, 639

Mayor, M., Lovis, C., Pepe, F., et al., 2011, AN, 332, 429

Mazeh T., Faigler S., 2010, A&A, 521, L59

McCullough P.R., Stys J.E., Valenti J., et al 2005, PASP, 117, 783

Mermilliod J.-C., Maeder A., 1986, A&A, 158, 45

Metcalfe T.S., Creevey O., Christensen-Dalsgaard J., 2009, ApJ, 1170, 5356

Metcalfe T.S., Monteiro M.J.P.F.G., Thompson M.J., et al., 2010, ApJ, 723, 1583

Micela G., 2002, ``Second Granada Workshop: The evolving Sun and its influence on the planetary environments'' Granada, Spain, Montesinos B., Gimenez A, and Guinan E. F., eds., 2002, ASP 269, 107

Michel, E., Baglin, A., Auvergne, M., et al., 2008, Science, 322, 558

n J., 2005, A&A, 441, 615 629

Miglio A., Montalbán, J., Carrier F., et al., 2010, A&A, 520, L6

Miglio A., Montalbán J., Noels A., Eggenberger P., 2008, MNRAS, 386, 1487

Miller N., Fortney J.J., 2011, revised for ApJL

Monteiro M J P F G,. Christensen-Dalsgaard J., Thompson M. J., 1994, A&A, 283, 247

Monteiro M.J.P.F.G., Christensen-Dalsgaard J., Thompson M. J., 2000, MNRAS 316, 165

Mordasini C., Alibert Y., Benz W., Naef D., 2009, A&A, 501, 1161

Mosser B., Appourchaux T. 2010, A&A, submitted

Moutou C., Hébrard G., Bouchy F., et al. 2009, A&A, 498, L5

Naef D., Mayor M., Pepe F., et al. 2001, A&A, 375, L27

Neckel, Th., Klare, G., 1980, A&AS, 42, 251

Miglio A., Montalbá

Noyes R., Hartmann L., Baliunas S., Duncan D., Vaughan A., 1984, ApJ, 279, 763

Ofek, E.O., 2008, PASP, 120, 1128

Pál A., Bakos G.Á., Torres G., et al., 2008, ApJ, 680, 1450

Palle P.L., Jimenez A., Perez Hernandez F., et al., 1995, ApJ, 441, 952

Pasquini L., Avila G., Dekker H., et al., 2008, Ground-based and Airborne Instrumentation for Astronomy II. Edited by McLean I.S., Casali M.M., Proceedings of the SPIE, 7014, 70141I

Perryman M.A.C., Brown A.G.A., Lebreton Y., et al. 1998, A&A, 331, 81

Pepe F., Lovis C., 2008, Physica Scripta, Vol 30, p. 14007

Pepe F., Lovis C., Segransan D., et al., 2011, A&A, submitted

Pickles, A.J., 1998, PASP, 110, 863

Pickles, A., Depagne, E., 2010, PASP, 122, 1437

Pollacco D., Skillen I., Collier Cameron A., et al. 2006, PASP, 118, 1407

Queloz D., Henry G.W., Sivan J.-P., et al., 2001, A&A, 379, 279

Queloz D., Bouchy F., Moutou C., et al. 2009, A&A, 506, 303

Quirrenbach A., Amado P.J., Mandel H., et al., 2010, Ground-based and Airborne Instrumentation for Astronomy III. Edited by McLean, I.S., Ramsay S.K., Takami H., Proceedings of the SPIE, 7735, 7735

Quirion P.-O., Christensen-Dalsgaard J., Arentoft T., 2010, ApJ, 725, 2176

Ragozzine D., Wolf A.S., ApJ, 698, 1778

Redfield S., Endl M., Cochran W.D., 2008, ApJ, 673, L87

Ribas I., Guinan E.F., Gudel M., Audard M., 2005, ApJ, 622, 680

Robin, A., Creze, M., 1986, A&A, 157, 71

Robin, A.C., Reyle, C., Derriere, S., Picaud, S., 2003, A&A, 409, 523

Roques, F., Moncuquet, M., 2000, Icarus, 147, 530

Rowe J.F., Matthews J.M., Seager S., et al., 2008, ApJ, 689, 1345

Roxburgh I.W., Vorontsov S.V., 1994a. MNRAS, 267, 297

Roxburgh I.W., Vorontsov S.V., 1994b. MNRAS, 268, 880

Roxburgh I.W., Vorontsov S.V., 2001, MNRAS 322, 85

Roxburgh I.W., Vorontsov S.V., 2003a, A&A, 411, 215

Roxburgh I.W., Vorontsov S.V., 2003b, Astrophysics & Space Science, 284, 187

Roxburgh I.W., Vorontsov S.V., 2006, MNRAS, 369, 1491

Roxburgh I.W., 2009a, A&A, 493, 185

Roxburgh I.W., 2009b, A&A, 506, 435

Saar S.H., Donahue R., 1997, ApJ, 485, 319

Saar S.H., Butler R., Marcy G., 2008, ApJ, 498, 153

Sagan, C., Salpeter, E.E., 1976, ApJS, 32, 737

Seager S., Deming D., 2010, Annual Review of Astronomy and Astrophysics, 48, 631

Seager S., Hui L., 2002, ApJ, 574, 1004

Seager S., Kuchner M., Hier-Majumder C.A., et al., 2007, ApJ, 669, 1279

Selsis F., Kasting J.F., Levrard B., et al., 2007, A&A, 476, 1373

Siebert, A., Williams, M.E.K., Siviero, A., et al., 2011, AJ, 141, 187

Shustov B., Sachkov M., Gómez de Castro A.I., et al., 2009, Astrophysics and Space Science, 320, 187

Snellen I.A.G., de Mooij E.J.W., Albrecht S., 2009, Nature, 459, 543

Snellen I.A.G., de Kok R.J., de Mooij E.J.W., Albrecht S., 2010a, Nature, 465, 1049

Snellen I.A.G., de Mooij E.J.W., Burrows A., 2010b, A&A, 513, A76

Spiegel D.S., Burrows A., 2010 ApJ, 722, 871

Stello D., Chaplin W. J., Bruntt H., et al. 2009, ApJ,, 700, 1589

Struve, O., 1952, The Observatory, 72, 199

Swain M.R., Deroo P., Griffith C.A., et al., 2010 Nature, 463, 637

Swain M., Vasisht G., Tinetti G., 2008, Nature, 452, 329

Swain M.R., Vasisht G., Tinetti G., et al., 2009, ApJL,690, L114

Tian H., Tu C.-Y., Xia L.-D., He J.-S., 2008, A&A, 489, 1297

Triaud A.H.M.J., Collier C.A., Queloz D., et al., 2010, A&A, 524, A25

Tsiganis K., Gomes R., Morbidelli A., et al., 2005, Nature, 435, 7041, 459

Udry S., Bonfils X., Delfosse X., et al. 2007, A&A, 469, L43

Udry S., Fischer D., Queloz D. 2007, Protostars and Planets V, B. Reipurth, D. Jewitt, and K. Keil (eds.), University of Arizona Press, Tucson, 685

Valencia D., Sasselov D.D., O'Connell R.J., 2007, ApJ, 665, 1413

van den Bergh S., 1995, Science, 270, 1942

Vauclair G., Fu J.-N., Solheim J.-E., 2011, A&A, 528, A5

Vergely, J.-L., Valette, B., Lallement, R., Raimond, S., 2010, A&A, 518, A31

Vidal Madjar A., Lecavelier des Etangs A., Desert J.-M., Ballester G.E., Ferlet R., Hebrard G., Mayor M., 2003, Nature, 422, 143

Vidal-Madjar A., Sing D.K., Lecavelier Des Etangs A., 2011, A&A, 527, A110

von Paris P., Gebauer S., Godolt M., et al., 2010, A&A, 522, A23

Vorontsov S.V., 1988, "A search of the effects of magnetic field in the solar five-minute oscillations", Proc. IAU Symposium No 123, Advances in helio- and asteroseismology, Eds J. Christensen-Dalsgaard, S. Frandsen, Reidel, Dordrecht, 151

Wagner F.W., Sohl F., Rückriemen T., Rauer H., 2011, accepted to the IAU 276 Proceedings: The Astrophysics of Planetary Systems: Formation, Structure, and Dynamical Evolution

Walsh K.J., Morbidelli A., 2011, A&A, 526, A126

Welsh W.F., Orosz J.A., Seager S., et al., 2010, ApJL, 713, L145

White, et al., 2011, in preparation

Willems, B., Kolb, U., 2002, MNRAS, 337, 1004

Willems, B., Kolb, U., 2004, A&A, 419, 1057

Willems, B., Kolb, U., Justham, S., 2006, MNRAS, 367, 1103

Winn, J.N., Howard, A.W., Johnson, J.A., et al. 2011a, AJ, 141, 63

Winn J.N., Matthews J.M., Dawson R.I., et al., 2011b, submitted to ApJL

Wolszczan, A., Frail, D. A., 1992, Nature, 355, 145

Wordsworth R.D., Forget F., Selsis F., et al. 2010, A&A, 522, A22

Wright J., Marcy G., Butler R., Vogt S., 2004, ApJS, 152, 261

Zahnle K.J., Walker J.C.G., 1982, Reviews of Geophysics, 20, 280

Zwintz, K., 2008, ApJ, 673, 1088

List of acronyms

AEU	Ancillary Electronics Units
AIT	Assembly, Integration and Testing
AO	Announcement of Opportunity
AOCS	Attitude and Orbit Control System
ASW	Application SoftWare
CCD	Charge Coupled Device
CDMU	Central Data Management Unit
CFRP	Carbon-Fibre Reinforced Plastic
CNES	Centre National d'Etudes Spatiales
CV	Cosmic Vision
DoF	Degrees of Freedom
DP	Data Product (DP1-DP6)
DPS	Data Processing System
DPU	(Telescope) Data Processing Unit
D/SRE	Director of Science and Robotic Exploration
EChO	Exoplanet Characterisation Observatory
EM	Electrical Model
EP-RAT	ExoPlanet Roadmap Advisory Team
ESA	European Space Agency
ESAC	European Space Astronomy Centre
ESOC	European Space Operations Centre
F-AEU	Fast Ancillary Electronics Units
FAS	Focus Adjustment Shims
FEE	Front End Electronics
FEU	Fast Electronics Unit
FGS	Fine Guidance Sensor
FM	Flight Model
FoV	Field of View
FPA	Focal Plane Assembly
FPI	Focal Plane Instrument
GFRP	Glass-Fibre Reinforced Plastic
GMSK	Gaussian Minimum Shift Key
GS	Ground station
GSE	Ground Support Equipment
HCMM	High capacity memory module
HDRM	Hold-down and Release Mechanism
HGA	High Gain Antenna
HK	House Keeping data
HP	Heat Pipe

ICU	Instrument Control Unit
ILS	Independent Legacy Scientist
IPPM	Integrated Processing Payload Module
IPRR	Instrument Preliminary Requirements Review
L0-L1	Data Product Level
LEOP	Launch and Early Orbit Phase
LGA	Low Gain Antenna
LOS	Line Of Sight
MAD	Mission Assumptions Document
MEU	Main Electronics Unit
MLI	Multi-Layer Insulation
MMU	Mass Memory Unit
MOC	Mission operations Centre
MRD	Mission Requirements Document
N-AEU	Normal Ancillary Electronics Units
N-DPU	Normal Data Processing Unit
NGTS	Next Generation Transit Survey
OB	Optical Bench
OBC	On-Board Computer
OGS	Optical Ground Station
P/L	Payload
PCL	PLATO Consortium Lead
PDAAS	PLATO Data Acquisition and Analysis System
PDC	PLATO Data Centre
PDD	Payload Definition Document
PDPC	PLATO Data Centre Processing Centre(s)
PDPM	PLATO Data Processing Manager.
PIP	Payload Interface Plate
PIPM	PLATO Instrument Project Manager
PLM	Payload Module
PPLC	Plato PayLoad Consortium
ppm	part per million
PRR	Preliminary Requirements Review
PSPM	PLATO Science Preparation Management
PSST	PLATO Study Science Team
PST	PLATO Science Team
PSF	Point Spread Function
PSU	Power Supply Unit
PVA	Photovoltaic Assembly
QE	Quantum Efficiency

RCS	Reaction Control System
RD	Reference Document
RFI	Radio Frequency Interference
RPE	Relative pointing Error
RTC	Remote Terminal Controller
S/C	Spacecraft
SciRD	Science Requirements Document
SiC	Silicone Carbide
SRR	System Requirements Review
SOC	Science Operations Centre
SSH	Sunshield
SSM	Second Surface Mirror
SVM	Service Module
SW	SoftWare
STM	Structural Model
TBC	To Be Confirmed
TOU	Telescope Optical Unit
TT&C	Tracking and Command subsystem